



Corso di dottorato di ricerca in
Scienze biomediche e biotecnologiche

Ciclo XXXI

Titolo della tesi

“Role of Ape1 acetylation in fine tuning its activity
on telomeric regions”

Dottoranda

Dott.ssa Silvia Burra

Supervisore

Prof. Gianluca Tell

Anno di discussione 2018-2019

*Niente nella vita va temuto, dev'essere solamente compreso.
Ora è tempo di comprendere di più, così possiamo temere di meno.*

Marie Curie

Summary

Summary.....	3
1. Abstract.....	5
2. Abbreviations	6
3. Figures <i>index</i>	7
4. Introduction	9
4.1. Cancer cells features	9
4.2. Base Excision Repair (BER) pathway	11
4.3. Apurinic/aprimidinic endonuclease 1 (Ape1)	12
4.4. Telomeres organization.....	21
4.5. Ape1 role at the telomeres.....	33
5. Aim of this study	36
6. Results	37
6.1. Structural analysis of G4 sequences by circular dichroism (CD) spectroscopy 37	
6.2. The 33-residue Ape1 N-terminus is required to stably bind telomeric G4 structures	40
6.3. The enzymatic activity of Ape1 on G4 telomeric structures is influenced by ionic strength and the N-terminus	44
6.4. Acetylatable lysine residues in the Ape1 N-terminus are required for binding and enzymatic activity on G4 telomeric structures	53
6.5. Activity of Ape1 protein variants from U2OS cells.....	56
6.6. The telomeric-binding ability of Ape1 depends on K ²⁷ , K ³¹ , K ³² and K ³⁵ residues.....	61
6.7. Interaction of NPM1 with Ape1 modulates its endonuclease activity on telomeric sequences	62
.....	66
7. Discussion.....	67
8. Future perspectives.....	72
9. Materials and Methods	74
9.1. Protein expression and FPLC purification	74
9.2. Oligonucleotides synthesis, purification and annealing.....	74
9.3. Circular dichroism (CD) spectroscopy.....	75
9.4. SDS-PAGE and Western blotting	76
9.5. Electrophoretic mobility shift assay (EMSA).....	77
9.6. UV-crosslinking experiments.....	77

9.7.	Cell cultures, transfection and Co-immunoprecipitation	77
9.8.	Chromatin immunoprecipitation and quantitative PCR.....	78
9.9.	AP site incision assays	79
9.10.	Surface Plasmon Resonance (SPR) experiments	80
9.11.	Telomeric length assay	80
9.12.	GST pull-down assay	80
9.13.	Statistical analysis	81
10.	References.....	82
11.	Published articles	101
12.	Acknowledgements.....	102

1. Abstract

One of the hallmarks of cancer is the loss of telomere stability. Unprotected telomeres are prone to aberrant end-joining reactions that lead to chromosomal fusions and translocations. Human telomeres are formed by the repeated TTAGGG sequence, in which the 3' exposed strand may adopt a G-quadruplex (G4) structure. The guanine-rich regions of telomeres are hotspots for oxidation forming 8-oxoguanine, a lesion that is handled by the base excision repair (BER) pathway. One key player of this pathway is Ape1, the main human endonuclease processing abasic sites. Recent evidences showed an important role for Ape1 in telomeric physiology, but the molecular details regulating Ape1 enzymatic activities on G4 telomeric sequences are lacking. Through a combination of *in vitro* assays, we demonstrate that Ape1 can bind and process different G4 structures containing an abasic site analog (THF) in two different locations and that the interaction involves specific acetyltable lysine residues (i.e. K²⁷/K³¹/K³²/K³⁵) present in the unstructured N-terminal domain of the protein. The cleavage of the abasic site located in a G4 structure by Ape1 depends on the DNA conformation or the position of the lesion and on electrostatic interactions between the protein and the nucleic acids. Moreover, Ape1 mutants mimicking the acetylated protein display increased cleavage activity for abasic sites. We found that nucleophosmin (NPM1), which binds the N-terminal domain of Ape1, plays a role in modulating telomere length and Ape1 activity at abasic G4 structures. Thus, the Ape1 N-domain is an important relay site for regulating the enzyme's activity on G4-telomeric sequences, and specific acetyltable lysine residues constitute key regulatory sites of Ape1 enzymatic activity dynamics at telomeres.

2. Abbreviations

ALT	Alternative Lengthening of Telomeres
AP	Apurinic/aprimidinic site
Ape1	AP endonuclease 1
BER	Base Excision Repair
F	Tetrahydrofuran
G4	G-quadruplex
OG	8-oxo-7,8-dihydroGuanine
Lys	Lysine
nCaRE	negative Calcium Responsive Element
NPM1	Nucleophosmin 1
PTM	Post-Translational Modification
ROS	Reactive Oxygen Species
TERC	Telomere RNA Component
TERT	Telomere Reverse Transcriptase
TERRA	Telomeric Repeat-containing RNA
TRF	Telomeric Repeat binding Factor

3. Figures index

Figure 1 The hallmarks of cancer.....	9
Figure 2 Overview of different damaging agents, DNA effects and relative DNA repair pathways	10
Figure 3 Graphical representation of the main BER steps	11
Figure 4 Structural organization of Ape1 protein	13
Figure 5 Cartoon representation of the Ape1-DNA complex.....	14
Figure 6 Representation of the product of guanine oxidation	17
Figure 7 Ape1 protein network.....	20
Figure 8 Representation of the chromosome ends protected by members of the shelterin complex	22
Figure 9 Representation of a planar tetrad	25
Figure 10 Possible G-quadruplex structure conformations	25
Figure 11 Mechanisms of telomerase-driven (A) and HR-driven (B) synthesis of telomeric DNA.....	27
Figure 12 Protein interactome network of telomeric partners	34
Figure 13 CD spectroscopy of the oligonucleotides used in this study	38
Figure 14 Schematic representations of G-quadruplex structures assumed by the oligonucleotides used in this work	39
Figure 15 Circular dichroism (CD) analysis for the G4 oligonucleotides used in this study	39
Figure 16 Gel analysis of purified human recombinant proteins used in this study	40
Figure 17 Ape1 stably binds the G4 oligonucleotides	41
Figure 18 Cross-linking analysis performed with Nat oligonucleotide	42
Figure 19 SPR sensorgrams for Ape1 ^{WT} and Ape1 ^{NA33} with Nat oligonucleotide	43
Figure 20 SPR sensorgrams for Ape1 ^{WT} and Ape1 ^{NA33} with Poly dT oligonucleotide	44
Figure 21 The position of the abasic site on the G4 influences Ape1 ^{WT} endonuclease activity	45
Figure 22 Ape1 ^{WT} endonuclease activity on control substrates	46
Figure 23 The position of the abasic site on the G4 influences Ape1 ^{NA33} endonuclease activity.....	47
Figure 24 Ape1 ^{NA33} endonuclease activity on control substrates.....	48
Figure 25 Ape1 ^{WT} cleaves AP sites in G4 substrates more efficiently at lower ionic strength	49
Figure 26 Ape1 ^{WT} cleaves AP sites in ds substrates more efficiently at lower ionic strength	49
Figure 27 Ape1 ^{NA33} cleaves AP sites in G4 substrates more efficiently at lower ionic strength	50
Figure 28 Ape1 ^{NA33} cleaves AP sites in ds substrates more efficiently at lower ionic strength	51
Figure 29 Ionic strength influences Ape1 endonuclease activity	52
Figure 30 Summary of AP site incision activity of Ape1 protein on the different substrates	52

Figure 31 Purified recombinant Ape1 mutant proteins check.....	53
Figure 32 Ape1 interacts with G4 oligonucleotides in a stoichiometric ratio	54
Figure 33 AP site incision activity graphs summarizing endonuclease activity of Ape1 protein and its mutants on the different substrates in a solution containing 50 mM KCl.	54
Figure 34 Endonuclease activity of Ape1 ^{K4pleA} on telomeric oligonucleotides and control substrate at high ionic strength.....	55
Figure 36 AP site incision activity graphs summarizing endonuclease activity of Ape1 protein and its mutants on the different substrates in a solution containing 5 mM KCl ...	56
Figure 35 Endonuclease activity of Ape1 ^{K4pleA} on telomeric oligonucleotides and control substrate at low ionic strength	56
Figure 37 Analysis of the interaction between Ape1 mutants and NPM1	57
Figure 38 Immunocaptured Ape1 ^{WT} and mutant proteins check.....	57
Figure 39 Analysis of gel mobility of Ape1 mutants from IP.....	58
Figure 40 Eukaryotic mutants of Ape1 are able to bind the telomeric substrates.....	58
Figure 41 AP site incision activity graphs summarizing endonuclease activity of eukaryotic Ape1 protein and its mutants on the telomeric substrates	59
Figure 42 Endonuclease activity of eukaryotic immunocaptured Ape1 protein and its mutants on telomeric oligonucleotides	60
Figure 43 Analysis of binding of Ape1 protein and its mutants on telomeric sequences	61
Figure 44 Ape1 presence is fundamental to maintain telomere integrity in vivo.....	63
Figure 45 NPM1 inhibits Ape1 endonuclease activity competing with the substrate for the interaction with the N-terminal domain of the endonuclease	64
Figure 46 NPM1 shows only a weak affinity toward Nat substrate	65
Figure 47 GST pull-down experiment showing that NPM1 is able to interact with Ape1 under physiologic conditions.....	65
Figure 48 NPM1, when present in a supra-stoichiometric ratio with Ape1, inhibits its endonuclease activity	66
Figure 49 A model for the regulation of Ape1 activity during the repair of abasic sites in G4 DNA.....	71

4. Introduction

4.1. Cancer cells features

Cancer cells are characterized by several hallmarks, which distinguish them from healthy cells. Tumor cells are able to avoid immune recognition, to favor tumor-promoting inflammation, to escape apoptosis and sustain proliferative signaling and also to overcome genomic instability (Hanahan and Weinberg 2011). Characterized by point mutations and chromosomal rearrangements, genome instability is one of the key elements that lead to cancer development through oncogene activation, or inactivation of tumor-suppressor genes (Figure 1) (Grandér 1998). Also, the majority of tumors are characterized by loss of checkpoint functions, compromised DNA repair activities and immortalization to reach a limitless replication (Ciccia and Elledge 2010; Hanahan and Weinberg 2011).

Furthermore, to achieve immortalization and to maintain telomere length, the activity of telomerase enzyme is fundamental (Olovnikov 1996). When damaged, telomeres can participate in aberrant end-joining reactions leading to chromosome fusions,

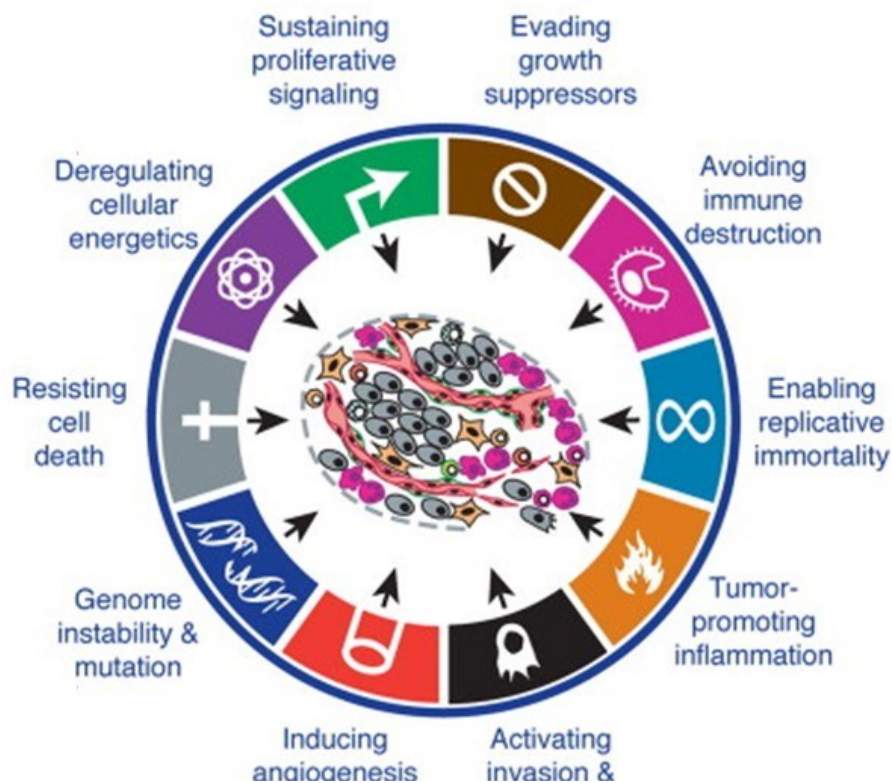


Figure 1 *The hallmarks of cancer*

The illustration lists the main hallmark capabilities of tumor cells, whose underlying mechanisms are still widely investigated. (Hanahan and Weinberg, 2011).

translocations or breakage (Bailey 2006). Eukaryotic cells are continuously exposed, during their life-span, to several environmental stimuli (i.e. tobacco, UV light, smog, infections), both endogenous and exogenous, which represent damaging agents because they can impair macromolecules (Hoeijmakers 2001). DNA retains an intrinsic reactivity which gets the molecule a susceptible target for damages from various sources. To avoid harmful consequences that could lead to lethal outcomes for the cells, they adopt several mechanisms to ensure DNA integrity (Figure 2). Unrepaired DNA damages could result in cell death, limitless proliferation and cancer (Wilson and Bohr 2007).

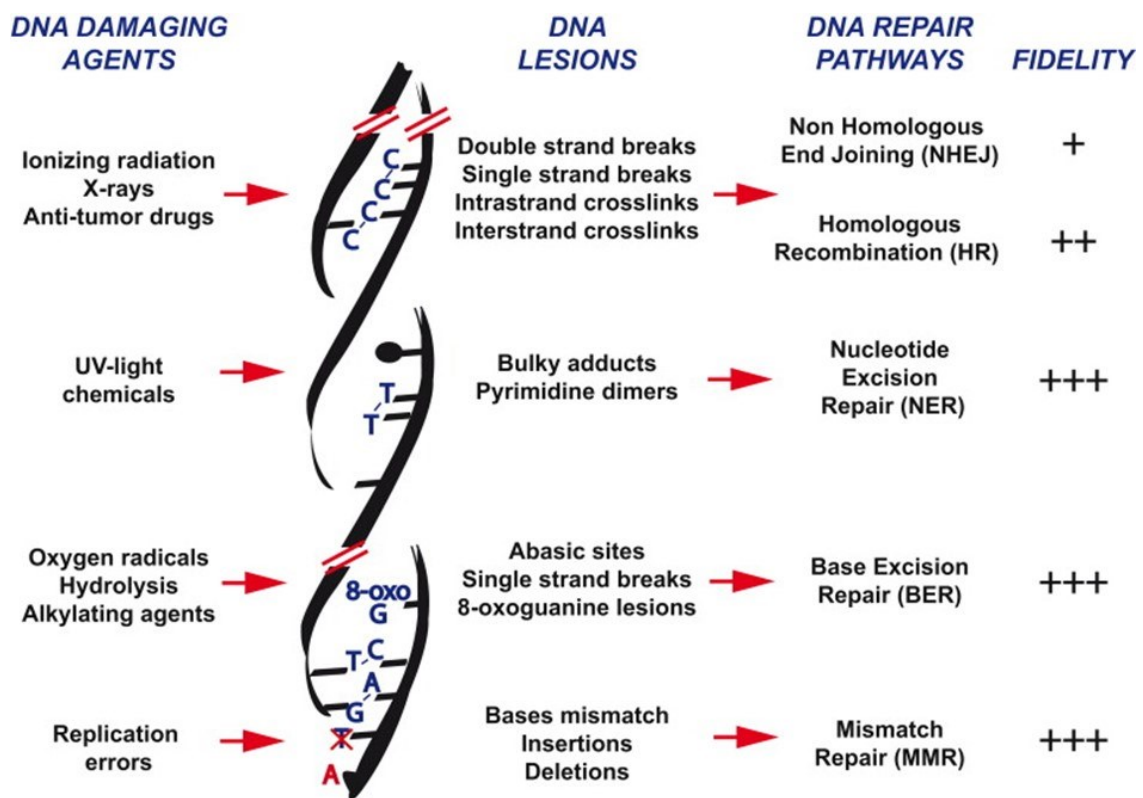


Figure 2 Overview of different damaging agents, DNA effects and relative DNA repair pathways

The figure recapitulates for each DNA damaging agent, the lesion induced on DNA and finally DNA repair pathways acting on the lesions (Blanpain et al. 2011).

To counteract these outcomes, several mechanisms are employed by the cells to maintain genome stability, including DNA repair, cell cycle checkpoints and apoptosis pathways (Bauer, Corbett, and Doetsch 2015). DNA damage response pathways include several systems to repair specific DNA lesions. DDR mechanisms include the base excision repair, the nucleotide excision repair, the mismatch repair, the homologous recombination and the non-homologous end joining pathways (Blanpain et al. 2011) (Figure 2). All these

pathways are finely tuned and coordinated thanks to a crosstalk that ensures the proper repair of the occurring lesion.

Most of the endogenous burden, associated with oxidative stress, is handled by the Base Excision DNA Repair (BER) pathway (Dempfle and Sung 2005; P. Liu and Dempfle 2010).

4.2. Base Excision Repair (BER) pathway

Base excision repair pathway is one of the most important pathways involved in the repair of DNA lesions and in the maintenance of genomic integrity, and it is essential to ensure viability of mammalian cells (Markkanen 2017). In fact, if key players of BER pathway are not expressed, this leads to embryonic lethality (Iyama and Wilson 2013).

BER is involved in the removal of damaged bases, for example, by oxidation, alkylation or deamination. Several enzymes are recruited to complete the process (Figure 3), which is composed of five essential steps (Akbari et al. 2015).

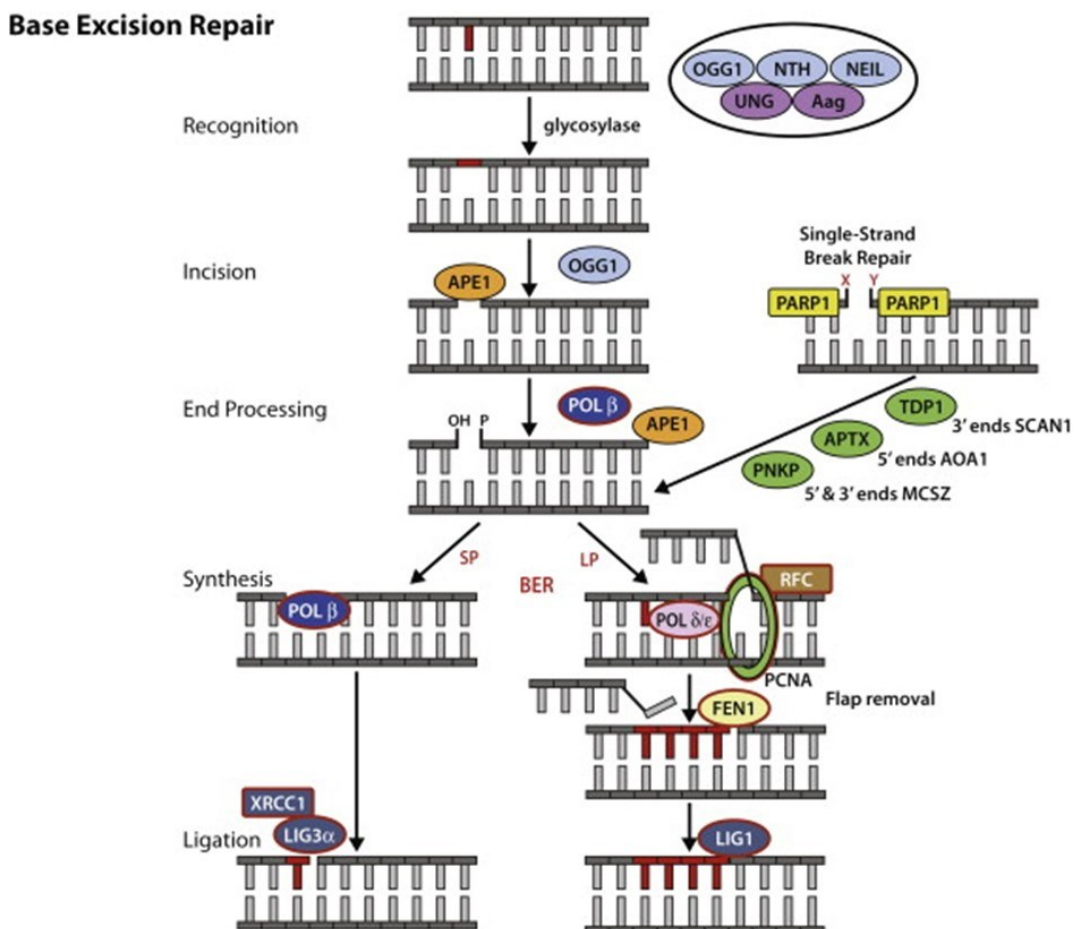


Figure 3 Graphical representation of the main BER steps

After the cleavage of the N-glycosyl bond by specific DNA glycosylases, AP endonuclease (Ape1) cuts the phosphodiester bond. The resulting gap is then filled by DNA polymerases and ligases (Akbari et al. 2015).

As a first step, this pathway identifies the abnormality in the DNA sequence through the intervention of a glycosylase, which specifically recognize the modified base. This is flipped out and cleaved, giving rise to an abasic site through the hydrolysis of the N-glycosyl bond (Wallace 2013). The abasic site is then processed by Ape1 (Apurinic/aprimidinic endonuclease 1, Bauer, Corbett, and Doetsch 2015) that cuts the phosphodiester backbone 5' to the AP site generating a 3' OH and 5'-deoxyribose-5-phosphate (Dempfle and Sung 2005). The nick is then handled by Pol β that replaces only the nucleotide containing the removed base (Howard and Wilson 2017), or alternatively by Pol δ/ϵ , which replace 2-12 nucleotides. In dependence of the involvement of the different polymerases, the pathway is called *short patch* or *long patch* respectively. In the short patch BER, ligase III is involved to seal the nick left after Pol β action (Sobol et al. 1996). In the long patch after Pol δ/ϵ intervention, FEN-1, PCNA and ligase I are recruited to remove the excess flap bases and complete the repair process (Sung, DeMott, and Dempfle 2005).

4.3. Apurinic/aprimidinic endonuclease 1 (Ape1)

Ape1 is the major AP endonuclease in mammals (Hadi et al. 2002). Besides its role in BER pathway, it was recently discovered that Ape1 has several other activities (Antoniali et al. 2017). Ape1 presence is important for the DNA repair process, so it is considered a key player in BER (Tell et al. 2009). Ape1 is an abundant protein, with a density of $\sim 10^4 - 10^5$ copies/cell, and with a relatively long half-life of almost 8 hours (Tell et al. 2009; Vascotto et al. 2009). The *APE1* gene is located on chromosome 14q11.2-q12 and it is 2.6 kbp long, composed of five exons and four introns (Robson et al. 1992). Multiple transcription start sites (TSSs) are present on the gene, to control both the constitutive and the inducible expression of the protein. In the proximal promoter region the consensus sequence for Sp1 transcription factor is located, which binds the promoter (Zaky et al. 2008). Sp1 is responsible for both constitutive transcription and for the increase during S-phase of the cell-cycle (Rivkees and Kelley 1994; Zaky et al. 2008).

Ape1 is a 35.55 kDa protein, composed of 318 amino acids. It is a monomeric protein with a globular structure containing α/β sandwiches and an unstructured N-terminal domain of 48 amino acids (Gorman et al. 1997).

Three functional domains of Ape1 can be defined:

- The N-terminal domain (aa 1-35) involved in protein-protein interaction and in interactions with nucleic acids (Poletto et al. 2013),
- The intermediate domain (aa 35-127), dedicated to transcription factors regulation through redox activity (Fantini et al. 2010; Lirussi et al., 2012),
- The C-terminal domain (aa 127-318) which conducts endonuclease activity (Tell et al. 2009).

Ape1 is subjected to several post-translational modifications, especially at its first 35 residues (Figure 4).

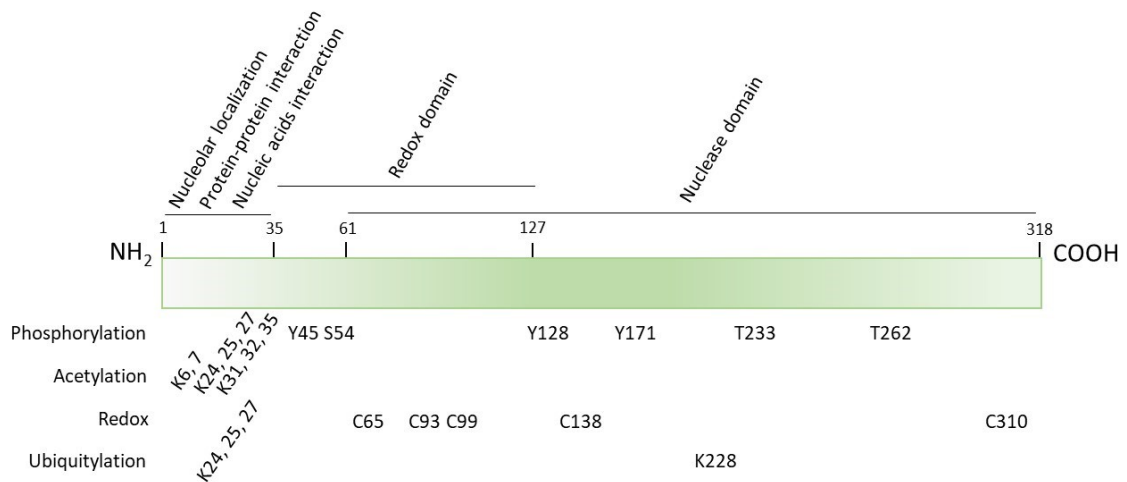


Figure 4 Structural organization of Ape1 protein

Each domain of Ape1 has a specific function. N-terminus is engaged in nucleolar localization, protein-protein interaction and nucleic acid binding. Redox domain interacts with transcription factors to regulate their action and C-terminal domain is the responsible for the endonuclease activity of the protein. The listed amino acids are involved in the specified post-translational modifications or activity.

A very well described *in vivo* post-translational modification is the truncation of the protein occurring at its first 33 amino acids (Bhakat et al. 2016; Timofeyeva et al. 2009). The cleavage reaction is carried on by a still not identified granzyme-like enzyme (Yoshida et al. 2003). The deletion mutant lacks the nucleolar localization signal located in the N-terminus domain, so this protein displays a cytoplasmic localization (Jackson et al. 2005), and its ability to interact with canonical protein partners is hampered (Vascotto et al. 2009). Phosphorylation of the N-terminal domain inhibits Ape1 endonuclease activity while enhancing its redox activity (Busso, Lake, and Izumi 2010; Huang et al. 2010). Acetylation involves lysine residues K⁶, K⁷, K²⁷, K³¹, K³² and K³⁵ with the effect of decreasing the interactions with other protein partners, such NPM1, inhibiting the accumulation of Ape1 in the nucleoli (Lirussi et al. 2012; Busso, Lake, and Izumi 2010).

Moreover, acetylation also affects the affinity of Ape1 toward nucleic acids, due to the neutralization of the positive charges of residues K²⁷, K³¹, K³² and K³⁵. Furthermore, the neutralization of the N-terminal arm of Ape1 induces a conformational change that increases the endonuclease activity of the protein (Roychoudhury et al. 2016; Fantini et al. 2010). Moreover, acetylated Ape1 results in a more enzymatically active form, so the protein can process DNA lesions faster (Fantini et al. 2008; Lirussi et al. 2012; Fantini et al. 2010; Roychoudhury et al. 2016).

The endonuclease activity incises in correspondence of the AP site, at its 5' on the phosphodiester backbone. After the cleavage, the single strand break is flanked by the 3'-hydroxyl (OH) and at the 5'-deoxyribose phosphate. Ape1 recognizes the abasic site, and subsequently excludes the dNTP, distorting the DNA backbone of about 35° (Figure 5).

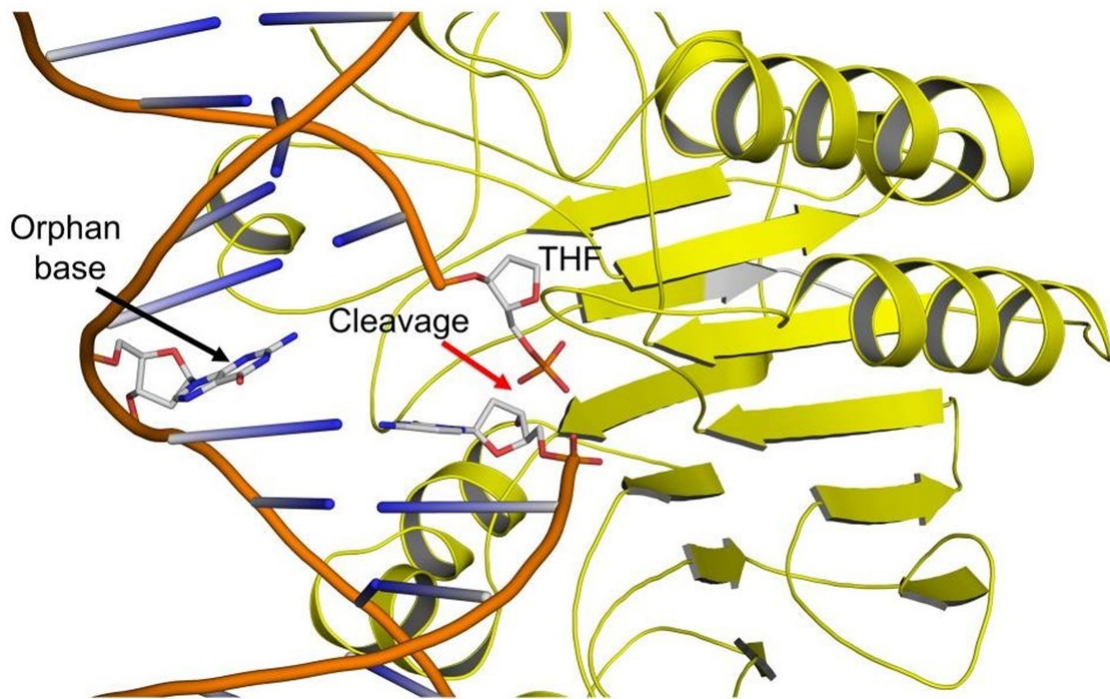


Figure 5 Cartoon representation of the Ape1-DNA complex

The protein is shown in yellow and the arrow indicates the cleavage. The abasic site is represented by the THF (Freudenthal et al., 2015).

The active site is defined by several residues. Phe226 is implicated in AP site recognition, Asp210 and Asn212 play a critical role in hydrolyzing the phosphodiester bond and Tyr171 with His309 direct the proper disposition of the AP substrate (Freudenthal et al. 2015; Mundle et al. 2009). Moreover, Asp283 and Asp308 are involved in maintaining the active site conformation (Evans, Limp-Foster, and Kelley 2000). The enzymatic reaction goes on upon a further rearrangement between Ape1 and DNA, which is

dependent on the presence of Mg^{++} acting as enzymatic co-factor, positioned at the active site (Glu 96 and Asp70), to promote the spatial reorganization (Erzberger and Wilson 1999; Tell, Wilson, and Lee 2010). A water molecule is also needed to carry on the cleavage reaction, which requires the presence of a nucleophile (Freudenthal et al. 2015; Manvilla et al. 2013). Quite recently, it has been demonstrated that Ape1 is also involved in RNA metabolism (Tell, Wilson, and Lee 2010; Antoniali et al. 2017). Furthermore, Arg177 and Met270 participate in DNA binding to maintain Ape1 locked on the substrate (Kaur et al. 2014).

Another fundamental function of Ape1 consists in its ability of working as co-activator of transcription factors through a redox mechanism, which allows to regulate gene expression. The key residues are Cys65 and Cys93 (Walker et al. 1993) and Cys99 (Luo et al. 2012), through which Ape1 keeps reduced critical Cys residues of some transcription factors. In particular, the crucial residue is represented by the Cys65, considered as the nucleophilic residue in the reduction of disulphide bonds in TFs. All the three cysteines are buried in a hydrophobic pocket, so it has been suggested that a conformational change is required to allow the contribution of these residues (Luo et al. 2012; Su et al. 2011).

Ape1 is also involved in nucleotide incision repair (NIR) by incising in a DNA glycosylase-independent manner substrates carrying a 3' OH (Gros et al. 2004). This pathway is activated to support BER pathway when glycosylases are absent or unable to process the lesion, usually resulting from oxidative stress (Timofeyeva et al. 2011). In the NIR context, Ape1 cuts at the 5' of the oxidized base without the intervention of a glycosylase, producing a 3' OH extremity that is then processed by FEN1. The repair is then completed by the action of polymerases (Ischenko and Sapparbaev 2002). Ape1 NIR activity is exerted at pH values of 6.4- 6.8 and KCl concentration of 50 mM. NIR is highly exerted by Ape1 at 100-fold lower $MgCl_2$ concentration, compared to AP-endonuclease activity (Gros et al. 2004). The N-terminal domain of the protein, fundamental for the protein-protein and protein-nucleic acid interaction, is not fundamental for the AP-endonuclease activity but is indispensable for the NIR activity (Izumi et al. 2005).

Ape1 is able to *in vitro* process single-stranded RNA containing abasic sites (Berquist, McNeill, and Wilson III 2008), to interact with ribosomal RNA to assist its processing (Vascotto et al. 2009), and to interact with several proteins implicated in RNA processing, i.e. NPM1. The interaction between Ape1 and NPM1 could compete with the contact of

each protein with RNA binding. The use of inhibitors of Ape1-NPM1 interactions in tumor cells, where both Ape1 and NPM1 are overexpressed and their interaction is functional for cancer cell proliferation, results in improvement of the contacts of each protein with rRNAs (Poletto et al. 2016). A recently published work highlights the action of Ape1 on abasic and oxidized ribonucleotides embedded in DNA (Malfatti et al. 2017). The protein can process ribonucleotide abasic sites incorporated in DNA with the same efficiency as deoxy-abasic sites (Malfatti et al. 2017). This evidence is interesting as it confirms the role of Ape1 in processing RNA substrates and it highlights the importance of the protein in the maintenance of genome integrity, as oxidative damage is a very common lesion involving ribonucleotides incorporated in DNA that is handled by BER.

4.3.1. Ape1 as regulator of gene expression

Besides its canonical role as fundamental enzyme in the BER pathway that is well characterized, Ape1 could be also considered a regulator of gene expression through different and yet not completely unveiled mechanisms. Indeed, Ape1 plays a role in the regulation of expression of human genes during oxidative stress conditions both through direct and indirect mechanisms, being therefore important for cancer biology (Tell, Wilson, and Lee 2010; Li and Wilson 2014; Antoniali et al. 2017).

Ape1 direct role in transcriptional regulation

Recent findings highlighted that epigenetic mechanisms seem to crosstalk with DNA damage. In detail, oxidative DNA lesions appear to act as epigenetic-like marks through the recruitment of the DNA repair machinery, thus modulating gene expression in cells exposed to oxidative stress (Fleming and Burrows 2017; Fleming, Ding, and Burrows 2017; Perillo et al. 2008). Oxidation of the guanine is a frequent event leading to 8-oxo-7,8-dihydroguanine (OG) formation, which is a highly mutagenic modification (Figure 6). If RNA polymerases face an OG during transcription, this could cause the stalling of the enzyme, leading to the repression of transcription. It was recently demonstrated that if OG is present at the promoter level of some genes, the transcription can be increased *via* the BER pathway (Fleming and Burrows 2017; Fleming, Ding, and Burrows 2017). The glycosylase OGG1 removes the OG, generating an AP site that unmarks the G-quadruplex structure and is bound but not efficiently cleaved by Ape1 (Fleming, Ding,

and Burrows 2017). So Ape1 may, in coordination with other BER partners, bridge other transcription factor regulators, intertwining DNA repair with transcription activation.

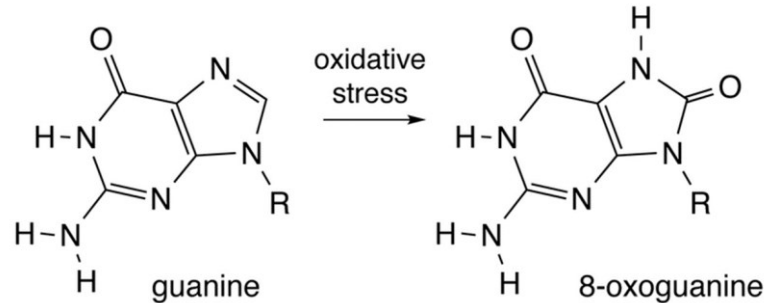


Figure 6 Representation of the product of guanine oxidation

8-oxo-7,8-dihydroguanine is one of the most common oxidative DNA lesions, formed under various oxidative conditions.

It was observed that Ape1 is able to regulate transcription through the binding *via* its N-terminal domain to bind specific DNA regulatory sequences, known as nCaRE, which are widely present among the genome (Antoniali, Lirussi, D'Ambrosio, et al. 2014, 1). These elements are found in the context of promoters of many genes. They are present also in the promoter of Ape1 gene, and Ape1 protein can bind it thanks to the involvement of a protein complex, including also hnRNPL, Ku70/80 and PARP-1, participating in a negative regulation of its own gene (Izumi, Henner, and Mitra 1996; Antoniali, Lirussi, D'Ambrosio, et al. 2014). On the contrary, when Ape1 binds the nCaRE sequences present on the SIRT1 promoter, this stimulates the transcription in case of oxidative stress. That is because, upon the AP endonuclease activity of Ape1, the promoter gains in flexibility and consequently the chromatin is locally relaxed, thus easing there the assembly of the transcription complex (Pastukh et al. 2015; Antoniali, Lirussi, D'Ambrosio, et al. 2014).

Ape1 indirect role in transcriptional regulation

Redox regulation is achieved through the modulation of TFs activity, especially targeting specific cysteine (Cys) residues located in their DNA-binding domains or regulatory sites, as pointed out by several studies (Evans, Limp-Foster, and Kelley 2000; Tell et al. 2005). Actually, these critical cysteines need to be in their reduced state to allow TFs proper binding to the target DNA sequences (Tell et al. 2005). So far, Ape1 is the only known DNA repair protein that also possesses nuclear transcriptional regulatory activity in mammals (Georgiadis et al. 2008). Through its intervention, Ape1 maintains several TFs

in their reduced and active state, influencing gene expression and maintaining genomic stability within the cells (Kelley, Georgiadis, and Fishel 2012). Ape1 modulates the redox status of both ubiquitous and tissue-specific transcription factors, such as AP-1, Egr-1, NF- κ B and p53 (Tell et al. 2005; Li and Wilson 2014; Kelley, Georgiadis, and Fishel 2012). These and others TFs are involved in the regulation of many different cellular mechanisms, ranging from cell proliferation and growth to apoptosis, included cancer promotion (Kelley, Georgiadis, and Fishel 2012; Kaur et al. 2014; Fantini et al. 2008). Ape1 role as a redox factor is exerted by its N-terminal domain, through a mechanism not yet fully understood. It was described that, after a partial structural rearrangement of the protein, Cys65 acts as the nucleophile residue for the reduction of the disulphide bond between two cysteines on the oxidized target TF, which is then reduced (Luo et al. 2012). Meanwhile, Cys65 establishes a new disulphide bond with Cys93 or 99 upon Ape1 oxidation process. In this way, Ape1 protein may contribute to preserve the cell from the genotoxic insults due to increased ROS concentration and unbalanced redox regulation.

Recent findings highlighted a novel role for Ape1 in RNA biology. As RNA is a single-stranded molecule, it is much more susceptible to oxidation compared to DNA. RNA damage is as a frequently observed feature in several human cancer types (Simms and Zaher 2016). Thus, RNA quality control mechanisms are crucial to avoid catastrophic effects such as ribosomal impairment, error-prone translation and, consequently, failed protein synthesis and altered gene expression (Vohhodina, Harkin, and Savage 2016). Ape1 was recently identified as a directly involved player in RNA control process, as through its N-terminal domain it interacts with RNA molecules and with other protein partners participating in RNA processing (Vascotto et al. 2009; Poletto et al. 2013). In particular, Ape1 interacts with the nucleolar ribosome biogenesis-related protein nucleophosmin 1 (NPM1) and with rRNA molecules in nucleoli. Moreover, Ape1 can process also RNA molecules, exerting an RNase H-like endoribonuclease activity (Berquist, McNeill, and Wilson III 2008; Tell, Wilson, and Lee 2010; Malfatti et al. 2017). Under oxidative stress conditions Ape1-NPM1 interaction is interrupted and Ape1 moves to nucleoplasm to exert its endonuclease function (Vascotto et al. 2009; Antoniali, Lirussi, Poletto, et al. 2014; Vohhodina, Harkin, and Savage 2016). Also acetylation of the lysine residues located in the N-terminus of the protein modulates Ape1 interaction with NPM1 and its cellular localization, suggesting that also PTMs play a role in regulating Ape1 functions (Lirussi et al. 2012). In this scenario, Ape1 serves as a scavenger of oxidatively damaged RNA molecules in order to maintain a functional

RNome (Tell, Wilson, and Lee 2010). Next, Ape1 can cleave c-myc RNA, controlling its half-life and tuning its turnover. These evidences support a role of Ape1 in RNA decay and quality control.

It was recently demonstrated that Ape1 is able to bind miRNA molecules too, so the protein is involved in gene expression regulation also through this mechanism (Kim, King, and Lee 2010; Antoniali et al. 2017). Micro RNAs are short non-coding RNA molecules able to regulate a variety of pathways, controlling the translation of RNA transcripts. These molecules are transcribed by RNA pol II and the product is called pri-miRNA because this primary transcript needs to be then modified to obtain a hairpin structure named pre-miRNA. Pre-miRNAs are exported in the cytoplasm and there processed to obtain the mature double-stranded RNA sequence that is 22 nucleotides long. Only one filament of the duplex constitutes the active effector on the target RNA, which is involved in transcription repression by pairing with the complementary RNA. Ape1 seems to be also involved in miRNA maturation as, when silenced, a different miRNA expression profile was detected (Antoniali et al. 2017). Upon depletion of Ape1, the oxidation of miRNAs increased, and an accumulation of pri-miRNAs was observed, coupled with a decrease of mature miRNAs. Probably Ape1 is involved in editing the precursors, consequently exerting a post-transcriptional key role in gene expression (Antoniali et al. 2017).

Furthermore, other evidences pointed out how Ape1 may be involved in epigenetic regulation (Fleming, Ding, and Burrows 2017; Chen et al. 2017).

Ape1 interactome

Ape1 takes active part in a plethora of pathways, thus when its functionality is compromised, the repercussions could be wide and severe (Tell, Wilson, and Lee 2010). The functions and interactions of Ape1 are modulated by PTMs, which control also the subcellular localization of the protein. Recently, a number of interactor proteins were identified, who belong to five major areas (Figure 7) (Antoniali et al. 2017).

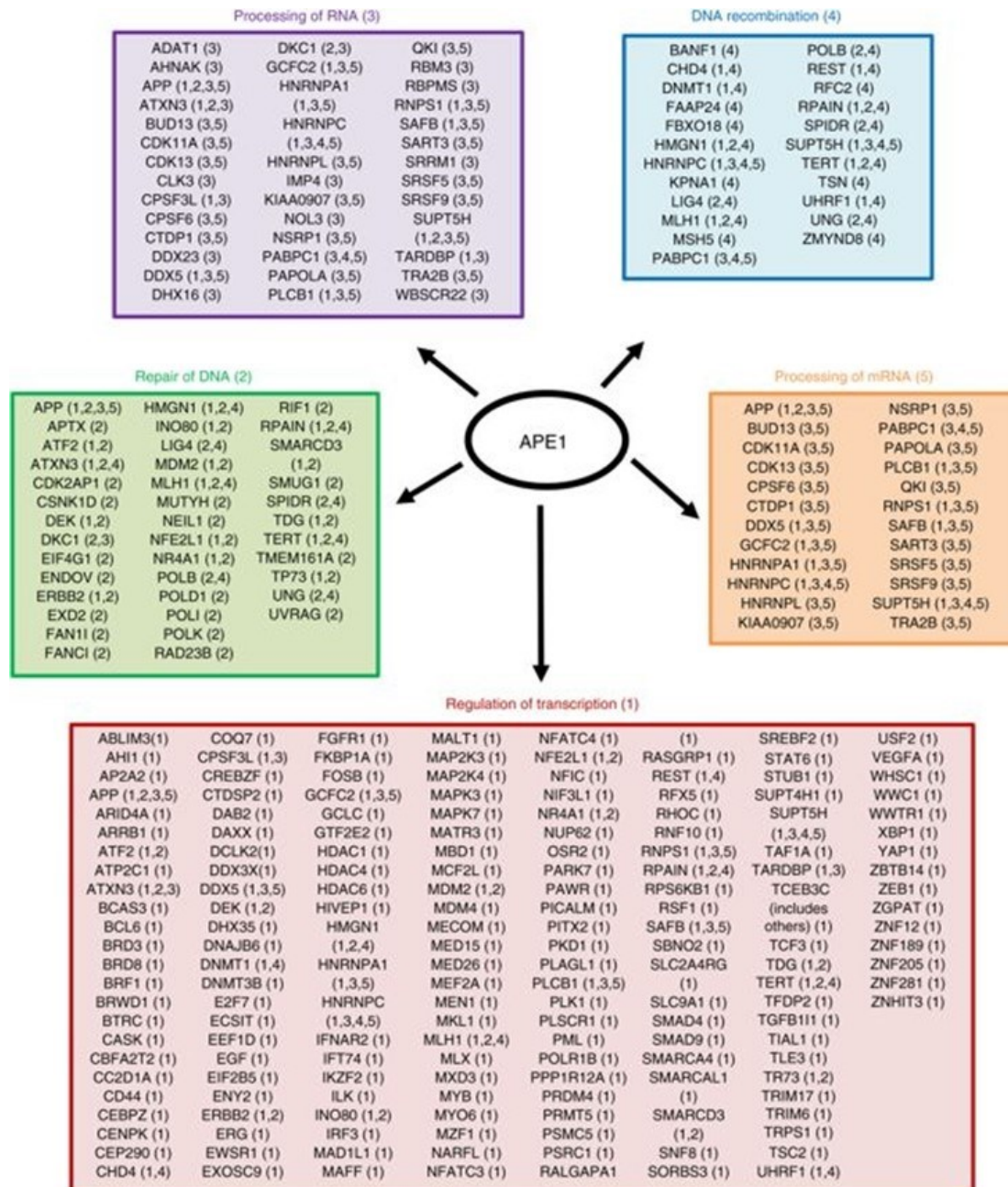


Figure 7 *Ape1* protein network

Top five biological pathways to which *Ape1* interactors are related: repair of DNA, apoptosis, double strand breaks repair, regulation of transcription and processing of RNA (Antoniali et al., 2017).

The recognized pathways are grouped in the regulation of transcription, apoptosis, DNA repair, double strand break repair and RNA processing fields. Of course, the DNA repair interactors mainly belong to the BER pathway, as *Ape1* works as a coordinator of downstream enzymes (Limpose, Corbett, and Doetsch 2017). Within the RNA processing area, are listed proteins involved in RNA metabolism and also RNA molecules, both coding and non-coding, as *Ape1* is also able to interact with these cellular components (Antoniali et al. 2017). Among the transcription regulation, several transcription factors

are listed, which are regulated by Ape1 through its redox function. Finally, apoptosis-regulating components include a lot of enzymes implicated in carrying post-translational modifications that act as signals influencing Ape1 interactions and localization (Fantini et al. 2010; Poletto et al. 2013; Lirussi et al. 2012).

Ape1 in cancer

Dysregulation of Ape1 is found in several human pathologies, including neurodegenerative disorders, cardiovascular diseases and carcinogenesis (Thakur et al. 2015). Overexpression of Ape1 is observed in a few cancer types, in which an altered intracellular distribution is also observed (Tell et al. 2009, 2005). In particular, cytoplasmic localization is correlated with poor prognosis and more aggressive tumours, as observed in lung, ovarian, thyroid, breast cancer and hepatocellular carcinoma (Tell et al. 2009). These features may be responsible for further cell resistance toward chemotherapy since it may reflect an adaptive response to chronic oxidative stress (Wilson and Simeonov 2010; Poletto et al. 2016; Rai et al. 2012), which is the main cause of hepatic carcinogenesis and its progression, so enhancing both Ape1 DNA repair and redox activities (Di Maso et al. 2015). Moreover, Ape1 is implicated in chemoresistance thanks to its ability to induce the expression of the multi-drug resistance gene (MDR1), through its interaction with YB-1 (Sengupta et al. 2011), and thanks to its regulatory action against the expression of the tumor suppressor PTEN (Fantini et al. 2008). The protein could be considered as a potential target to sensitize the cells to chemotherapy, thus its altered expression levels could be employed as a predictive biomarker to evaluate the sensitivity of the tumour (Thakur et al. 2014, 1). As lysine residues (i.e. K²⁷, K³¹, K³² and K³⁵) were found acetylated in cancer cells (Fantini et al. 2010; Poletto et al. 2012), this PTM might be employed as a mechanism to regulate the protein function. Base excision repair, and Ape1 action, are fundamental also at the telomeric level, as the disruption of the physiology of these regions play a role in tumor development, being involved in the raise of telomeric aberrations (Madlener et al. 2013).

4.4. Telomeres organization

Human telomeres extend for 10-15 kbp and are composed by the non-coding repeated sequence TTAGGG (Blasco 2003). Chromosome extremities end with a single-stranded overhang that is bound by the shelterin complex (de Lange 2005). This complex is composed by a group of proteins (Figure 8) that are required to maintain DNA integrity

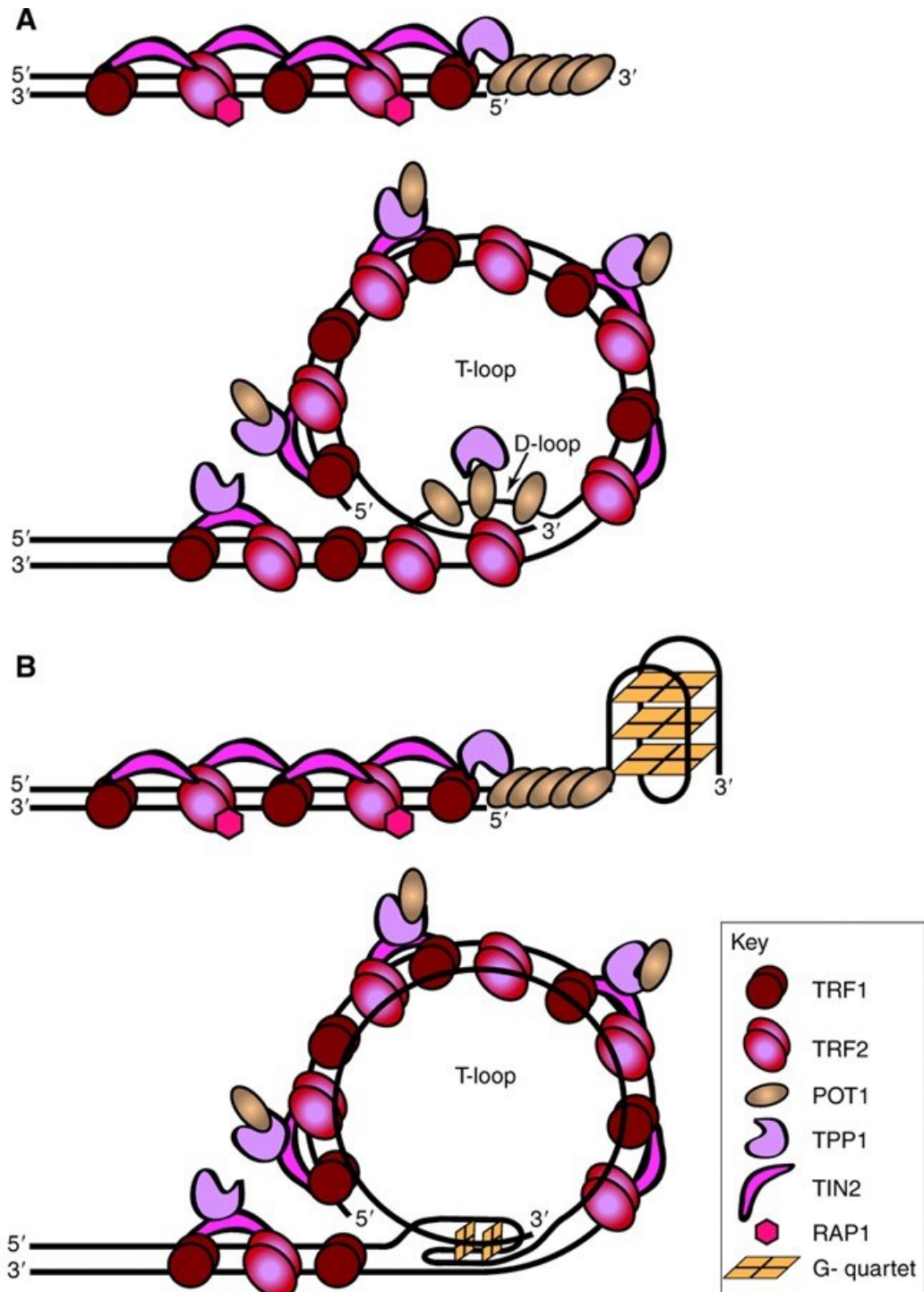


Figure 8 Representation of the chromosome ends protected by members of the shelterin complex

(A) Linear (top) and folded T-loop (bottom) structural states of the telomere are depicted. (B) An anti-parallel intramolecular G-quadruplex either alone (top) or in the context of a T-loop (bottom) might cap the chromosome terminus to avoid their degradation or extension (Oganesian and Karlseder 2009).

and to mediate interactions with other protein partners (Oganesian and Karlseder 2009). The shelterin complex proteins are: TRF1, TRF2 (Telomeric repeat binding factor 1 and 2), POT1 (Protection of telomeres 1), TIN2 (TRF-interacting protein), TPP1 (TIN2 and

POT-interacting protein) and RAP1 (Repressor/activator protein 1), whose presence is fundamental to ensure protection to telomeres (Liu et al. 2004). In particular, this complex also contributes to the folding of telomere into a structure called telomeric loop (T-loop), which guarantees the protection of the single-stranded filament, thanks to the pairing with the upstream complementary strand, creating a displacement loop (D-loop) (Doksani et al. 2013). The structure assumed by the protruding strand is functional to avoid the activation of the DNA damage machinery which would detect the unpaired filament as a site to be repaired (de Lange 2004). A feature of telomeres is the guanine-rich composition of the protruding strand, which is called G-overhang. The G-overhang is bound by a specific single-strand binding protein, POT1, Protection of telomeres (Baumann and Cech 2001). POT1 is essential in the formation of the T-loop, stabilizing the D-loop by binding the displaced filament (Oganesian and Karlseder 2009). The other proteins which establish a direct contact with the telomeres are TRF1 and TRF2, which specifically recognize the double-stranded tract of telomeric DNA. The presence of these two protein partners is essential: the homozygous deletion of either gene results in early embryonic lethality in mice (Celli and de Lange 2005). TRF2 contains a basic domain and a DNA-binding domain; if these two domains are deleted from TRF2 gene, that leads to the activation of DNA-damage response, marked by the presence of γ H2AX, 53BP1, the loss of G-overhang and by end-to-end fusions (Agata Smogorzewska et al. 2002). Thus, TRF2 is involved in the inhibition of NHEJ pathway (Ribes-Zamora et al. 2013). Moreover, TRF2 is also involved in the suppression of illegitimate homologous recombination events at the telomeres. This is a fundamental role, as the D-loop resembles a Holliday junction recombination intermediate, so the HR pathway must be blocked in this context. The expression of a mutant TRF2 deprived of the basic domain results in loss of the T-loop, that leads to the formation of extrachromosomal telomeric circles, which provoked the activation of the DNA damage response and the induction of senescence (Wang, Smogorzewska, and de Lange 2004). It was demonstrated that TRF2 also associates with the NER endonuclease complex XPF-ERCC1, which represses telomere recombination. This complex is also involved in promoting overhang removal, resulting in chromosome fusions in case of TRF2 deletion (Zhu et al. 2003). TRF1 and TRF2 are both involved in DNA remodeling. Through its homodimerization domain, TRF1 is able to loop, bend and induce synapsis of telomeric DNA (Griffith, Bianchi, and de Lange 1998). TRF2 can also induce strand invasions stimulating topological changes at the telomeres (Griffith et al. 1999; Verdun and Karlseder 2006). TRF2 is involved in

the stabilization of the T-loop invasion site by the overhang (Fouché et al. 2006). RAP1 was demonstrated to be essential to protect telomeres from homology-directed repair of telomeres as it cooperates with the basic domain of TRF2 to repress PARP1 and SLX4 localization to telomeres. Without RAP1 and TRF2B, PARP1 and SLX4 HR factors promote rapid telomere resection, resulting in telomere loss and in generation of chromosome fusions in human cells (Rai et al. 2016, 1).

As DNA polymerase works only toward the 3' direction, the leading strand is duplicated until the end, while the duplication of the lagging strand leaves out about 200 nucleotides at each cell cycle (d'Adda di Fagagna et al. 2003). Consequently, telomeres are progressively shortened by each cell replication (Harley, Futcher, and Greider 1990), until they reach a threshold length, which determines the exit from the cell cycle and the start of the senescence phase. The threshold at which the cell stops proliferating and enters in the senescent phase is called Hayflick limit (Hayflick and Moorhead 1961). Some cell types, such as germline cells, stem cells and cancer cells, are not subjected to telomere shortening because they activate some mechanisms to avoid senescence (Flores and Blasco 2010).

4.4.1. G-quadruplex structures and their functions

Telomeric sequences, which are guanine-rich, are characterized by the assumption of a G-quadruplex (G4) folding (Bugaut and Alberti 2015). The acquirement of this folding is supported by TRF2 protein (Pedroso, Hayward, and Fletcher 2009). G-quadruplex (G4) structures derive from the stacking of at least three planar tetrads which are established thanks to the formation of Hoogsten hydrogen bonds between the guanines interspersed in the sequence (Figure 9).

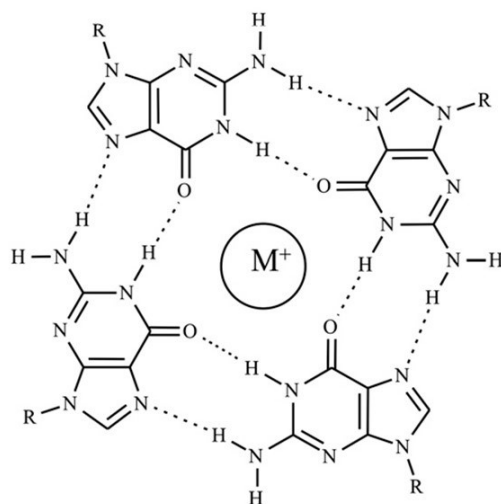


Figure 9 Representation of a planar tetrad

The tetrad is established thanks to the hydrogen bonds, here dotted, between the hydroxyl and aminic groups of each guanine and to the coordination of a cation, indicated by M^+ (Huppert et al 2008).

They form in the presence of monovalent cations, such as Na^+ or K^+ which are coordinated between the stacked tetrads. Several quadruplex conformations exist: they are defined as parallel, antiparallel or hybrid in dependence of the direction in which the filament runs at each “corner” of the tetrad. The different conformation assumed depends on the type of cation, and on the length of the loops, which are the tracts interspersed between the guanine runs (Figure 10).

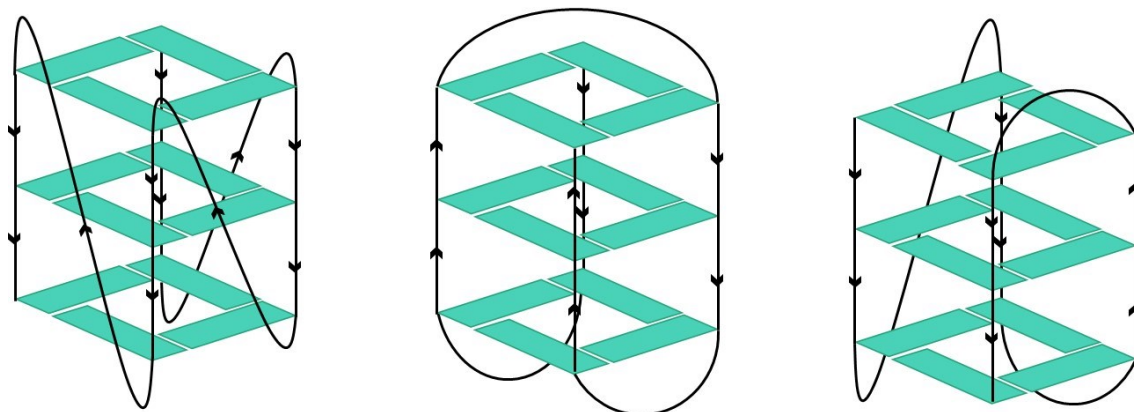


Figure 10 Possible G-quadruplex structure conformations

The representation shows the different G-quadruplex structures that can be assumed by a single stranded DNA sequence containing guanines. Guanine bases are represented by parallelepipeds and non-G residues located in the loops were omitted for clarity. Parallel (left), antiparallel (center) and hybrid (right) G4 are indicated and the arrows show the direction in which each strand runs.

The parallel G4 is characterized by strands running all in the same direction, linked by double-chain reversal loops; the antiparallel G4 contains two strands running in one direction and the other two in the opposite and lateral or diagonal loops. The hybrid quadruplex is also called “3+1” as it results from three strands running in the same direction and one in the other; the loops are also mixed (Dai et al. 2007). Several G4 types can be formed *in vitro* and these structures are thermodynamically characterized by a higher stability than double-stranded DNA and DNA or RNA hairpins (Lane et al. 2008). The formation of G-quadruplex structures *in vivo* plays an important role in regulating DNA replication (Bochman, Paeschke, and Zakian 2012), indeed these secondary structures are unfolded by helicases (RecQ protein-like 4) which are cell-cycle dependent (Postberg et al. 2012). Rif1 also was demonstrated to participate in temporal and spatial regulation of DNA replication (Yamazaki, Hayano, and Masai 2013; Kanoh et al. 2015). Rif1 (Rap1 interacting factor) is a protein able to bind G4-structured binding sequences containing a consensus sequence (Masai et al. 2018). Rif1 preferentially binds to target sequences containing multiple G-tracts, suggesting that higher-order G4 structures allow a more efficient recognition by the protein. G4 structures are present at the promoter region of many genes (i.e. c-Myc, VEGF, SIRT1, TNF α), thus controlling the transcription through the unfolding of the region (Balasubramanian, Hurley, and Neidle 2011).

4.4.2. Telomere maintenance pathways

Two telomere maintenance mechanisms are known: the telomerase-mediated telomere elongation and the ALT (alternative lengthening of telomere) pathway (Figure 11).

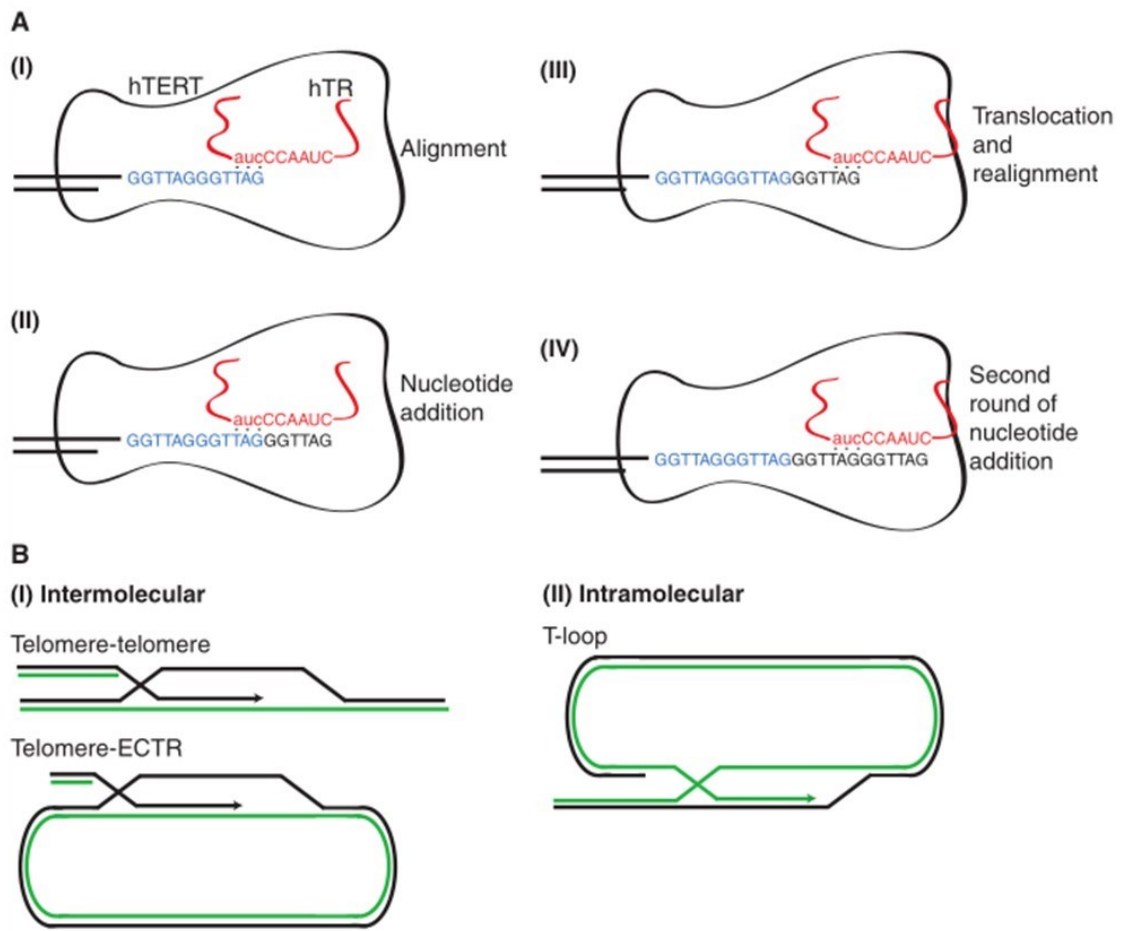


Figure 11 Mechanisms of telomerase-driven (A) and HR-driven (B) synthesis of telomeric DNA

(A.I) DNA synthesis is initiated with the alignment of the 3' telomeric G-overhang (in blue) with the RNA template (in red). (A.II) Telomerase catalyzes nucleotide addition to the overhang until the 5' end of the template is reached. (A.III) The enzyme translocates and realigns with the newly synthesized 3' end of the overhang. (A.IV) A second round of nucleotide addition starts. (B) Both inter- and intratelomeric recombination events have been hypothesized to promote telomere maintenance in ALT. In both types of recombination, the 3' overhang of the telomere initiates invasion and uses its host DNA as a template for DNA copying. (B.I) Intermolecular recombination might involve telomeres from two adjacent chromosomes or chromatids. (B.II) The telomere could also use itself as a template and synthesize DNA via rolling circle replication (Oganesian and Karlseder 2009).

Telomerase is a special enzyme, which works as a reverse transcriptase (RT) from an RNA template. These two components are respectively called TERT and TERC (Feng et al. 1995; Harrington et al. 1997). The other key factor of the human telomerase complex, with TERT and TERC, is dyskerin that is involved in binding and stabilizing TERC (Cohen et al. 2007). While TERC and dyskerin are constitutively expressed, TERT constitutes the limiting factor in telomerase activity (Li et al. 2003). TERC is localized in Cajal bodies, small nuclear organelles implicated in RNA biogenesis and maturation. It was demonstrated that telomerase Cajal body protein1 (TCAB1) mediates the passage of

telomerase RNA through Cajal bodies and assists the fully assembled complex in reaching the telomeres (Venteicher et al. 2009). The telomerase complex is highly expressed during embryonic development and its expression levels decrease after birth. In tumor cells the complex is often re-expressed to allow telomere elongation and ensure immortalization. TERT is, in somatic cells, under strict transcriptional control, while in cancer cells this regulation is lost. It was demonstrated that the expression of hTERT is influenced by epigenetic modifications on the promoter of the gene. Methylation of the promoter of hTERT leads to transcriptional inactivation, but it was stated that when CpG islands in the only proximal promoter region are methylated, this prevents the binding of transcriptional repressors such as CTCF (Renaud et al. 2007), thus leading to transcription activation. Also, acetylation of histone H3 and H4 activates the transcription of TERT gene, as it was demonstrated that after treatment with TSA, a histone deacetylase inhibitor, the methylation levels decrease, thus allowing CTCF binding and consequently suppressing TERT expression (Choi et al. 2010). TRF1 is involved in the negative regulation of telomerase-dependent maintenance of telomere length. This regulation is possible thanks to the crosstalk of TRF1 with POT1-TPP1 complex which controls the access of telomerase to the G-overhang. Telomere length is correlated to TRF1 occupancy, as longer telomeres carry more TRF1 on them. The information is transmitted by TPP1 to POT1, which renders the G-overhang inaccessible to telomerase thanks to a stronger association with it (Loayza and De Lange 2003; Xin et al. 2007; Ye et al. 2004). This is supported by the fact that if TRF1 levels are altered through overexpression or downregulation, this results in telomere shortening or lengthening respectively (Loayza and De Lange 2003; Smogorzewska et al. 2000; Ancelin et al. 2002). The 85-90% of the tumors exploit telomerase re-expression to maintain telomere length, while the remaining 10-15% of the cancer types use ALT. ALT pathway consists of homologous recombination, mainly post-replication, that can occur inter-molecularly using the telomere of the sister chromatid as template, or can be intramolecular, exploiting the T-loop structure (De Vitis, Berardinelli, and Sgura 2018). As the ALT pathway is less strictly regulated, cells that exploit this system show heterogeneous telomere length. For example, if the alignment is asymmetric, this leads to unequal telomere elongation between the two chromatids. Asymmetric chromatid alignment could also give rise to uneven telomere-sister chromatid events (Oganesian and Karlseder 2009). The outcome would show a telomere-less chromosome and its sister with a proliferative advantage (Muntoni et al. 2009). In case of intramolecular recombination, T-loop junction resolution

can occur, generating truncated telomeres and T-circles that represent extra-chromosomal telomeric repeats (Cesare and Reddel 2008). In some cases, telomeres are not allowed to form T-loops due to their insufficient length. If so, TRF2 surveillance might be compromised.

Telomeres were considered transcriptionally inactive, due to the high methylation levels of the subtelomeric regions and to the density of heterochromatic marks (trimethylation of histone H3 and H4 at lysine 9 and 20 respectively) at the telomeric level (Blasco 2007). Surprisingly, it was demonstrated that the transcription at the telomeric level occurs and it gives an RNA consisting of the repeated sequence UUAGGG, which was called TERRA (telomeric repeat-containing RNA) (Azzalin et al. 2007). This long non-coding RNA transcript derives from the activity of RNA polymerase II on the C-rich strand toward the chromosome end. TERRA molecules can range between 100 bp and 9 kb, but the most of them are approximately 200 bp long (Cusanelli and Chartrand 2015). The promoter is localized at the subtelomeric portion, in correspondence of the CpG islands (Luke and Lingner 2009). These islands are maintained non-methylated from the intervention of the insulator proteins CTCF and cohesin, to allow the transcription of TERRA (Ng et al. 2009). TERRA exerts several protective functions towards telomeres. When telomeres shorten, the heterochromatin histone marks are lost as well as the DNA methylation. In this context, TERRA molecules expression is induced. TERRA clusters on shortened telomeres (Yu, Kao, and Lin 2014) from which it was originated, acting as a signaling molecule with multiple functions. One effect is the recruitment, on that site, of the telomerase during S phase (Cusanelli, Romero, and Chartrand 2013), so that telomerase can elongate short telomeres and consequently TERRA levels decrease at these sites (Porro et al. 2010).

An additional effect of TERRA is the stabilization of the telomeric complex and the maintenance of the heterochromatin (Deng et al. 2009). TERRA interacts with TRF1 and TRF2 with a stabilizing effect, moreover, TERRA also binds to methylated histone H3K9me3 and participates in heterochromatin formation (Deng et al. 2009). Thus, TERRA acts as a scaffold molecule that promotes the recruitment of various proteins at the telomeric level. Moreover, the presence of TERRA is required to properly cap the telomeres. TERRA is able to bind hnRNPA1, a ribonucleoprotein that in S phase is brought in proximity of telomeres (López de Silanes, Stagno d'Alcontres, and Blasco 2010) and here displaces RPA, a ssDNA binding protein which is required to activate ATR checkpoint. POT1 substitutes RPA on the G-overhang, repressing ATR-mediated

DDR at telomeres (Flynn et al. 2011). Due to its complementarity with the C-rich strand, TERRA is able to form DNA-RNA hybrids, called R-loops (Arora et al. 2014), involved in transcription termination and regulation of gene expression (Ginno et al. 2012). Formation of R-loops is strictly controlled and these hybrids are resolved by RNaseH1 and 2, or unwound by helicases such as Pif1 (Paeschke et al. 2013). R-loops stimulate homologous recombination in ALT-positive cells and recruit there the telomerase complex in telomerase-positive cells (Arora et al. 2014).

4.4.3. Telomere interactome and its involvement in telomeric DNA repair

Telomeres are preserved by the shelterin proteins, which ensure protection to the chromosome termini. However, the telomeric G-quadruplex represent a vulnerable target for oxidation (Fleming and Burrows 2013) and the presence of OG could displace the shelterin complex (Opresko et al. 2005). One of the key players responsible for the removal of OG is NEIL3, which preferentially processes lesions located in single-stranded or quadruplex DNA (Zhou et al. 2013). NEIL3 participates in telomere integrity maintenance, thanks to the interaction with TRF1 during late S-phase and its absence leads to telomeric aberrations (Zhou et al. 2017). It was demonstrated that Ape1 is also localized at the telomeric level, where it interacts with TRF2, and this interaction ensures the integrity of telomeric DNA (Madlener et al. 2013). In the absence of TRF2, the binding of POT1 is increased, to stimulate the endonuclease activity in case of DNA damage (Lee et al. 2011; Miller et al. 2012).

RPA (replication protein A) is another fundamental protein that binds to single stranded DNA in eukaryotic cells. Its partial depletion by RNA interference dramatically reduces cell proliferation, diminishes DNA synthesis, causes genomic instability, and decreases DNA repair (Hass, Lam, and Wold 2012). RPA dynamically interacts with helicases belonging to the RecQ family, such as RECQL1, WRN, BLM and FANCD1. Moreover, RPA recruits to the site of action also DNA translocases, such as SMARCAL1 that indirectly interacts with the helicases to solve the stalling of replication forks (Awate and Brosh, Jr. 2017). Furthermore, an important protein involved in telomere homeostasis is Rif1 (Rap1-interacting factor 1), which interacts with a component of the shelterin complex. In mammals Rif1 is not associated with intact telomeres: the interaction takes place in case of telomere shortening or DSB at the telomeric level (de Lange 2005). Rif1 acts as a mediator of DSB repair pathway choice: the protein is involved in determining

the activation of HR or NHEJ (Fontana et al. 2018). As HR requires the commitment of the end resection, which is dependent on the cell cycle and CDK activity (Hustedt and Durocher 2016), a counterbalance is established between CtIP, which promotes resection together with BRCA1, and Rif1 that pairs with 53BP1 (Yun and Hiom 2009). 53BP1 acts as a reader of histone marks such as H4K20me2 and H2AK15ub, so it promotes NHEJ during G1 and early S phase (Zimmermann and de Lange 2014) together with Rif1 that attenuates end resection, though in mammalian cells the mechanism of action has still to be elucidated. H/ACA ribonucleoproteins also contribute to the assembly and stabilization of telomerase complex and to post transcriptional processing of nascent ribosomal RNA and pre-mRNA splicing (Meier 2005). Within these RNPs, NOP10 and DKC1 are listed as key telomerase components that handle the effects of oxidative stress at the telomeric level. When DKC1 or NOP10 are silenced, the cells produce much lower levels of TERC and show a decreased telomerase activity (Lin et al. 2015). Another effect of the silencing of these components is the increase of oxidative stress, that reflects on the levels of oxidized peroxiredoxin and glutathione. Moreover, cells silenced for NOP10 or DKC1 are more susceptible to DNA damage. So, the depletion of these RNPs affects RNA maturation process and generates oxidative stress, which is a significant factor determining telomere shortening (Ibáñez-Cabellos et al. 2018).

4.4.4. Oxidation damage repair at telomeric structures

Oxidative damage is quite common at the telomeric level (Park et al. 1992), originating a considerable amount of OG. As base oxidation can cause a substantial loss of thermostability to the DNA sequence and, possibly, disrupt sheltering protein contacts with the telomeres (Opresko et al. 2005), several proteins are involved in the repair of such type of lesion. When located in a G-quadruplex structure, oxidation damage is handled by NEIL1 and NEIL3 glycosylases (Zhou et al. 2013). It was demonstrated that NEIL1 and NEIL3 are able to remove, beyond OG, also hydantoin lesions deriving from further oxidation within a Na⁺-coordinated antiparallel quadruplex (Zhou et al. 2015). In the same work the processing of several sequences was investigated, in particular, the teamwork of Wallace examined the processing of both telomeric sequences containing lesions in different positions, and sequences that are found within the promoter of many genes, such as VEGF and c-Myc. In this study, the authors state that OGG1 can process OG only when they are located in a duplex substrate, and that Ape1 is able to process furan in quadruplex DNA Na⁺-coordinated (Zhou et al. 2015). The authors conclude

hypothesizing a possible involvement of NEIL glycosylases in both telomere maintenance and gene regulation. Additionally, NEIL3 interacts also with TRF1, and appears to be an essential player ensuring telomere integrity by coordinating the repair of oxidation damages, as in the absence of this glycosylase the cells display telomere dysfunctions (Zhou et al. 2017). NEIL3 cleaves the damaged base and then recruits the LP-BER machinery, included Ape1, to facilitate the repair at telomeric *loci* (Zhou et al. 2017). Anyway, the mechanism of action and regulation of Ape1 on telomeric G-quadruplex structures needs to be further elucidated.

4.4.5. Role of G-quadruplex in transcription regulation

Oxidation damage at the level of gene promoters organized as G4 could be taken as a transcription activating signal (Fleming, Ding, and Burrows 2017). When a purine in a duplex sequence is oxidized, the repair of this modification creates an AP site that decreases the thermostability of the double strand, driving to the formation of a more stable quadruplex structure (Fleming, Ding, and Burrows 2017). It was suggested that the oxidized guanine-containing tract within the promoter of VEGF gene can be looped out from the quadruplex structure so to maintain the G4 folding and to facilitate the repair proteins in their activity (Fleming, Ding, and Burrows 2017). Consequently, the presence of an oxidized guanine leads to the recruitment of the BER components, but the quadruplex folding reduces the processivity of the repair process. As a result, transcription machinery is engaged, thus oxidation could be considered an epigenetic-like modification driving DNA repair-coupled transcription initiation (Zhou et al. 2015; Fleming, Ding, and Burrows 2017). It was confirmed that, when Ape1 idles on the abasic site within a G4, the protein activates some transcription factors through its redox domain (Fleming and Burrows 2017). The group of Burrows employed a luciferase assay to report the transcription of VEGF gene to determine whether the localization of OG on the template or the coding strand influences the outcome (Fleming et al. 2017). Depending on the strand on which the OG is formed, the effect is activation or repression of translation. In particular, if the lesion is located on the coding strand, this reflects on transcriptional activation, while if it is positioned on the template strand, transcription is switched off (Fleming et al. 2017). The oxidation of guanines seems not to be randomly distributed throughout the genome: these events appear to be more frequent at the promoters of actively transcribed genes (Zarakowska et al. 2014), and this can regulate their transcription. The Burrows teamwork demonstrated that the folding of quadruplexes at

the promoter level is the responsible for gene expression depending on the localization of the potential quadruplex sequence on the coding versus template strand (Fleming et al. 2018). They highlighted that the frequency of potential quadruplex-forming sequences was 1.8-fold higher in promoters of DNA repair genes, compared to other random genes of the human genome, so these secondary structures play a very important role in regulating gene transcription (Hänsel-Hertsch et al. 2016; Fleming et al. 2018). Employing the luciferase reporter assay, the authors used G4-specific ligands to stabilize G-quadruplex structures at the promoter level of NEIL1, NEIL3 and BLM genes. They observed that activation of transcription occurred when the quadruplex was formed on the coding strand, while G4 structures folded on the template strand interfere with transcription, which was down-regulated (Fleming et al. 2018). In this context, the oxidation of guanine is defined as a friend and foe signal: when solid tumors grow they become hypoxic, inducing oxidative stress. This lead to VEGF activation and vascularization to permit tumor expansion (Fleming and Burrows 2017). Thus, OG behaves both as an epigenetic-like regulator and an initiator of mutagenesis in this scenario. Intertwining between DNA repair and transcription activation is starting to earn increasing interest.

4.5. **Ape1 role at the telomeres**

Figure 12 shows the network of proteins that interact with both the telomeric regions and Ape1 protein. It includes, besides TRF1, TRF2 and RAP1, components of the shelterin complex, some players involved the DNA repair processes like XRCC1, XRCC5, XRCC6, FEN1, PCNA, DNA-PK and DDB1 and regulation factors such as MCM4, MCM7 and HP1 γ , which respectively allow DNA replication initiation and contributes to the maintenance of transcriptional silencing recognizing heterochromatin histone marks.

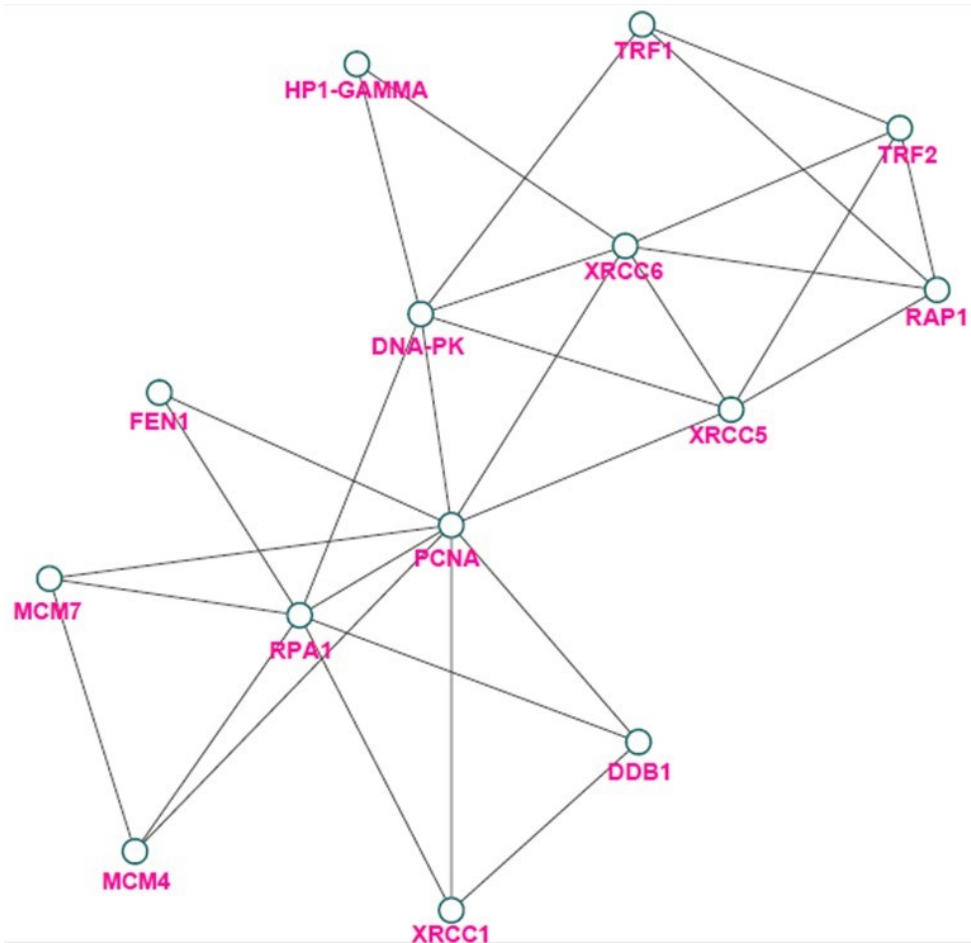


Figure 12 *Protein interactome network of telomeric partners*

The figure shows the cross-talk of proteins that are associated to the telomeric region and that belong also to Ape1 interactome.

It was demonstrated that depletion of Ape1 leads to telomere shortening and losses and to a higher rate of chromosome fusions (Madlener et al. 2013) and that Ape1 deficiency promotes cell senescence and premature aging features (Li et al. 2018). It was proved that a mutant form of Ape1, carrying lysine residues 6 and 7 substituted with alanines, mimicking the acetylation of these amino acids, display an *in vivo* increase in the rate of telomeric aberrations, despite maintaining its DNA repair activity (Madlener et al. 2013). Within the amino-terminus of the protein, several other residues exist which can be acetylated, in particular the lysines in position 27, 31, 32 and 35. Moreover, the acetylation status of these lysine residues may be modulated by lysines 6 and 7 (Lirussi et al. 2012). It was previously found in our lab that a mutant of Ape1 which carries the four cited lysine residues substituted with alanines displays enhanced endonuclease activity on double-stranded DNA containing an abasic site (Fantini et al. 2010), but reduced ability of recognition and processing of the abasic site on a single-stranded substrate (Fantini et al. 2010; Poletto et al. 2013). Moreover, cancer cells that express the

Ape1 mutant, bearing Lys/Ala substitution in the four specified positions (i.e. Ape1^{K4pleA}), display a reduced proliferation rate (Lirussi et al. 2012). The role of Lys 27-35 in the processing of telomeric sequences has not been elucidated yet, so we hypothesize that the post-translational modification status of the specified lysines may be a mechanism to regulate the enzymatic activity of the protein at the telomeric level.

As the guanine is the base with the lowest redox potential (Steenken and Jovanovic 1997), it is a susceptible target of oxidation. Consequently, the telomeric sequences are vulnerable regions and, under oxidative stress conditions, the formation of oxidized and abasic sites is frequent. The structure of the quadruplex is highly destabilized by the presence of an apurinic site which disrupts the tetrad (Virgilio et al. 2012; Esposito et al. 2010; Babinský et al. 2014). Ape1 can exert its endonuclease activity *in vitro* on abasic sites located in telomeric repeats-containing double strands (Broxson et al. 2014; Li et al. 2014; Theruvathu et al. 2014), and also on the quadruplex structure of the c-Myc promoter, though with an attenuated cleavage rate (Broxson et al. 2014). It seems that Ape1 activity on G-quadruplex structures containing an abasic site is influenced by the coordinated cation, which may induce a different folding (Zhou et al. 2015). As mentioned before, Ape1 stalling on a G4 while processing the abasic site here located may induce partial unfolding of the DNA secondary structure to extrude the lesion. However, nowadays, little is known about the ability of Ape1 to process abasic sites located in structured telomeric sequences.

5. Aim of this study

Cancer cells are frequently characterized by the dysregulation of telomere homeostasis. In particular, tumors display aberrations at the telomeric level due to shortened telomeres that are illicitly elongated to ensure the maintenance of a required length which allows unlimited cellular replication (Hanahan and Weinberg 2011). Moreover, cancer cells often exhibit telomeric fusions, bridges, telomeric translocations and breakages. Human telomeres are composed of the repeated sequence TTAGGG and are characterized by the protrusion of the 3' extremity (de Lange 2005). The single stranded filament assumes a secondary structure called G-quadruplex (G4), thanks to the hydrogen bonds established between the guanines. As the guanine is the most susceptible base toward oxidative damage (Steenken and Jovanovic 1997), these regions are a hotspot for oxidation. When a guanine is oxidized, the modification leads to a lower stability of the G-quadruplex (Babinský et al. 2014). Base excision repair is active also at the telomeric level, where ensuring the maintenance of integrity is crucial for cellular proliferation. A key player of the BER is Ape1, the major human endonuclease (Hadi et al. 2002). Recently it was shown that Ape1 presence is fundamental in the maintenance of telomere physiology (Madlener et al. 2013), however the details regarding the molecular regulation of its enzymatic activity have not been elucidated yet.

We already investigated the Ape1 ability to process single-stranded nucleic acids that resulted strictly dependent on the propensity of the substrate to adopt secondary structures and is modulated by the N-terminal basic unstructured portion of the protein (Poletto et al. 2013). Here, we want to shed light on the role of the N-terminal arm of Ape1 for the stable recognition and enzymatic processing of telomeric substrates. We particularly focused on the function of lysine residues, which can be modulated through acetylation, that represents a mechanism to regulate the affinity of the protein toward nucleic acids. We employed several substrates mimicking the telomeric structure and containing an abasic site analog located in different positions to perform endonuclease activity assays in two different saline conditions with several Ape1 protein mutants mimicking acetylation of crucial lysine residues within N-terminal domain.

Understanding the inherent need for Ape1 at telomeres is critical to define the precise mechanism that underlies cancer progression.

6. Results

6.1. Structural analysis of G4 sequences by circular dichroism (CD) spectroscopy

Previous studies, performed on dsDNA, demonstrated that Ape1 exhibits a substrate-dependent endonuclease activity (Berquist, McNeill, and Wilson III 2008; Marenstein, Wilson III, and Teebor 2004) and may play a role in telomere maintenance (Madlener et al. 2013). The potential of Ape1 to process telomeric G-quadruplex structures containing abasic sites has been barely investigated (Madlener et al. 2013; M. Li et al. 2018; Zhou et al. 2015; Fleming, Ding, and Burrows 2017). In order to fill in this gap, we used three labelled oligonucleotides (ODN) (Table 1), including telomeric sequences already known to fold into G4 structures (Virgilio et al. 2012), some bearing abasic sites in different positions. Specifically, the ODN, indicated as S4 and S8 contain a tetrahydrofuran (F) residue resembling an abasic site (Takeshita et al. 1987), replacing the 4th or the 8th guanosine, respectively, while Nat represents the natural telomeric sequence containing undamaged DNA. In order to obtain structural insights, we first analyzed the ODN by CD spectroscopy, under several buffer conditions including those required for the enzymatic assays. The profile of the labeled Nat sequence (Figure 13 A) (annealed at 70 mM KCl) appears almost superimposable on that of its unlabeled counterpart (Virgilio et al. 2012), thus indicating that the presence of the IRDye moiety does not influence G-quadruplex conformation. This profile is characteristic of the hybrid 3+1 strand arrangement (Dai, Carver, and Yang 2008). On the other hand, the CD spectrum of sequence S4 (Figure 13 B) shows a positive band around 265 nm, typical of parallel G-quadruplexes, and a further positive band at 295 nm. In turn, S8 exhibits a negative band at 243 nm and a positive band at 265 nm (Figure 13 C), that are characteristic of parallel G-quadruplex structures adopted by telomeric sequences in molecular crowding conditions (Heddi and Phan 2011). These data would suggest the coexistence of parallel and other types of G-quadruplex conformations for S4 and S8, with a clear prevalence of the parallel conformation in the case of S8 (Virgilio et al. 2012). Overall, the CD profiles of the three labeled ODN in the conditions tested appear very similar to those obtained in KCl 70 mM solution alone, thus indicating that the changes of buffer composition, due to addition of Tris and MgCl₂, and KCl, do not affect the G-quadruplex folding topology adopted following the annealing procedure. Schematic representations of the hybrid 3+1

conformation, adopted by Nat, and that of the parallel G-quadruplex are reported in [Figure 14](#).

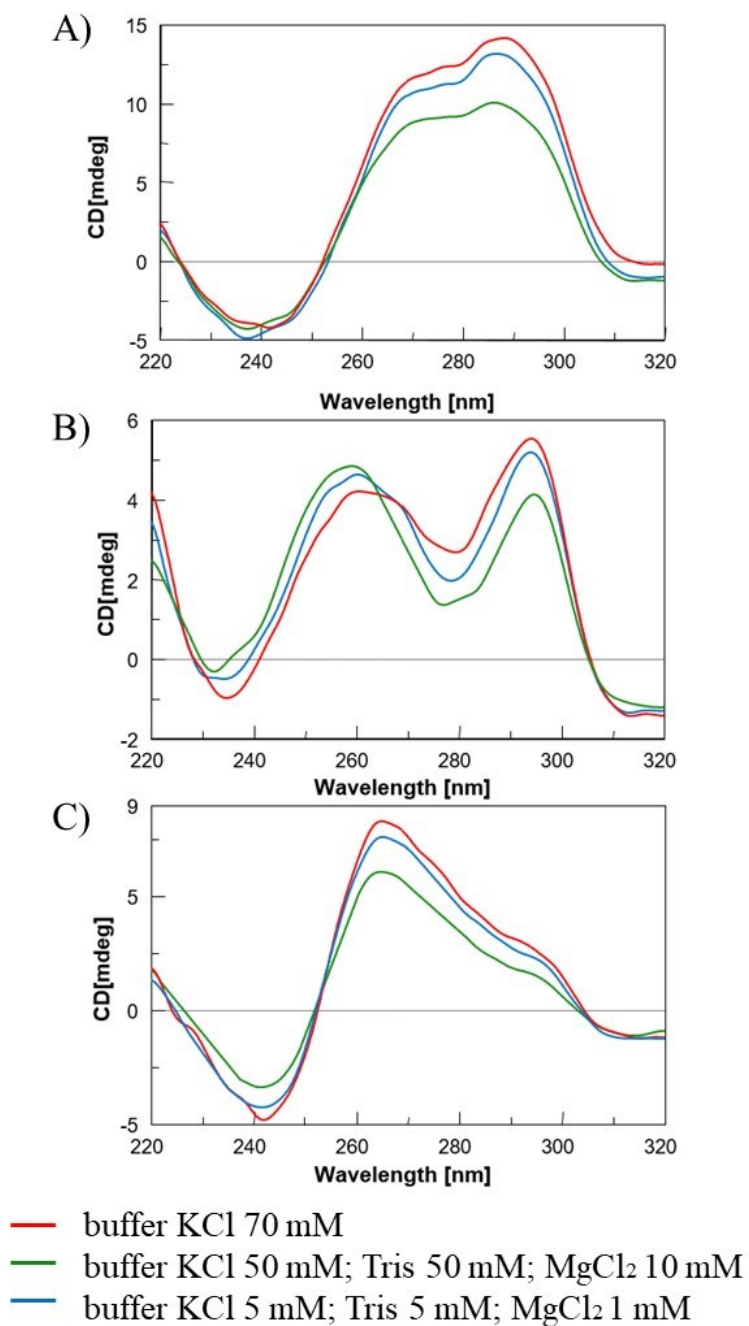


Figure 13 CD spectroscopy of the oligonucleotides used in this study

Overlay of CD spectra of telomeric oligonucleotides Nat (A), S4 (B) and S8 (C) acquired at indicated buffer conditions.

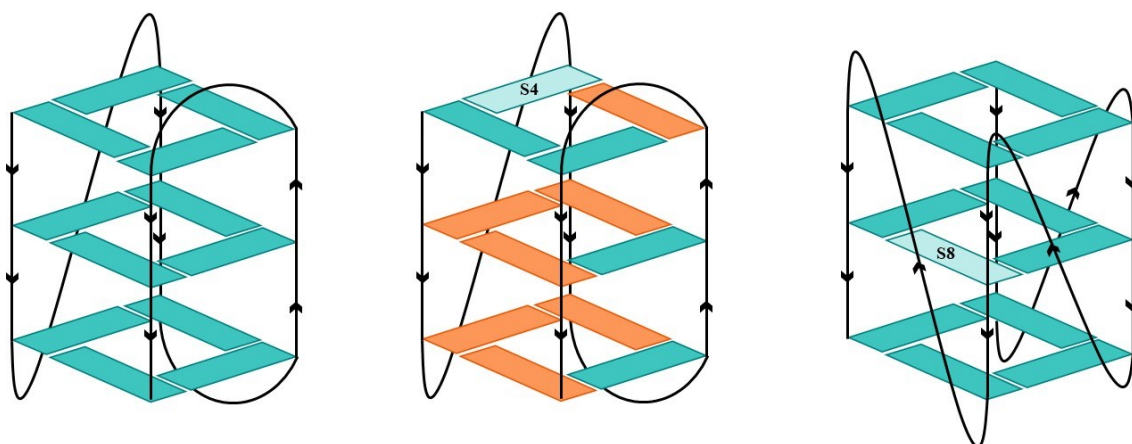


Figure 14 Schematic representations of G-quadruplex structures assumed by the oligonucleotides used in this work

Hybrid G-quadruplex (left, Nat, and center) formed by the original sequence and the parallel G4 (right) adopted in molecular crowding conditions. Guanosines adopting anti and syn glycosidic conformations are indicated in blue and orange, respectively. S4 and S8 indicate the positions in which abasic sites have been introduced. For clarity, the loop residues have been omitted.

CD-melting experiments were also carried out to investigate the thermal stability of the G-quadruplex structures adopted by the labeled ODN at the lowest salt concentration, namely the least favorable conditions for the G-quadruplex stability. The CD-melting profiles (Figure 15) showed that all the G-quadruplex structures start to melt at around 45-50°C and thus the three ODN were completely folded at 37°C. These data clearly indicate the presence of suitable amount of G-quadruplex structures in all the conditions used for the following assays.

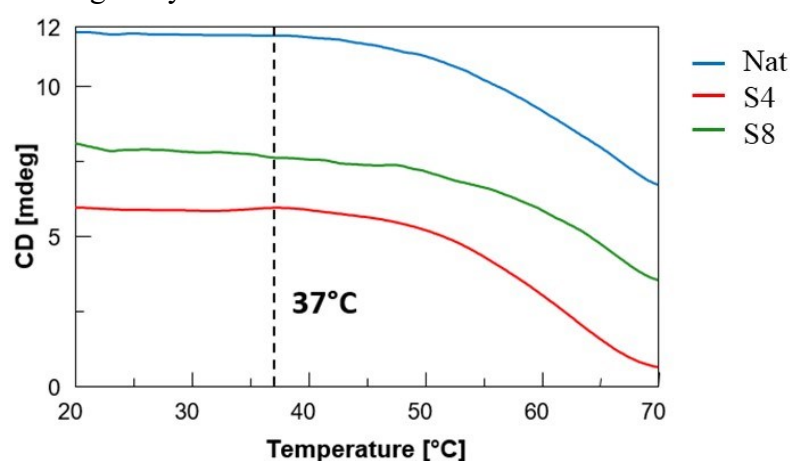


Figure 15 Circular dichroism (CD) analysis for the G4 oligonucleotides used in this study

CD melting profiles of each telomeric oligonucleotide acquired at the maximum CD λ values for each sample in a buffer containing KCl 5 mM, Tris 5 mM and MgCl₂ 1 mM.

6.2. The 33-residue Ape1 N-terminus is required to stably bind telomeric G4 structures

The 33 N-terminal residues of Ape1 play a role in the recognition of single stranded nucleic acids (Poletto et al. 2013). Therefore, we analyzed the functional role of this domain of Ape1 for interaction with telomeric sequences. The recombinant proteins used here (unmodified Ape1 or Ape1^{WT}, and a derivative lacking the first 33 N-terminal residues called Ape1^{NΔ33}) were expressed and purified in *E. coli* as previously described (Fantini et al. 2010) and verified by SDS-PAGE analysis (Figure 16).

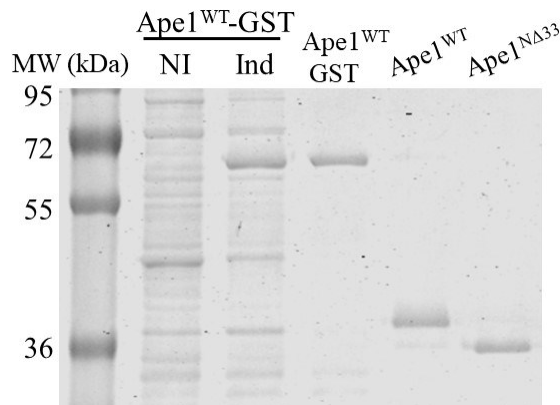


Figure 16 **Gel analysis of purified human recombinant proteins used in this study**

Proteins were separated onto 10% SDS-PAGE followed by Coomassie brilliant blue staining. 5 μ g loaded of each bacterial lysate (“NI” means not IPTG-induced bacteria and “Ind” means IPTG-Induced bacteria); 0.5 μ g Loaded of each purified protein. The molecular weight (MW) is expressed in kilodaltons (kDa).

The binding ability of purified recombinant Ape1 proteins to the ODN was tested through electrophoretic mobility shift assay (EMSA) analyses (Figure 17). These assays were performed by incubating the proteins with the telomeric substrates (i.e. Nat, S4 and S8) and the unstructured Poly dT-F, a poly dT oligonucleotide containing an abasic site, as a control. The analysis of native gels (Figure 17, left) revealed that Ape1^{WT} bound the telomeric sequences whereas this ability was lost when the N-terminal domain was missing. Specifically, three different shifted bands (indicated by asterisks in the figure) are clearly visible that correspond to protein-DNA complex formation between Ape1^{WT} and the telomeric sequences (lanes 2, 4, 6). Lower bands, with weaker intensities, may have increased mobility due to conformational differences (Kladova et al. 2018). As

expected, there was no indication of complex formation between Ape1 and the unstructured Poly dT-F (lane 8), confirming the importance of ODN secondary structure for stable binding (Poletto et al. 2013). Furthermore, the band pattern among the three ODN demonstrated that Ape1^{WT} is proficient in binding the G-quadruplex sequences with no significant differences among the G4 substrates used. In addition, EMSA experiments with the Ape1^{NΔ33} (Figure 17, right) highlight the requirement of the 33 N-terminal domain residues for binding to each G4 substrate (lanes 3-5-7). Again, no detectable complex was observed for the unstructured Poly dT-F (lane 9) incubated with Ape1^{NΔ33}.

Notably, UV-crosslink experiments (Figure 18) showed that the more stable complex between Ape1 and the substrate has relative mobility corresponding to ~44 kDa in the case of the Ape1^{WT} protein, and of about 42 kDa in the case of the Ape1^{NΔ33} deletion mutant, consistent with a 1:1 stoichiometry in the complex. Moreover, the presence of a UV-crosslinked complex between Ape1^{NΔ33} and the ODN (Figure 18) suggests that the

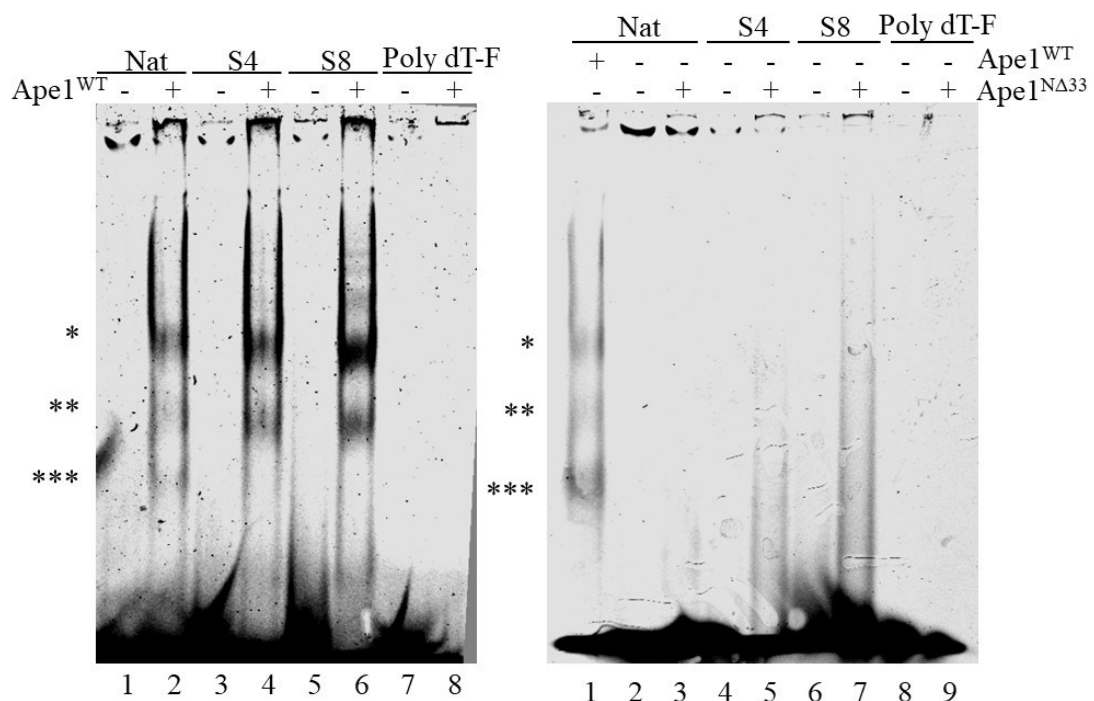


Figure 17 Ape1 stably binds the G4 oligonucleotides

Representative native EMSA polyacrylamide gel of recombinant Ape1^{WT} (left) and Ape1^{NΔ33} (right). Binding on the indicated ODN substrates (25 nM) is shown. Poly dT-F was used as negative control whereas Nat was used as positive control. The difference between this signal and the corresponding sample in the left panel relies only the intensity. *, ** and *** indicate the signals derived from metastable complexes that display different migration. Reactions were performed as explained in Materials and methods section.

absence of the 33 N-terminal domain does not hamper the ability of the protein to interact with the DNA substrate, at least transiently.

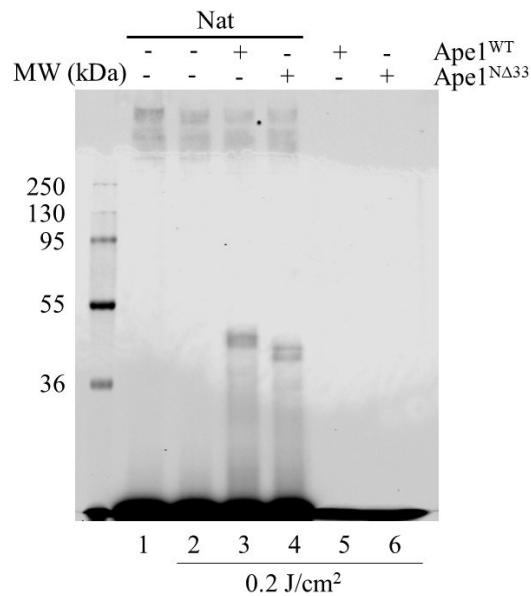


Figure 18 Cross-linking analysis performed with Nat oligonucleotide

The substrate was challenged with Ape1^{WT} (lane 3) or Ape1^{NΔ33} (lane 4) as described in Materials and methods section. Reactions were resolved onto SDS-PAGE 10%. Lane 1 and 2: non-crosslinked or crosslinked Nat ODN respectively. Lane 5 and 6: Ape1^{WT} and Ape1^{NΔ33} respectively crosslinked without Nat.

Altogether, these results demonstrated that: i) the molar ratio between the protein and the substrate is close to 1:1 as detected by the calculated molecular weight of the Protein-DNA complexes through UV-crosslink experiments; ii) the different mobility of the complexes and the weak signals of the retarded complexes, as seen from EMSA experiments, is possibly due to metastable complexes formation during the electrophoretic run (Kladova et al. 2018) and iii) the absence of the 33 N-terminal domain may probably affect the binding equilibrium of Ape1 with the substrate, possibly accelerating the dissociation step.

In order to quantitatively evaluate the affinity of both Ape1^{WT} and $\text{Ape1}^{\text{N}\Delta 33}$ for the telomeric Nat sequence, we used surface plasmon resonance (SPR) analyses. The overlays of the binding profiles are shown in [Figure 19](#) (and in [Figure 20](#)). Both proteins exhibited concentration-dependent binding: whereas Ape1^{WT} exhibited a low nanomolar value for its dissociation constant with the Nat sequence ([Figure 19](#), left), the binding of $\text{Ape1}^{\text{N}\Delta 33}$ to the Nat sequence ([Figure 19](#), right), exhibited a 9-fold reduced affinity (K_D) compared to Ape1^{WT} ([Table 2](#)).

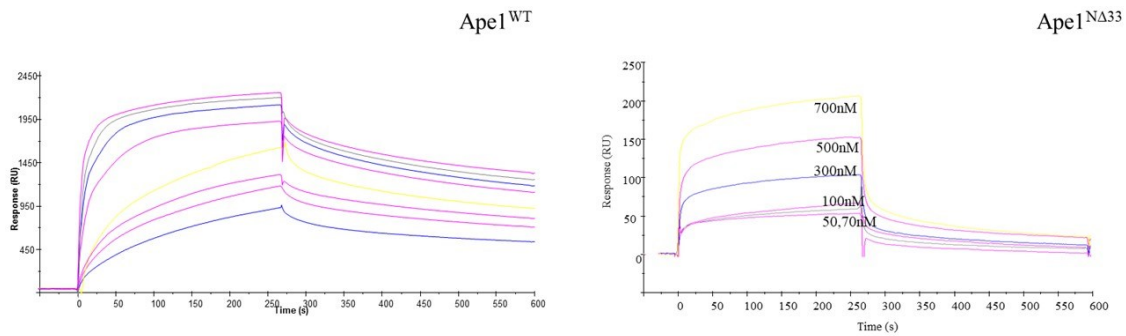


Figure 19 SPR sensorgrams for Ape1^{WT} and $\text{Ape1}^{\text{N}\Delta 33}$ with Nat oligonucleotide

Overlay of sensorgrams relative to SPR experiments for the binding to immobilized Biot- Nat of Ape1^{WT} (left) and $\text{Ape1}^{\text{N}\Delta 33}$ (right), respectively.

Protein	ODN	k_{on} ($\text{M}^{-1} \text{s}^{-1} \times 10^4$)	k_{off} ($\text{s}^{-1} \times 10^{-3}$)	K_D (nM)
Ape1^{WT}	Nat	8.23	2.6	31.6
	Poly dT	2.82	4.79	170
NPM1	Nat	2.04	2.99	147
	Poly dT	0.696	1.78	255
$\text{Ape1}^{\text{N}\Delta 33}$	Nat	3.04	8.67	285
	Poly dT	Not valuable		

Table 1 SPR based equilibrium dissociation constants (K_D) and kinetic parameters for the interaction of Ape1^{WT} and $\text{Ape1}^{\text{N}\Delta 33}$ and NPM1 with Nat and Poly dT ODN using the BIAevaluation v.4.1 software. Data reported were obtained through SPR analyses using proteins as analyte on the indicated biotinylated ODN ligands.

This was further corroborated by the SPR analysis of Poly dT/Ape1^{NΔ33} interaction, that, in the range of concentrations tested, does not allow the evaluation of the K_D value (Figure 20); while Ape1^{WT} shows an affinity toward this unstructured ligand five-fold reduced with respect to the G-quadruplex sequence (Table 2). The absence of a visible signal arising from the interaction between Ape1^{NΔ33} and Nat substrate in EMSA assay, despite a five-fold difference in K_D with respect to Ape1^{WT}, may be due to the shifting of the equilibrium during the electrophoretic run toward the dissociated form of the complex. These data further confirm the crucial role exerted by the N-terminal region of Ape1 in the recognition of the G4 ODN, reflected in both dissociation and association phases shown by Ape1^{NΔ33} with respect to full-length (Table 2).

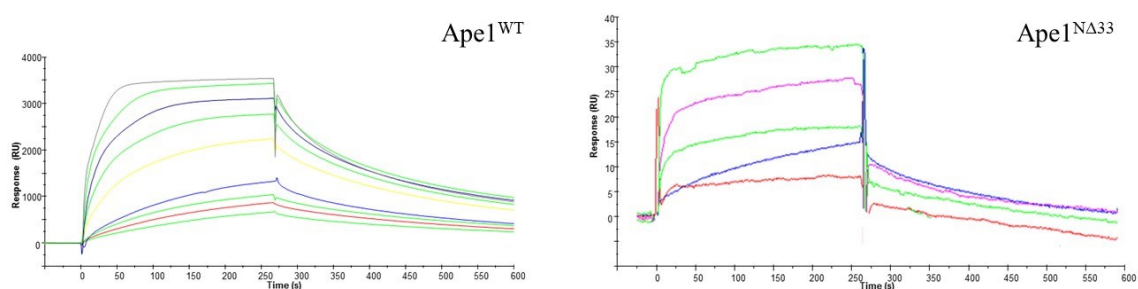


Figure 20 SPR sensorgrams for Ape1^{WT} and Ape1^{NΔ33} with Poly dT oligonucleotide

Overlay of sensorgrams relative to SPR experiments for the binding to immobilized Biot- Poly dT of Ape1^{WT} (left) and Ape1^{NΔ33} (right), respectively.

6.3. The enzymatic activity of Ape1 on G4 telomeric structures is influenced by ionic strength and the N-terminus

In order to test the endonuclease activity of Ape1 on telomeric substrates, we performed AP-site incision assays under different salt concentrations including, as substrate, a conventional dsDNA oligonucleotide containing an abasic site in the middle, named ds-F (Sanderson et al. 1989).

Cleavage assays were performed by incubating the indicated amounts of Ape1^{WT} with a fixed amount of each G4 substrate in a high ionic strength solution (50 mM KCl). As Figure 21 shows, Ape1^{WT} exhibited different endonuclease activities on the three substrates: it did not significantly cleave the S4 ODN, generating a maximum of only about 4% of product. In contrast, Ape1 cleaved about one third of the S8 ODN substrate at the highest protein concentration (Figure 21).

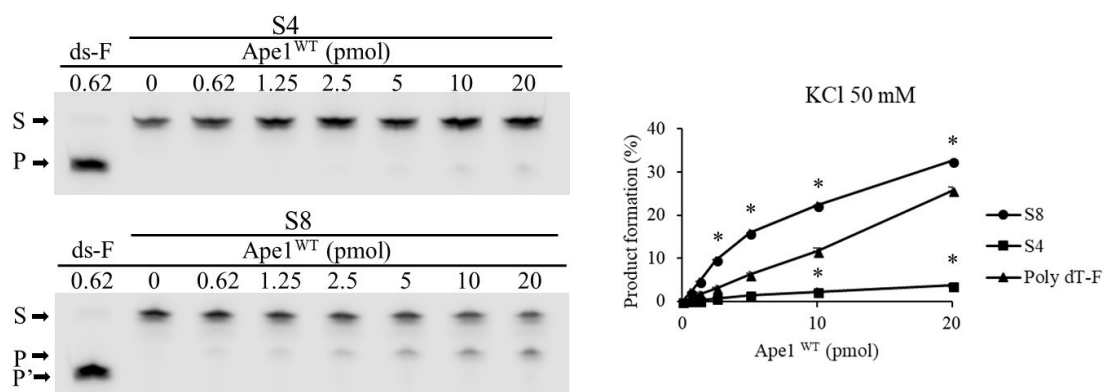


Figure 21 *The position of the abasic site on the G4 influences Ape1^{WT} endonuclease activity*

Representative denaturing polyacrylamide gels of AP site incision by Ape1^{WT} on S4 and S8 incubated with the indicated amount of protein in a solution containing 50 mM KCl as described in Materials and methods section (left). Graph describes the percentage of conversion of substrate (S) into product (P) as a function of the dose of Ape1 protein on the specified substrate (right). ds-F ODN was used as positive control. S denotes the substrate position; the length of the generated products is 1 nt different between S8 (P) and ds-F (P'). Average values are plotted with standard deviations of three loadings of the same experiment as a function of protein dosage. Standard deviation values were always less than 10% of the mean of experimental points. Asterisks indicate a statistically significant difference between the indicated substrate and Poly dT-F oligonucleotide processing.

As expected, the Poly dT-F was cut less efficiently than S8, as it does not adopt secondary structures, and the Nat sequence was not processed (Figure 22). Moreover, as expected, the ds-F ODN was the best substrate, with a 1000-fold higher rate of cleavage by Ape1 than found for the G4 structures (Figure 22).

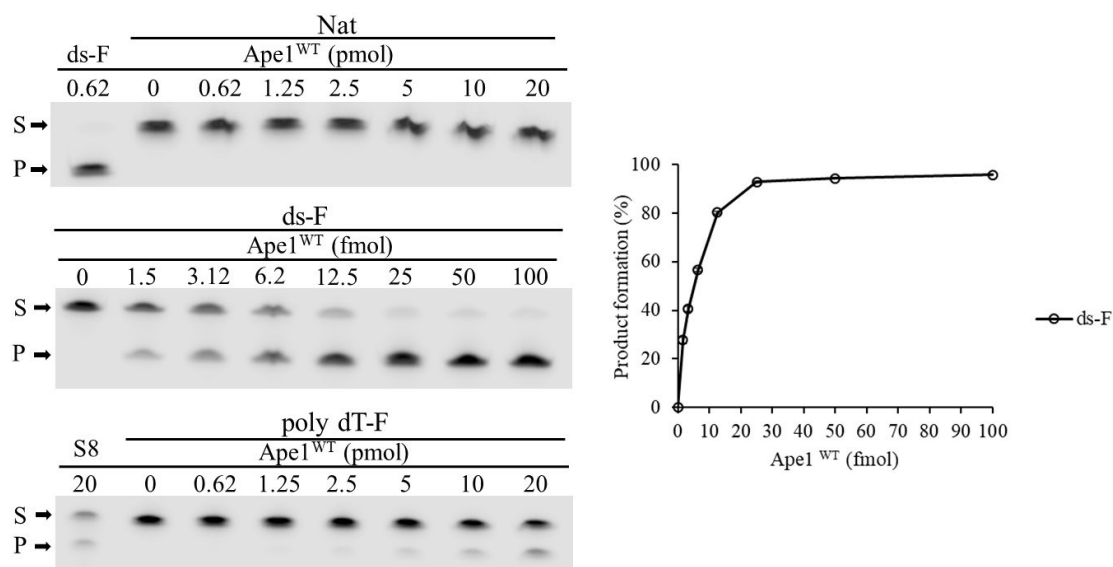


Figure 22 *Ape1^{WT}* endonuclease activity on control substrates

Representative denaturing polyacrylamide gels of AP site incision by *Ape1^{WT}* on the indicated oligonucleotides incubated with the specified amount of protein in a solution containing 50 mM KCl as described in Materials and methods section (left). Graph describes the percentage of conversion of substrate (S) into product (P) as a function of the dose of protein on the specified substrate (right). *ds-F* or *S8* oligonucleotides were used as positive controls. S denotes the substrate position, P denotes the product position. Average values are plotted with standard deviations of three loadings of the same experiment. Standard deviation values were always less than 10% of the mean of experimental points.

Prompted by the importance of the *Ape1* N-terminal domain in binding G4 structures (Figures 13 and 17), we analyzed the endonuclease activity of the *Ape1^{NΔ33}* on the same telomeric substrates (Figure 23). At high ionic strength (i.e. 50 mM KCl), *Ape1^{NΔ33}* cleaved the G-quadruplex structures much less efficiently than *Ape1^{WT}* protein. Cleavage of the *S8* substrate reached a maximum of nearly 15%, while both the *S4* and Poly dT-F ODN gave maxima of only about 1% product (Figure 23).

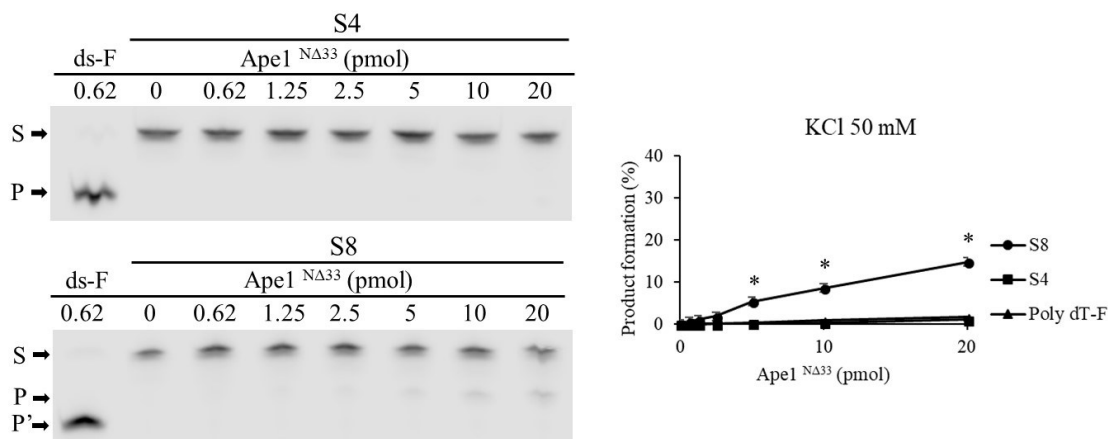


Figure 23 *The position of the abasic site on the G4 influences Ape1^{NΔ33} endonuclease activity*

Representative denaturing polyacrylamide gels of AP site incision by Ape1^{NΔ33} on S4 and S8 incubated with the indicated amount of protein in a solution containing 50 mM KCl as described in Materials and methods section (left). Graph describes the percentage of conversion of substrate (S) into product (P) as a function of the dose of Ape1 protein on the specified substrate (right). ds-F ODN was used as positive control. S denotes the substrate position; the length of the generated products is 1 nt different between S8 (P) and ds-F (P'). Average values are plotted with standard deviations of three loadings of the same experiment as a function of protein dosage. Standard deviation values were always less than 10% of the mean of experimental points. Asterisks indicate a statistically significant difference between the indicated substrate and Poly dT-F oligonucleotide processing.

The activity of Ape1^{NΔ33} on ds-F, was weaker than that of the full-length protein but, at the highest concentration, Ape1^{NΔ33} was able to process nearly all the substrate, with no activity on the Nat or the Poly dT-F ODN (Figure 24).

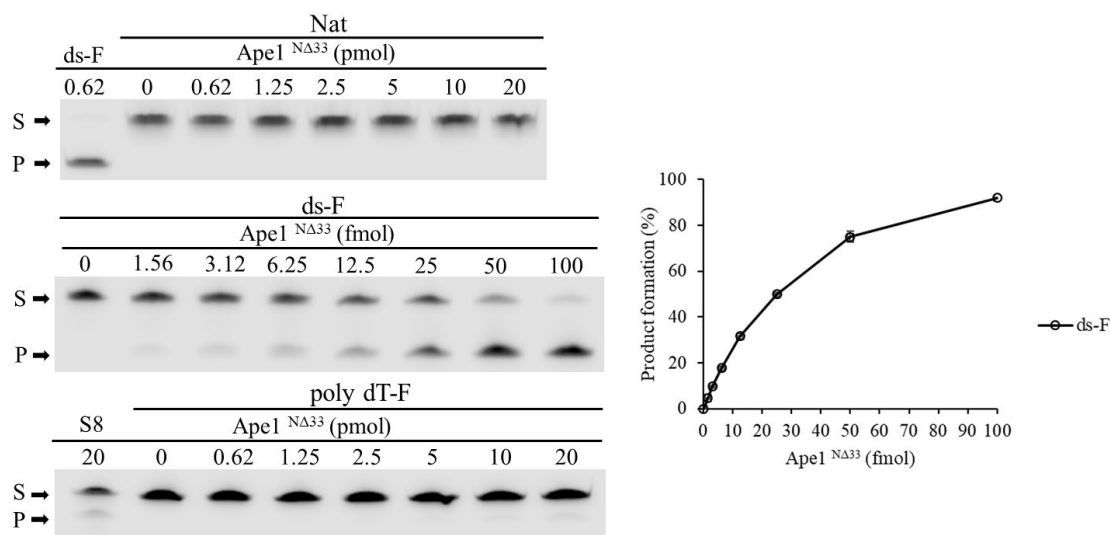


Figure 24 *ApeI*^{NΔ33} endonuclease activity on control substrates

Representative denaturing polyacrylamide gels of AP site incision by *ApeI*^{NΔ33} on the indicated oligonucleotides incubated with the specified amount of protein in a solution containing 50 mM KCl as described in Materials and methods section (left). Graph describes the percentage of conversion of substrate (S) into product (P) as a function of the dose of protein on the specified substrate (right). ds-F or S8 oligonucleotides were used as positive controls. S denotes the substrate position and P denotes the product position. Average values are plotted with standard deviations of three loadings of the same experiment. Standard deviation values were always less than 10% of the mean of experimental points.

At low ionic strength, the *ApeI* N-terminus affects the catalytic activity of the protein, via the product-release step of the reaction (Fantini et al. 2010). We therefore tested the effects of reduced salt concentration on *ApeI*-cleavage activity, by performing enzymatic experiments in 5 mM KCl (vs. 50 mM in the previous experiments). Under these conditions, *ApeI*^{WT} displayed increased endonuclease activity on G4 structures (Figure 25), then seen at higher KCl (Figure 21).

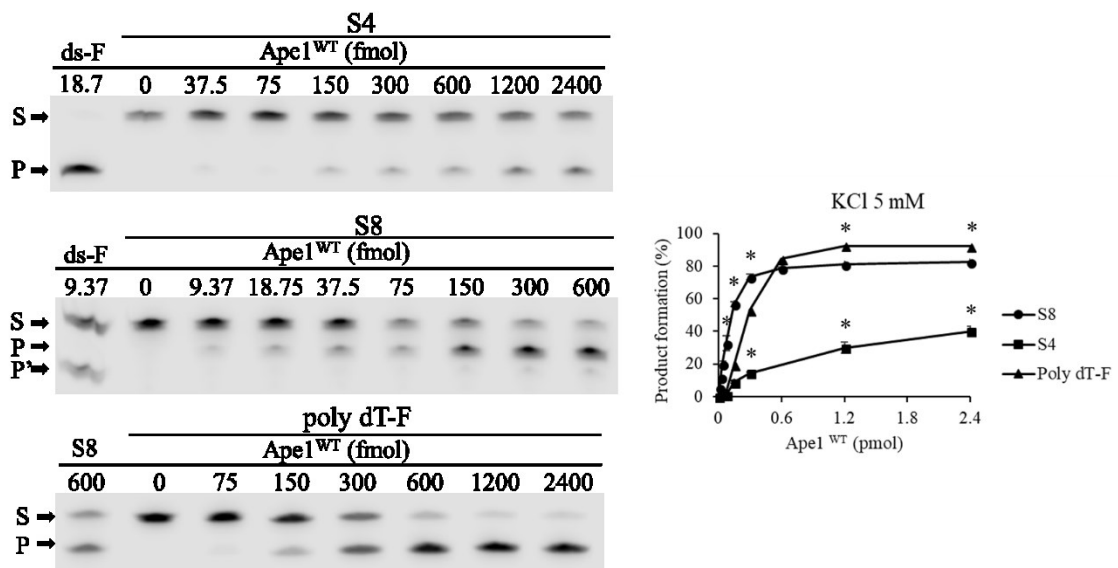


Figure 25 *Ape1^{WT} cleaves AP sites in G4 substrates more efficiently at lower ionic strength*

Representative denaturing polyacrylamide gels of AP site incision by *Ape1^{WT}* on the indicated substrates with the indicated amount of protein in a solution containing 5 mM KCl as described in Materials and methods section; ds-F or S8 were used as positive control (left). Graph depicting AP site incision activity of *Ape1^{WT}* on the specified substrate in a solution containing 5 mM KCl. Graph describes the percentage of conversion of substrate (S) into product (P) as a function of the dose of protein on the specified substrate. Average values are plotted with standard deviations of three loadings of the same experiment as a function of protein dosage. Standard deviation values were always less than 10% of the mean of experimental points. Asterisks indicate a statistically significant difference between the indicated substrate and Poly dT-F oligonucleotide processing.

In detail, the S4 resulted to be better processed under low ionic strength conditions (Figure 25) by *Ape1^{WT}*, with an increase of about ten-fold with respect to high salt concentration (50 mM KCl). Similarly, the S8 appeared more efficiently processed at low ionic strength

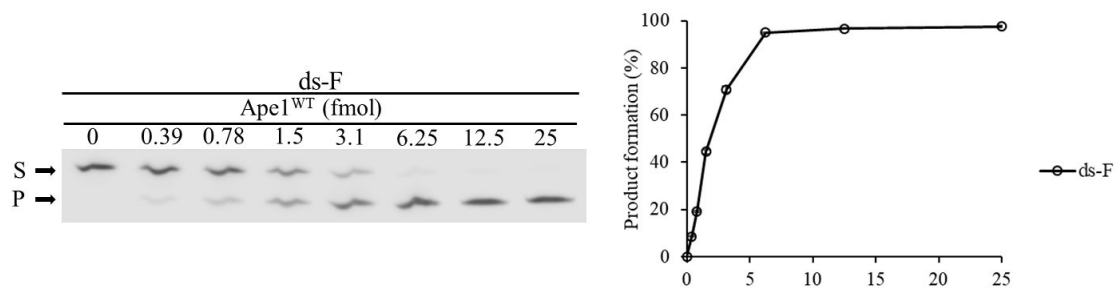


Figure 26 *Ape1^{WT} cleaves AP sites in ds substrates more efficiently at lower ionic strength*

Representative denaturing polyacrylamide gel of AP site incision by *Ape1^{WT}* on ds-F substrate (left). The substrate was incubated with the indicated amount of *Ape1* in a solution containing 5 mM KCl as described in Materials and methods section. S denotes the substrate position and P denotes the product position. Graph describes the percentage of conversion of substrate (S) into product (P) as a function of the dose of protein on ds-F (right). Average values are plotted with standard deviations of three loadings of the same experiment. Standard deviation values were always less than 10% of the mean of experimental points.

with a more than two-fold increase in product formation. Notably, also the Poly dT-F was processed under these conditions, with an efficiency similar to that displayed on the S8 (Figure 25). As expected for ds-F, the efficiency was significantly higher (about 100-fold), compared to the two G4 structures (Figure 26), and 4-fold higher with respect to the activity measured at 50 mM KCl. Therefore, the ApeI enzymatic activity was significantly affected by the KCl concentration and it was modulated by an electrostatic effect possibly involving the contribution of the basic amino acids of the N-terminal arm (Fantini et al. 2010; Poletto et al. 2013).

Then, also the activity of ApeI^{NΔ33} was tested under low ionic strength conditions. Both S4 and S8 substrates were processed more actively than the previous condition (Figure 27).

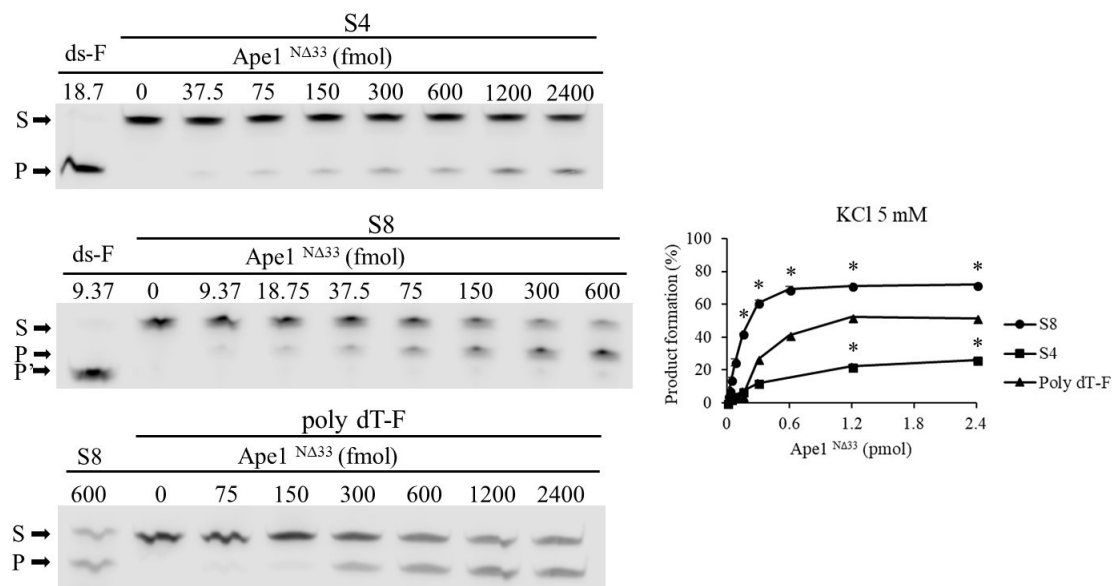


Figure 27 *ApeI^{NΔ33} cleaves AP sites in G4 substrates more efficiently at lower ionic strength*

Representative denaturing polyacrylamide gels of AP site incision by ApeI^{NΔ33} on the indicated substrates with the indicated amount of protein in a solution containing 5 mM KCl as described in Materials and methods section; ds-F or S8 were used as positive control (left). Graph depicting AP site incision activity of ApeI^{NΔ33} on the specified substrate in a solution containing 5 mM KCl. Graphs describe the percentage of conversion of substrate (S) into product (P) as a function of the dose of protein on the specified substrate. Average values are plotted with standard deviations of three loadings of the same experiment as a function of protein dosage. Standard deviation values were always less than 10% of the mean of experimental points. Asterisks indicate a statistically significant difference between the indicated substrate and Poly dT-F oligonucleotide processing.

Moreover, the activity of $Ape1^{N\Delta33}$ on ds-F was even higher than the one displayed by $Ape1^{WT}$ protein (Figures 28), since the maximum product formation is reached at 1.5 fmol of $Ape1^{N\Delta33}$. These data are in agreement with previous results and are due to an increase of the k_{off} in the catalytic reaction (Fantini et al. 2010).

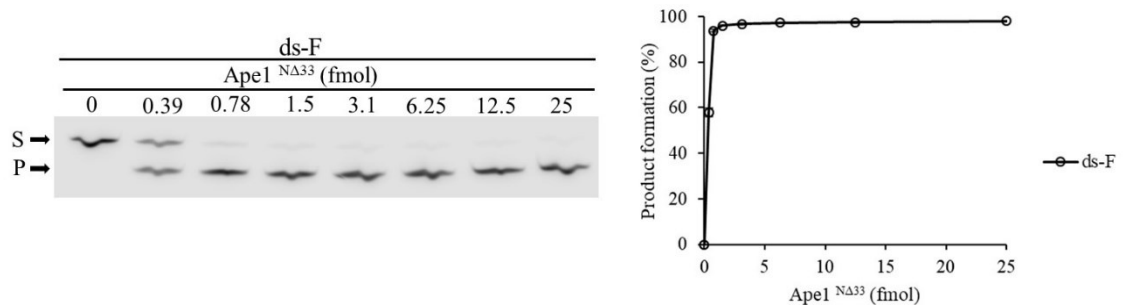


Figure 28 $Ape1^{N\Delta33}$ cleaves AP sites in ds substrates more efficiently at lower ionic strength

Representative denaturing polyacrylamide gel of AP site incision by $Ape1^{N\Delta33}$ on ds-F substrate (left). The substrate was incubated with the indicated amount of $Ape1$ in a solution containing 5 mM KCl as described in Materials and methods section. S denotes the substrate position and P denotes the product position. Graph describes the percentage of conversion of substrate (S) into product (P) as a function of the dose of $Ape1^{N\Delta33}$ on ds-F (right). Average values are plotted with standard deviations of three loadings of the same experiment. Standard deviation values were always less than 10% of the mean of experimental points.

In order to evaluate the dependence of the $Ape1$ activity on ionic strength, we analyzed the variation of enzyme products formation by $Ape1^{WT}$ and $Ape1^{N\Delta33}$ on the S8 substrate, as a function of KCl concentrations (Figure 29). Data obtained clearly indicated a linear dependence of the $Ape1$ endonuclease activity on KCl concentrations even though to a different extent for the two proteins since the trend line of $Ape1^{N\Delta33}$ showed a greater steepness ($m = -1.574$) with respect to that of $Ape1^{WT}$ ($m = -1.136$).

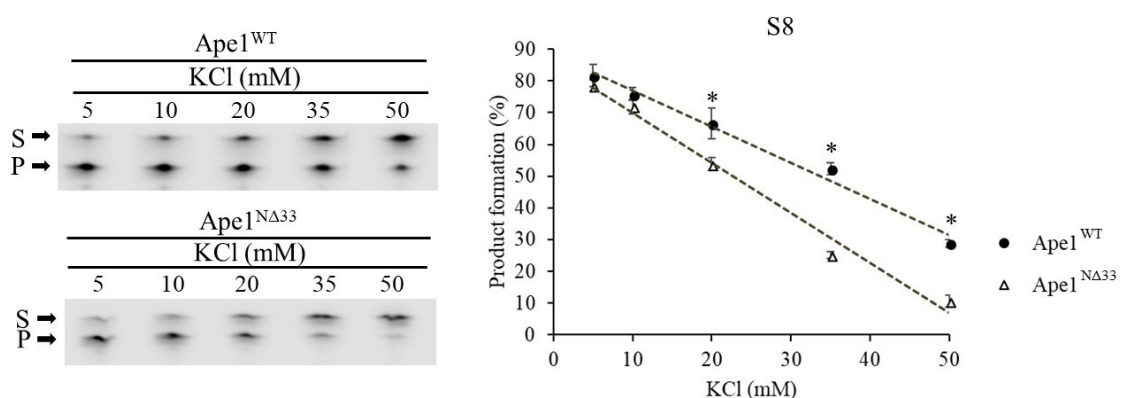


Figure 29 Ionic strength influences Ape1 endonuclease activity

Representative denaturing polyacrylamide gels of AP site incision by Ape1^{WT} or Ape1^{NΔ33} on S8 substrate. The substrate was incubated with the indicated amount of Ape1 in a solution containing the indicated concentrations of KCl. S denotes the substrate position and P denotes the product position (left). AP site incision activity on S8 ODN decreases in raising ionic strength. Graph depicting endonuclease activity experiments performed with Ape1^{WT} or Ape1^{NΔ33} as described in Materials and methods section. Average values are plotted with standard deviations of three loadings of the same experiment as a function of KCl concentration used (right). Standard deviation values were always less than 10% of the mean of experimental points. Asterisks indicate a statistically significant difference between the endonuclease activity displayed by Ape1^{WT} with respect to Ape1^{NΔ33}.

In Figure 30, the quantifications of the amount of products obtained under the different salt concentration conditions, as above, are summarized showing that the dependence of the enzymatic activities of Ape1^{WT} and Ape1^{NΔ33} proteins on salt concentrations appeared more pronounced for S4 and the S8 ODN with respect to the ds-F substrate.

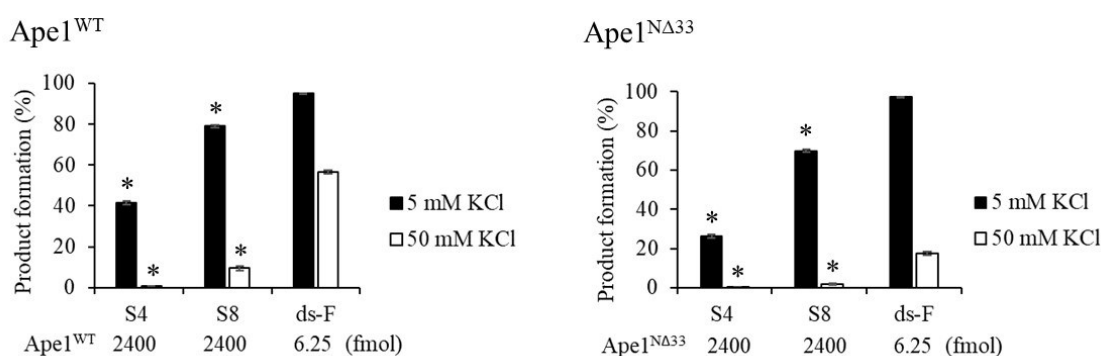


Figure 30 Summary of AP site incision activity of Ape1 protein on the different substrates

Histograms summarizing the different endonuclease activities of Ape1^{WT} (left) and Ape1^{NΔ33} (right) on the specified substrates at the indicated doses (fmol) of the enzyme in the stated KCl concentrations on the different substrates. Each bar was compared with the activity of the protein on ds-F in the corresponding saline condition.

Overall, these data demonstrated that the enzymatic activity of Ape1 on G4 telomeric structures strongly depends on the ionic strength and on the presence of the N-terminal unstructured domain. Therefore, these findings suggest that the charged residues present in the N-terminus of Ape1 may modulate its enzymatic activity on G4 structures.

6.4. Acetylatable lysine residues in the Ape1 N-terminus are required for binding and enzymatic activity on G4 telomeric structures

In order to investigate whether the positive charges (i.e. acetylatable lysine residues) in the Ape1 N-terminal domain might affect the processing of damaged telomeric substrates, we evaluated the endonuclease activity on the S4 and S8 substrates of Ape1^{K4pleA}, in which replacement of the lysine by alanine residues mimics acetylation by neutralizing the positive charges of the side chains (Fantini et al. 2010; Lirussi et al. 2012).

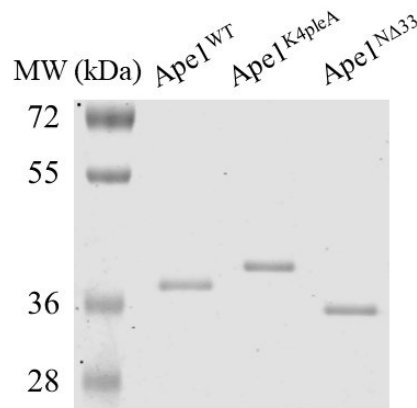


Figure 31 Purified recombinant Ape1 mutant proteins check

Gel analysis of human purified recombinant proteins used in this study. 0.5 μ g of each protein were loaded and separated onto 10% SDS-PAGE followed by Coomassie brilliant blue staining.

Purified Ape1^{K4pleA} (Figure 31) displayed an altered mobility with respect to Ape1^{WT}, which was likely due to the alteration of the overall charge, as we previously observed (Fantini et al. 2010). First, we evaluated the ability of Ape1^{K4pleA} to interact with the telomeric sequences. UV-crosslinking experiments (Figure 32) demonstrated that all the proteins form complexes with both S4 and S8, and that the complexes had the same relative mobility as the proteins.

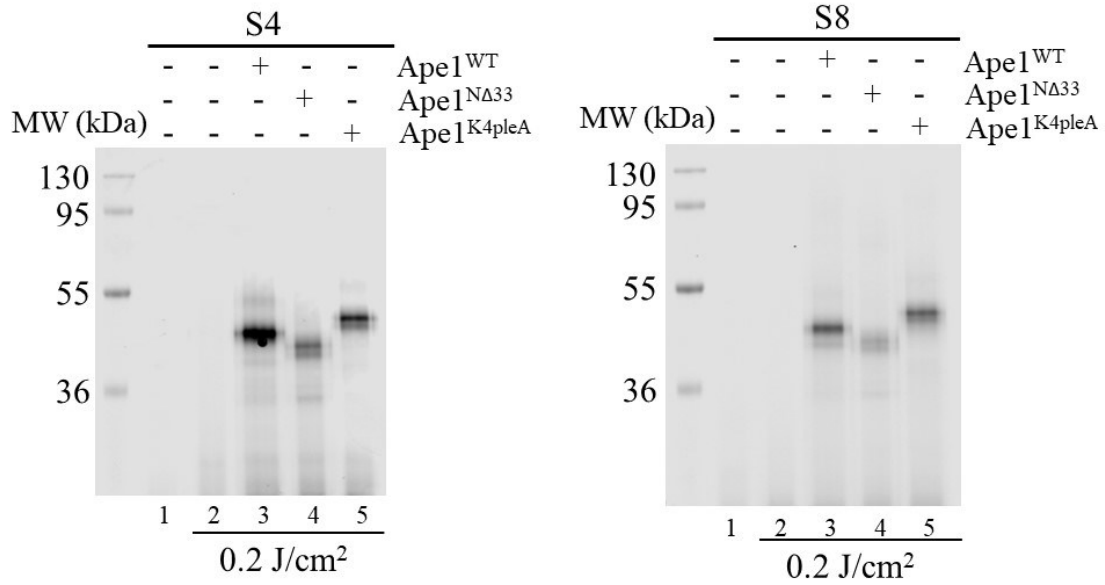


Figure 32 *ApeI* interacts with G4 oligonucleotides in a stoichiometric ratio

Interaction between recombinant wild type and mutant *ApeI* with S4 (left) and S8 (right) was evaluated through crosslinking analysis. The substrates were challenged with *ApeI*^{WT} (lane 3), *ApeI*^{NΔ33} (lane 4) or *ApeI*^{K4pleA} (lane 5) as described in Materials and methods section. Reactions were resolved onto SDS-PAGE 10%. Lane 1 and 2: non-crosslinked or crosslinked ODN respectively.

The enzymatic activities were assessed under different salt concentration conditions. At 50 mM KCl, none of the proteins had strong activity on S4 (<3% product formation). All the proteins had some activity on S8 at 50 mM KCl, with *ApeI*^{WT} having a 2- to 3-fold higher rate of cleavage than *ApeI*^{NΔ33} and *ApeI*^{K4pleA} (Figures 33 and 34). In contrast, the activity of *ApeI*^{K4pleA} on ds-F at 50 mM KCl resembled that of the *ApeI*^{WT}, while *ApeI*^{K4pleA} activity was somewhat lower (Figures 33 and 34).

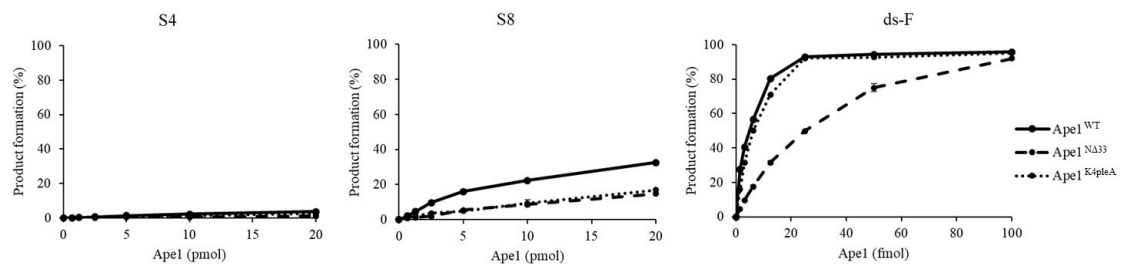


Figure 33 AP site incision activity graphs summarizing endonuclease activity of *ApeI* protein and its mutants on the different substrates in a solution containing 50 mM KCl.

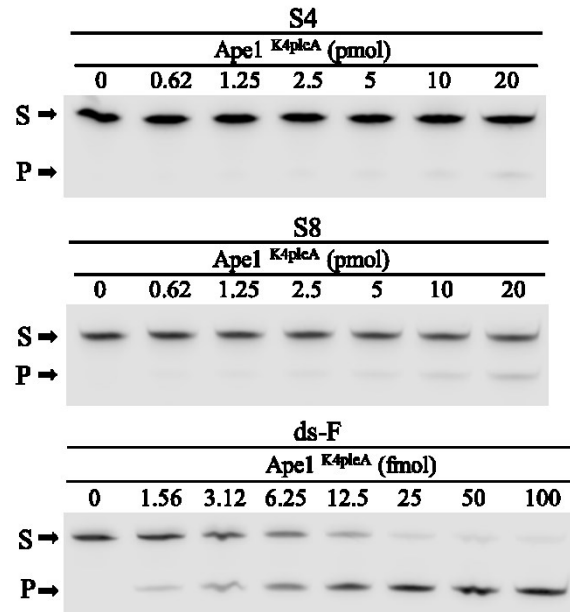


Figure 34 Endonuclease activity of *Ape1*^{K4pleA} on telomeric oligonucleotides and control substrate at high ionic strength

Representative denaturing polyacrylamide gels of AP site incision by *Ape1*^{K4pleA} on the indicated substrates with the specified amount of protein in a solution containing 50 mM KCl as described in Materials and methods section.

At 5 mM KCl, the lower salt concentration strongly increased the activity of all the proteins on both the S4 and the S8 substrates (Figure 35 and 36). On the S4 substrate, *Ape1*^{K4pleA} was more active (~44% product) than *Ape1*^{WT} (Figure 35 and 36). Notably, the activity of both modified *Ape1* proteins on ds-F was similar and higher than that of *Ape1*^{WT} (Figure 35 and 36).

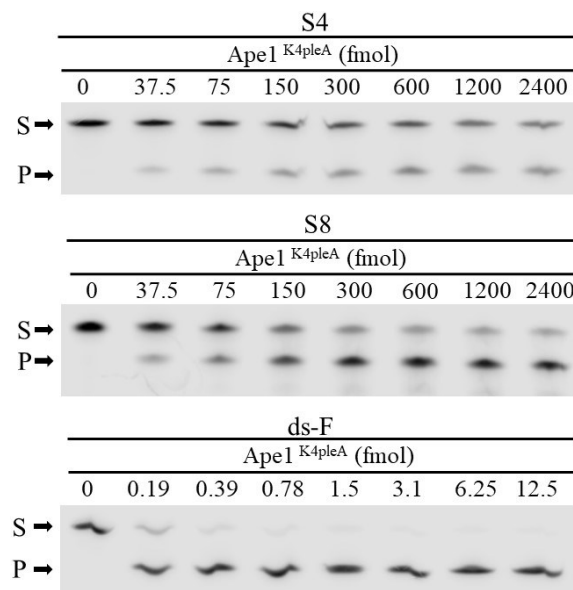


Figure 365 Endonuclease activity of *Ape1*^{K4pleA} on telomeric oligonucleotides and control substrate at low ionic strength

Representative denaturing polyacrylamide gels of AP site incision by *Ape1*^{K4pleA} on the indicated substrates with the indicated amount of protein in a solution containing 5 mM KCl as described in Materials and methods section.

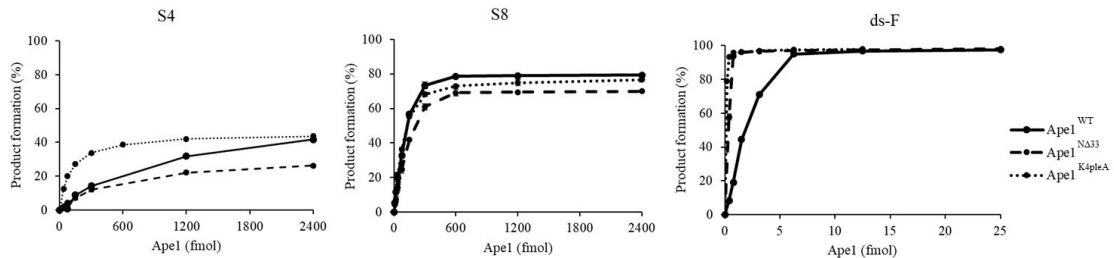


Figure 356 AP site incision activity graphs summarizing endonuclease activity of *Ape1* protein and its mutants on the different substrates in a solution containing 5 mM KCl

Overall, these data clearly demonstrate that lysine 27-35 of *Ape1* contribute strongly to the binding and cleavage activity of the enzyme for a DNA lesion in telomeric sequences; acetylation to neutralize these residues *in vivo* may modulate *Ape1* function at telomeres.

6.5. Activity of *Ape1* protein variants from U2OS cells

The *Ape1* enzymatic activity could be dynamically modulated by interacting proteins in cells (Vascotto et al. 2014; Moor et al. 2015). With the aim to evaluate the contribution of such partners on the enzymatic activity of *Ape1*, we carried out enzymatic assays employing *Ape1*-protein complexes isolated from human cell lines. In these assays, in addition to the K-to-A protein, we introduced the alternative K-to-R protein (a non-acetylatable form - *Ape1*^{K4pleR}) and the K-to-Q protein (mimicking a constitutive acetylated *Ape1* form retaining the side chain with the charge neutralized - *Ape1*^{K4pleQ}) substitutions (Lirussi et al. 2016). We measured the activity of the *Ape1* proteins on telomeric substrates using immunocaptured *Ape1*-protein complexes obtained from U2OS human cells (Figure 37 and 38). These complexes were affinity purified following transfection of vectors expressing the FLAG-tagged mutant proteins (Lirussi et al. 2016)

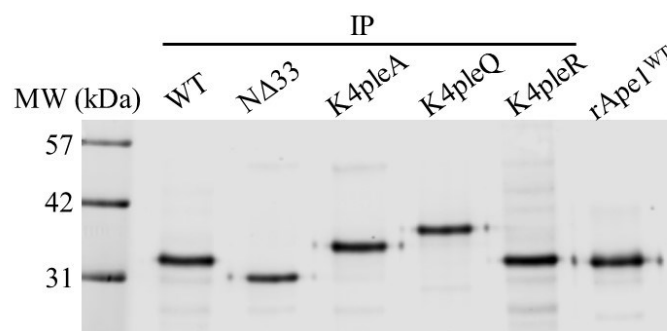


Figure 387 Immunocaptured *Ape1*^{WT} and mutant proteins check

Western blot analysis of *Ape1* IP samples used in this study. Co-IP proteins were separated onto 10% SDS-PAGE and immunoprobed with anti *Ape1* antibody. *rApe1* was included for comparison.

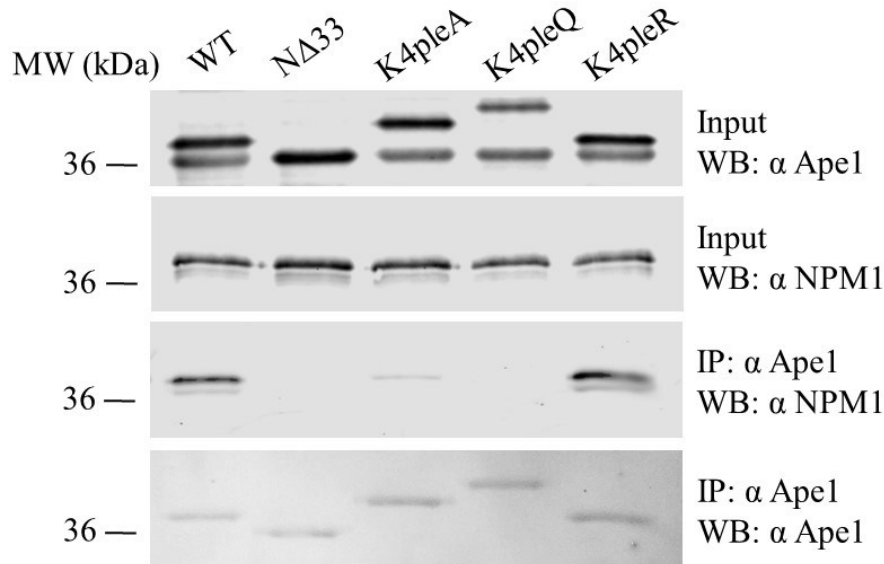


Figure 378 Analysis of the interaction between *Ape1* mutants and NPM1

Evaluation of *Ape1* IP from U2OS cells overexpressing *Ape1* mutants resolved on 10% SDS-PAGE analyzed through Western blot. Total cell extracts were immunoprobed with anti *Ape1* and anti NPM1 antibodies (First and second panel respectively); each lane of the first panel displays a lower band corresponding to the endogenous *Ape1* and an upper band corresponds to the exogenous flagged protein. Co-IP proteins were immunoprobed with anti NPM1 antibody (Third panel) and *Ape1* was detected through Ponceau red staining (Fourth panel).

and checked for the presence of *Ape1*'s partners such as nucleophosmin (NPM1) (Figure 38 and Antoniali et al. 2017).

The *Ape1*^{K4pleA} and *Ape1*^{K4pleQ} proteins obtained from U2OS cells had different electrophoretic mobility than *Ape1*^{WT} (Figure 37), consistent with the recombinant proteins obtained from *E. coli* (Figure 31). The separation of these IP samples on a urea-gel demonstrated that the altered migration obtained in SDS-PAGE gels was not due to a different apparent molecular weight of the mutants *Ape1*^{K4pleA} and *Ape1*^{K4pleQ}, but

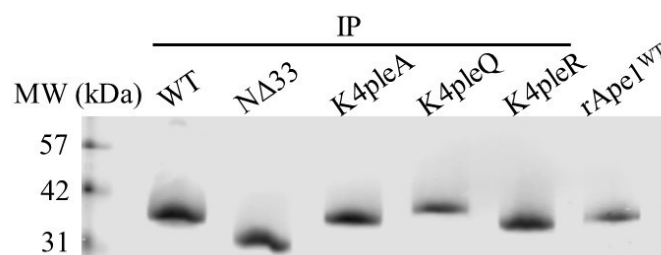


Figure 39 Analysis of gel mobility of Ape1 mutants from IP

Samples were separated on a 10% SDS-PAGE containing 7 M urea and immunoprobed with anti-Ape1 antibody. The altered electrophoretic mobility observed for the Ape1^{K4pleA} and Ape1^{K4pleQ} mutant is due to an alteration of the overall charge.

presumably to the change of the overall charge (Figure 39), as previously shown (Fantini et al. 2010).

We then conducted UV-crosslinking experiments with these different Ape1 variants and Ape1^{WT}, (Figure 40). The ability of each mutant protein to stably interact with the

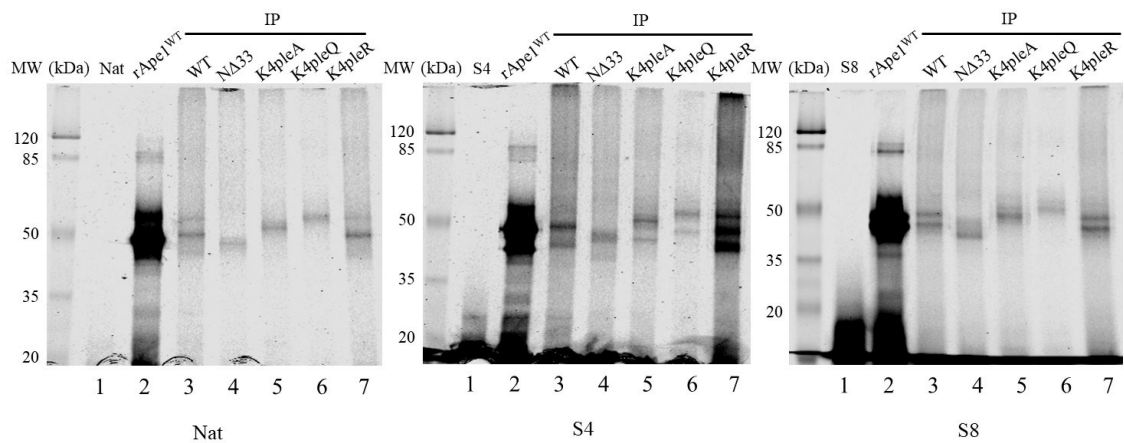


Figure 40 Eukaryotic mutants of Ape1 are able to bind the telomeric substrates

Crosslinking analysis of Immunoprecipitated (IP) samples were performed as described in Materials and methods section and run onto an SDS-PAGE 10%. Recombinant protein, rApe1^{WT} was used as control.

substrates was at least comparable to that of the immunocaptured Ape1^{WT}. Interestingly, the Ape1^{K4pleR} protein displayed an enhanced binding ability, relative to Ape1^{WT}, with all the substrates used in the UV-crosslinking assay (Figure 40, lanes 7).

We performed cleavage experiments, at low KCl concentration (5 mM), to compare with Ape1^{WT} the activity of the two acetylation-mimicking proteins (Ape1^{K4pleA} and Ape1^{K4pleQ}) and the protein that mimicks non-acetyltable Ape1 (Ape1^{K4pleR}).

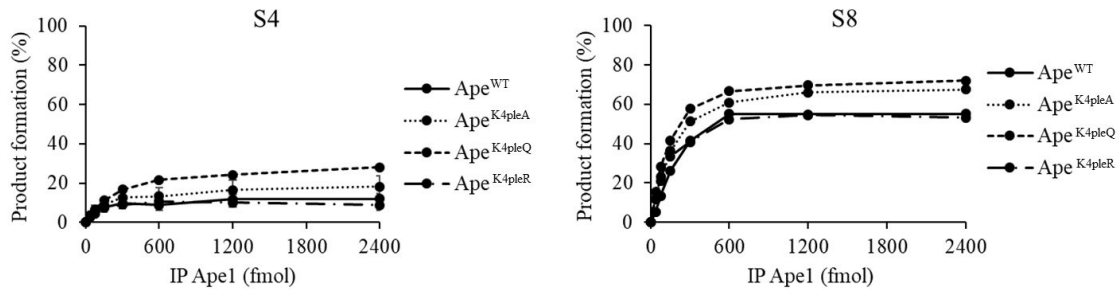


Figure 41 AP site incision activity graphs summarizing endonuclease activity of eukaryotic Ape1 protein and its mutants on the telomeric substrates

Graphs depicting AP site incision activity of IP for Ape1^{WT}, Ape1^{NΔ33}, Ape1^{K4pleA}, Ape1^{K4pleQ} and Ape1^{K4pleR} on the specified substrate in a solution containing 5 mM KCl. Graphs describe the percentage of conversion of substrate into product as a function of the dose of protein on the indicated substrate. Average values are plotted with standard deviations of three loadings of the same experiment as a function of protein dosage.

Endonuclease assays (Figure 41 and 42) demonstrated that, particularly with the S8 substrate, the acetylation-mimicking mutants displayed a higher endonuclease activity than did the Ape1^{WT} and Ape1^{K4pleR} proteins, suggesting that the loss of positive charges of several Lys residues confers on the enzyme an increased ability to release the product upon cleavage, as we previously hypothesized (Fantini et al. 2010).

The S4 substrate was significantly less processed by all the tested proteins, similarly to previous data obtained with recombinant proteins from *E. coli* with the activities of acetylation-mimicking proteins higher than those of the Ape1^{WT} and Ape1^{K4pleR} proteins. Similar experiments, performed at 50 mM KCl, indicated that the enzymatic activity of the tested proteins was significantly lower under those conditions, as found for the purified proteins (data not shown).

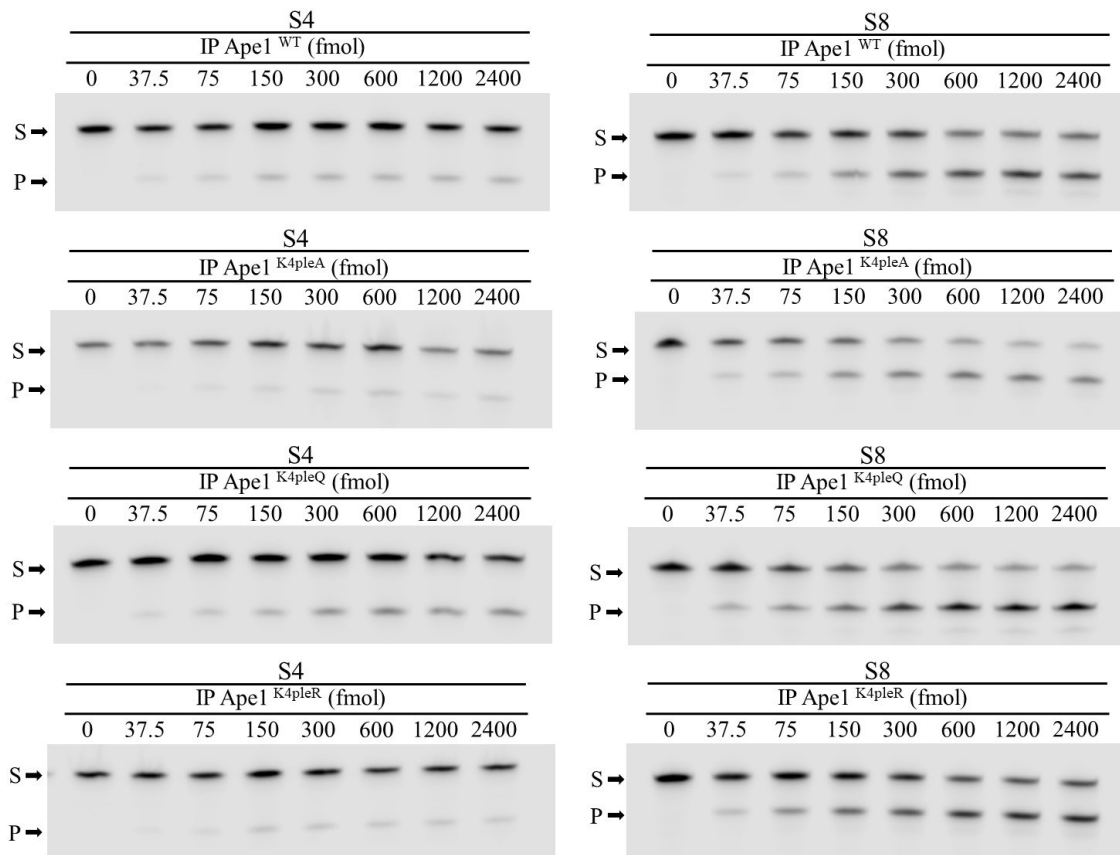


Figure 42 *Endonuclease activity of eukaryotic immunocaptured Ape1 protein and its mutants on telomeric oligonucleotides*

Representative denaturing polyacrylamide gels of AP site incision by co-IP samples of Ape1^{WT} or the indicated mutants on the specified G4-structured substrates. The substrate was incubated with the indicated amount of Ape1-IP in a solution containing 5 mM KCl as described in Materials and methods section. S denotes the substrate position and P denotes the product position.

Overall, our data clearly indicate that the acetylation of lysine residues K²⁷⁻³⁵ is important for controlling the overall enzymatic activity of Ape1 on telomeric sequences, as in the case for ordinary abasic dsDNA substrates (Fantini et al. 2010).

6.6. The telomeric-binding ability of Ape1 depends on K²⁷, K³¹, K³² and K³⁵ residues

Next, we checked the ability of Ape1 wild-type and mutated proteins to physiologically interact with telomeres by using Telomeric-Chromatin Immuno-Precipitation analysis (Telo-ChIP) analyses (see *Materials and methods*). Telo-ChIP analysis was performed on HeLa cells stably expressing FLAG-tagged Ape1 mutant proteins in place of the endogenous wild-type (which was down-regulated through a specific siRNA (Lirussi et al. 2012; Vascotto et al. 2009; Antoniali et al. 2017)). The expression levels of the ectopic forms of Ape1 in these cells was similar to that of the endogenous protein (Antonioli et al. 2017), which should minimize off-target and other confounding effects of overexpression. The DNA recovered from the ChIP assay was then analysed by quantitative PCR (Q-PCR). As shown in [Figure 43](#), the telomeric binding ability of Ape1^{NΔ33} was considerably reduced, compared to Ape1^{WT} protein. In contrast, Ape1^{K4pleA} showed a binding ability comparable to that of Ape1^{WT} while Ape1^{K4pleR} bound telomeric DNA with an activity 9-fold higher than that of Ape1^{WT}. These data are consistent with the binding detected using UV-crosslinking ([Figure 32](#)).

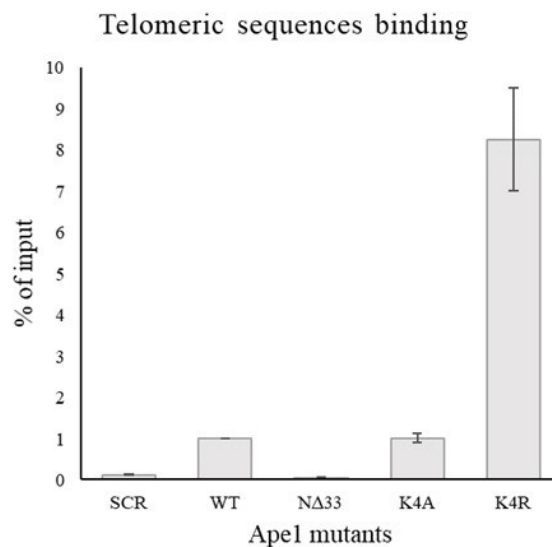


Figure 43 Analysis of binding of Ape1 protein and its mutants on telomeric sequences

U2O2 cells were transfected with pCMV plasmids for the expression of Flag-tagged Ape1 mutants as indicated in Materials and methods section. Empty vector used as control. Histogram shows the amount of telomeric sequences by each mutant of Ape1 resulting from ChIP experiments as percentage of input DNA. Error bars correspond to SDs of qPCR from one ChIP experiment.

6.7. Interaction of NPM1 with Ape1 modulates its endonuclease activity on telomeric sequences

Since the N-terminal domain of Ape1 is involved in modulating protein-protein interactions (Poletto et al. 2013), we next checked whether the interaction with a known Ape1 partner NPM1 (Vascotto et al. 2009) may affect Ape1 enzymatic activity on telomeric DNA. We previously demonstrated that stable interaction between Ape1 and NPM1 requires charged K²⁷⁻³⁵ residue on Ape1 (Lirussi et al. 2012), and that this interaction modulates Ape1 endonuclease activity *in vitro* and in cancer cells (Vascotto et al. 2014). Interestingly, NPM1 can bind G-quadruplex structures in the *c-Myc* promoter (Federici et al. 2010).

First, we checked whether NPM1 affects telomere physiology by testing whether telomere length is affected in the OCI/AML3 cell line, which stably expresses the aberrant NPM1^{c+} protein, which is localized to the cytoplasm, compared to OCI/AML2 cells expressing wild-type NPM1 localized to the nucleus (Tiacci et al. 2012). Telomere-length assays clearly demonstrated an evident shortening of telomeres in OCI/AML3 cells with respect to control OCI/AML2 cells, confirming a role for nuclear NPM1 in telomere maintenance (Figure 44, left). To verify the importance of Ape1 role in the maintenance of telomere integrity, we inhibited the Ape1 endonuclease activity treating OCI/AML2 cells with sublethal doses of compound #3 for one week (Rai et al. 2010). Upon the inhibition of Ape1 activity, we could detect a shortening of the telomeric signal, as the mean telomere length was 3.12 kbp compared with 3.28 kbp of the control sample (DMSO). This evidence suggests that the protein exerts its endonuclease activity at the telomeric level and its inhibition indeed affects telomere dimension. In order to confirm a role for Ape1 in telomere maintenance, we performed the telomere length analysis in CH12F3 cells, a mouse lymphoma cell line devoid of Ape1 ($\Delta\Delta\Delta$) or retaining one copy of Ape1 gene (Δ^{++}) (Masani, Han, and Yu 2013). The Ape1-proficient line had a telomere length averaging ~18 kbp, as expected for mouse telomeres. The Ape1 deficient cells showed a significantly shorter telomeres averaging 14 kbp (Figure 44, right). These results show a role for Ape1 in telomere maintenance in murine lymphocytes, consistent with a previous study on human cell lines (Madlener et al. 2013).

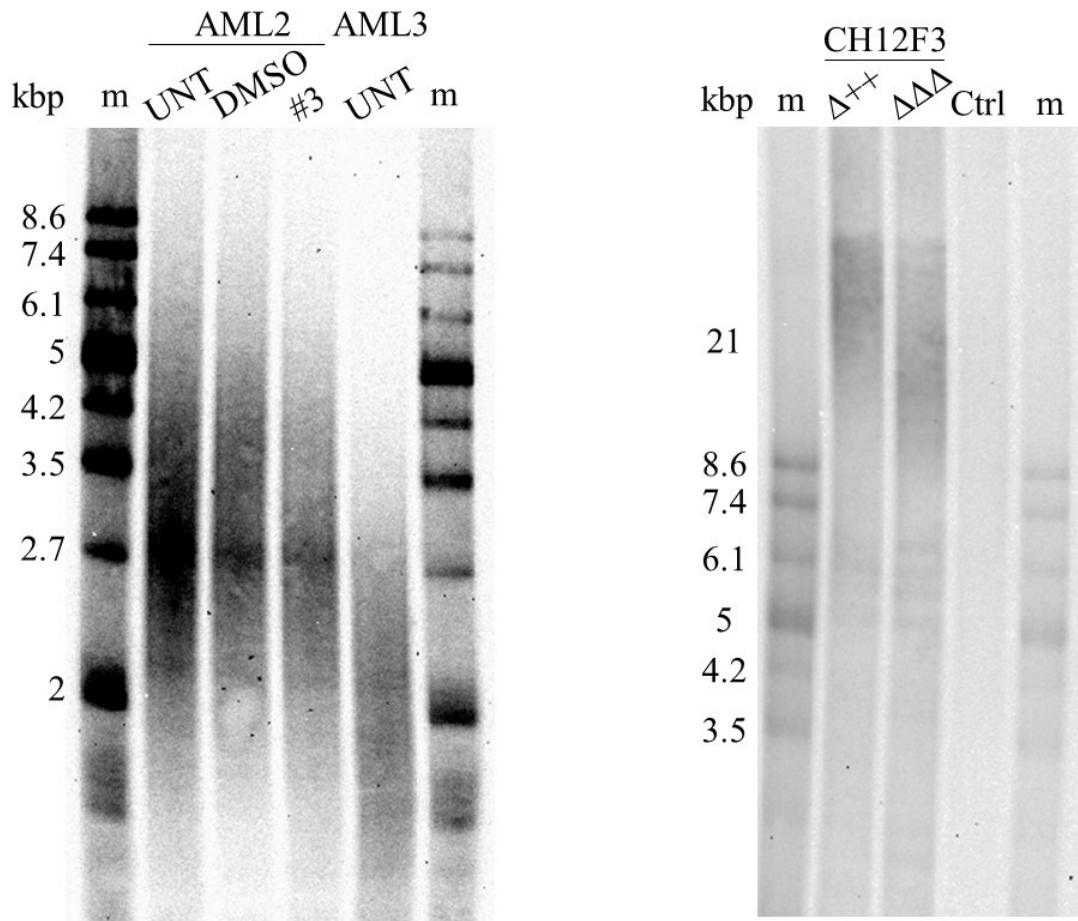


Figure 44 *Ape1* presence is fundamental to maintain telomere integrity in vivo

Telomeric length assay as a function of NPM1 localization (left). Telomere length assay was performed as described in Materials and methods section on acute myeloid leukemia (AML) cells showing the different length of telomeres in cell types characterized by different NPM1 localization. AML2 cells were untreated (UNT) or treated with compound #3 or DMSO.

*Telomeric length assay as a function of *Ape1* expression level (right). Telomere length was assayed on mouse CH12F3 cells expressing (Δ^{++}) or depleted for *Ape1* ($\Delta\Delta\Delta$) protein. Ctrl refers to a DNA control with a mean length of 7.4 kbp provided by the kit. The molecular weight marker (m) is provided by the kit; the weight of each band is indicated as kbp.*

We then investigated the effects of NPM1 on *Ape1* binding of the telomeric Nat substrate by EMSA assays. NPM1 did not form detectable complexes with the Nat, while there clearly was binding by *Ape1* (Figure 45, lanes 2 and 3). When increasing amounts of NPM1 were added to reactions with a constant amount of *Ape1*, the extent of the protein-telomeric DNA complex was progressively decreased (Figure 45, lanes 4-7). As expected, *Ape1*^{NA33} did not form detectable complexes with the Nat sequence, independently of NPM1 presence (Figure 45, lanes 8-12). GST-pulldown experiments (Figure 46)

confirmed the interaction of Ape1 with NPM1 recombinant proteins under these conditions.

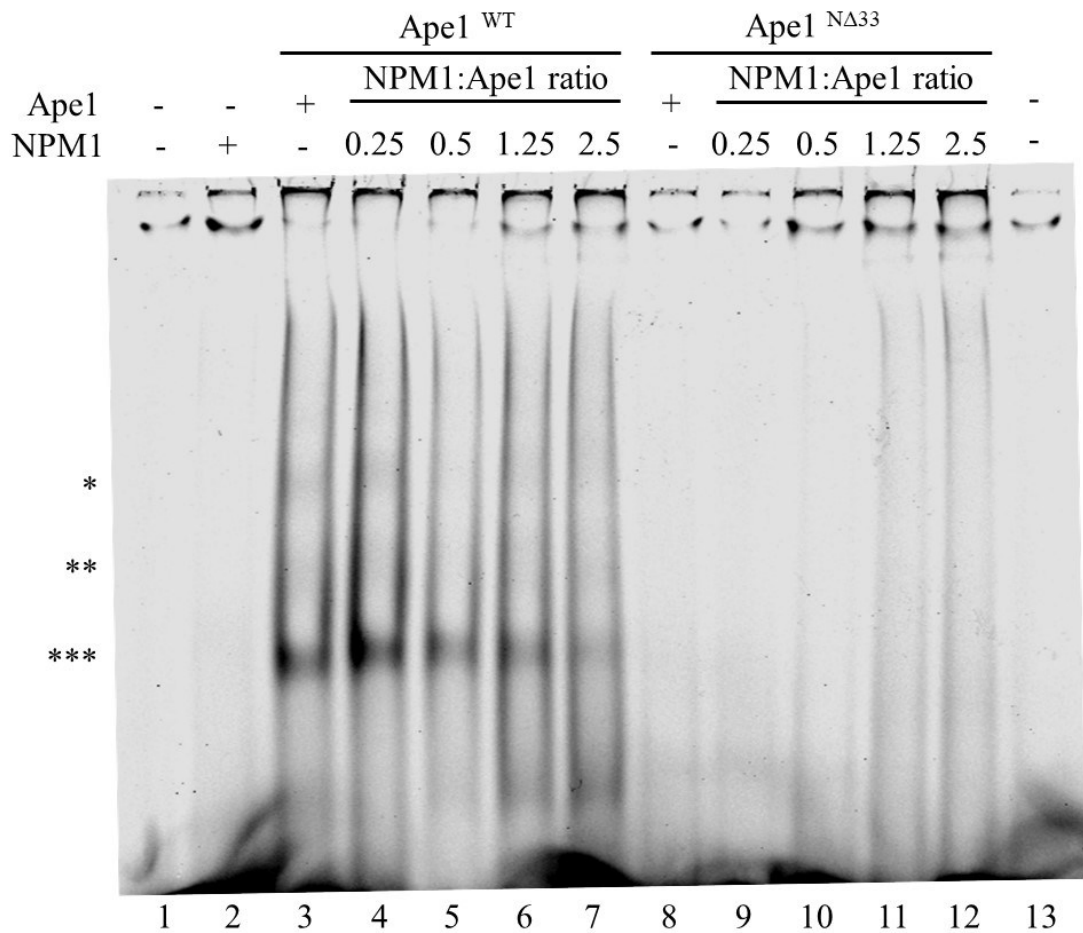


Figure 45 NPM1 inhibits Ape1 endonuclease activity competing with the substrate for the interaction with the N-terminal domain of the endonuclease

Representative native EMSA polyacrylamide gel of recombinant Ape1^{WT} and Ape1^{NΔ33} pre-incubated with increasing concentrations of NPM1. Binding on Nat substrate (25 nM) is shown. Reactions were performed as explained in Materials and methods section.

The reported ability of NPM1 to bind G-quadruplex structures (Gallo et al. 2012; Federici et al. 2010; Scognamiglio et al. 2014) prompted us to investigate telomere binding using SPR. As shown in [Figure 47](#), NPM1 does interact with the Nat, although with a 4.6-fold lower affinity than Ape1^{WT} ([Table 2](#)), consistent with the EMSA results ([Figure 45](#)).

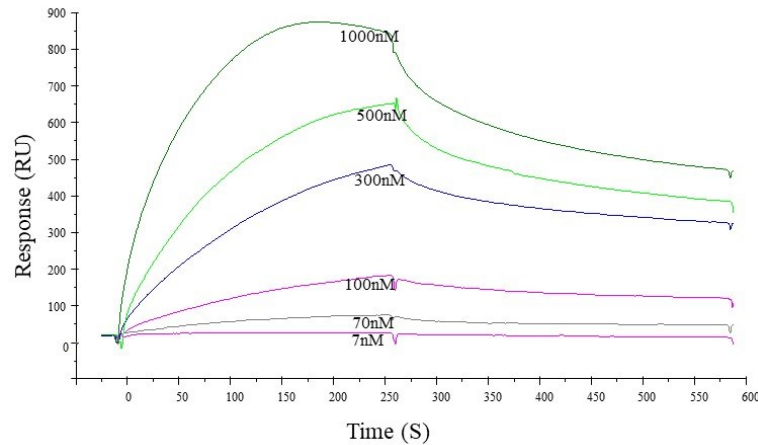


Figura 46 NPM1 shows only a weak affinity toward Nat substrate

Overlay of sensorgrams relative to SPR experiments for the binding to immobilized Biot- Nat of NPM1

We then analysed the effect of the interaction with NPM1 on the Ape1-AP endonuclease activity. When NPM1 was present in a sub-stoichiometric ratio with respect to Ape1, the endonuclease activity was modestly enhanced; in contrast when NPM1 was present in a

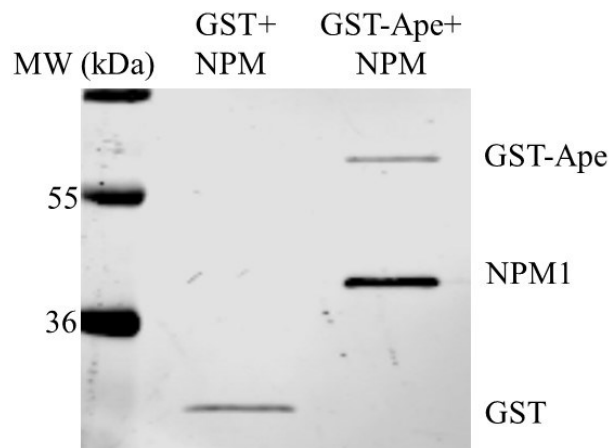


Figura 47 GST pull-down experiment showing that NPM1 is able to interact with Ape1 under physiologic conditions

GST pull-down assay was performed as described in Materials and methods section using GST or GST-tagged recombinant Ape1^{WT} as the bait and NPM1 as the prey. After the incubation, the samples were loaded on a 10% SDS-PAGE and subsequently immunoprobed with anti-GST and anti-NPM1 antibodies.

supra-stoichiometric ratio with Ape1, the endonuclease activity was inhibited ~2-fold (Figure 48). From these data, we can conclude that interaction of NPM1 with Ape1 modulates its endonuclease activity on telomeric sequences, at least *in vitro*.

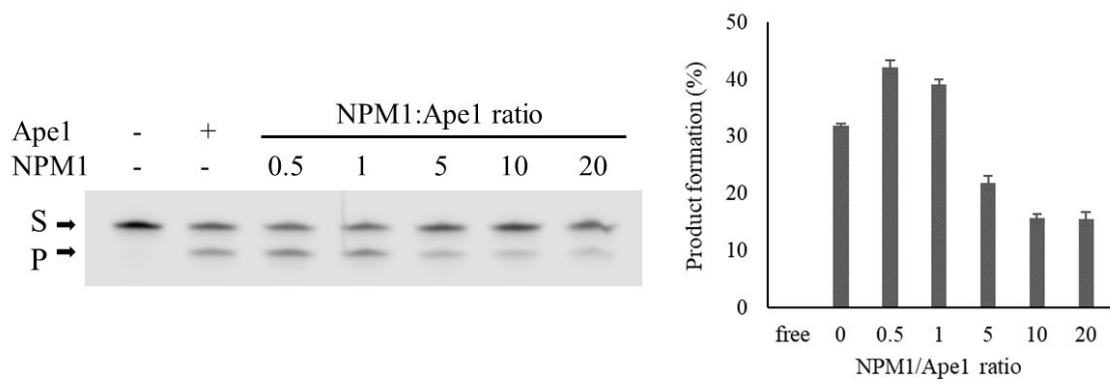


Figura 48 *NPM1, when present in a supra-stoichiometric ratio with Ape1, inhibits its endonuclease activity*

Representative denaturing polyacrylamide gel of AP site incision by *Ape1*^{WT} on S8 substrate in the presence of increasing amounts of *NPM1* (left). The proteins were incubated in a solution containing 50 mM KCl as described in Materials and methods section. S denotes the substrate position and P denotes the product position. Histogram showing the level of substrate processing upon the increasing ratio between *NPM1* and *Ape1*^{WT} (right). Average values with standard deviations of three loadings of the same experiment are presented.

7. Discussion

This work was aimed at characterizing the ability of Ape1 to recognize and process telomeric DNA substrates containing abasic sites in different positions. Moreover, we wanted to evaluate the role of the unstructured N-terminal domain and, in particular, that of the acetyltable Lys residues we previously identified (Fantini et al. 2010; Lirussi et al. 2012). To this end, we analyzed the ability of the wild type and several mutant forms of Ape1 to recognize and process different oligonucleotides that are able to fold into different G-quadruplex structures.

We found that Ape1^{WT} was able to bind each G4 structured ODN, independently of the presence of the abasic site (Table 1 and Figures 17 and 19). K_D values obtained through SPR assays showed that the affinity of the protein toward the G4 structured substrates was considerably higher than that for an unstructured substrate, highlighting the importance of DNA secondary structure for recognition by Ape1, as we previously suggested (Poletto et al. 2013).

While the G-quartet structure appears to be an important determinant, a possible effect of the abasic site position on Ape1 activity cannot be ruled out. In fact, the enzymatic activity on S4 was significantly lower than that on the S8 substrate, and the CD data indicate that the solution composition of G4 structures for S4 and S8 is different. There was a clear preference of Ape1 for a parallel G4 structure for S8, with this conformation the one preferred under molecular crowding conditions. Consistent with our results, other studies report a dependence of Ape1 activity on the type of G4 structure in telomeric sequences containing abasic sites (Zhou et al. 2015). Since the variation of ionic strength plays a crucial role in similar enzymes (Correa et al. 2013; Abeldenov et al. 2015), we evaluated the enzymatic activity of Ape1^{WT} under KCl concentrations of 5-50 mM. There was only a small effect of KCl for Ape1 acting on canonical abasic dsDNA (Figures 33 and 35), as previously shown (Fantini et al. 2010); the KCl concentration does not affect the secondary structure of the G4-substrates (Figure 13). Remarkably, Ape1^{NA33} was not able to form any stable complexes with the substrates (Figures 17 and 19) and exhibited a significantly lower efficiency in processing the abasic lesions in both the S4 and S8 structures (Figure 23), despite active Ape1 binding as demonstrated by UV-crosslinking experiments (Figure 18). These findings further indicate that the unstructured N-terminal tail of Ape1, though not directly participating in the enzymatic activity of the protein, can

modulate stable DNA binding by Ape1, as we previously hypothesized (Poletto et al. 2013) and as recently corroborated by other studies (Kladova et al. 2018).

The Ape1 N-terminal domain is rich in positively charged amino acids (8 Lys and 2 Arg residues); several of these lysine residues (K²⁷, K³¹, K³², K³⁵) can undergo acetylation in cells under genotoxic stress conditions (Fantini et al. 2010; Lirussi et al. 2012). Similarly to Ape1^{NΔ33}, the mutant Ape1^{K4pleA}, which mimics the acetylated status by replacing all four Lys with Ala residues, displayed an endonuclease activity on S4 and S8 that was significantly lower than that of Ape1^{WT}. Despite this difference, the Ape1^{K4pleA} did not show a reduced ability to bind to G4-DNA (Figure 32). Interestingly, at lower ionic strength, the activity of the Ape1^{K4pleA} and Ape1^{NΔ33} mutants was higher than that of Ape1^{WT} protein. This result indicates that additional charged amino acids outside the N-terminus may contribute to the catalytic activities of Ape1. In addition, the increased enzymatic activities at low ionic strength of Ape1^{K4pleA} and Ape1^{K4pleQ} on S4 and S8, relative to Ape1^{WT} and Ape1^{K4pleR} (Figures 41 and 42), suggest that charged K residues in the Ape1 N-terminus may regulate the product-release step, as we previously hypothesized (Fantini et al. 2010). These findings are in line with previous observations showing that release of the incision product may represent the limiting step in Ape1 turnover, particularly for dsDNA and structures such as the telomere G-quadruplex (Marenstein, Wilson III, and Teebor 2004; Poletto et al. 2013; Mol, Hosfield, and Tainer 2000; Masuda, Bennett, and Demple 1998).

The observation that the Ape1^{K4pleR} protein has increased telomere binding ability (Figures 40, 41 and 43), also supports the conclusion that the charged residues in the N-domain significantly contribute to the stability of Ape1-telomeric substrates complexes.

Recent studies pointed to the unstructured Ape1 N-terminus as a relay for regulating the different functions of the protein through modulation of the Ape1-protein interactome (Fantini et al. 2010; Vascotto et al. 2014; Antoniali, Lirussi, Poletto, et al. 2014; Antoniali et al. 2017). We previously demonstrated that NPM1 stimulates Ape1 endonuclease activity on abasic dsDNA *in vitro* and in cells through interaction with the unstructured Ape1 N-terminus (Fantini et al. 2010; Vascotto et al. 2014). Moreover, NPM1 by itself interacts with G-quadruplex-forming DNA (Federici et al. 2010), and mouse cells lacking NPM1 display general signs of genetic instability and activation of DNA damage responses (Colombo et al. 2005). In addition, Acute Myeloid Leukemia (AML)-associated mutations in the *NPM1* gene, cause the re-localization of part of the protein to

the cytoplasm (NPM1c+). This mis-localization hampers DNA binding of non-telomeric G4 structures by NPM1 (Bañuelos et al. 2013; Chiarella et al. 2013) and may affect Ape1 nuclear BER function in cancer cells (Vascotto et al. 2014). Therefore, the investigation of a potential effect of NPM1 in modulating the activity of Ape1 on G4-structures may represent an important model for understanding the role of mutual interactions between Ape1 and its interacting partners in the processing of damaged DNA. Using AML cell lines, we demonstrated that functional NPM1 is required for maintenance of appropriate telomeric length. Depending on the NPM1/Ape1 ratio, recombinant NPM1 may modulate the enzymatic activity of Ape1 on abasic telomeric substrates by having a stimulatory function under sub-stoichiometric ratio, and an inhibitory effect at supra-stoichiometric ratio. It must be noted that functional NPM1 may act as a pentameric molecule (Mitrea et al. 2014), so it is possible that, *in vivo*, a supra-stoichiometric ratio between NPM1 and Ape1 may represent a more physiologic condition, though further experiments are needed to better circumstantiate these findings in the telomeric context. Overall, the data show that, depending on the relative stoichiometric ratio between NPM1 and Ape1, the enzymatic activity of Ape1 on telomeric substrates may be strictly modulated by Ape1 protein interacting partners. Moreover, these findings suggest that an effort should be made to directly determine whether telomere maintenance is compromised, as a result of disrupting the normal Ape1-NPM1 interaction.

Since the interaction between NPM1 and Ape1 is also modulated by acetylation of the Lys residues at positions 27/31/32/35 (Lirussi et al. 2012), we may also infer that their acetylation may significantly affect the Ape1 role on telomere maintenance, not only through a direct effect on Ape1 binding on these substrates (Figure 46), but also by means of protein-protein mediated effects. Interaction of NPM1 with Ape1 involves mainly the N-terminal portion of Ape1 (Poletto et al. 2013) and positive charges on Lys residues at positions 27/31/32/35 (Lirussi et al. 2012). Thus, these data support the hypothesis that the Ape1 positively charged N-terminus is an important player in regulating the kinetics of the interaction of Ape1 with the telomeric substrates. Moreover, the endonuclease activity data support the conclusion that, depending on the relative stoichiometric ratio between NPM1 and Ape1, the enzymatic activity of Ape1 over telomeric substrates may be strictly modulated by Ape1 protein interacting partners. Therefore, these findings require an effort to directly determine whether telomere maintenance is compromised, as a result of disrupting the functional normal Ape1-NPM1 interaction.

Madlener et al. (Madlener et al. 2013) showed that cells expressing an Ape1 mutant bearing substitution of K⁶/K⁷ with Ala residues underwent severe chromosomal instability. Though we did not evaluate the role of these residues in modulating the enzymatic activity and binding properties of Ape1 on telomeric G-quadruplex, we may speculate that our data might provide the molecular basis for those unexplained findings. In fact, we previously found that deacetylation of K⁶/K⁷ by Sirtuin 1 (SIRT1) is dependent on the charged status of the K²⁷⁻³⁵ residues (Lirussi et al. 2012). Only when K²⁷⁻³⁵ are positively charged, K⁶/K⁷ may be de-acetylated by SIRT1, providing the positive charges essential for the normal function of Ape1 at telomeres. These observations support the hypothesis that dynamic cross-talk between the Lys residues in the Ape1 N-terminus may fine-tune the enzymatic activity of the protein and we speculate that there is a general role for acetylation of these residues in regulating Ape1 function at telomeres (Figure 49).

In another recent work (Kladova et al. 2018), stimulation of the OGG1, MBD4 and ANPG glycosylases activities by Ape1 strictly depended on the presence of an intact Ape1 N-terminus. Through oligomerization of Ape1 along the DNA duplex, which depends on its N-terminus, the protein was able to promote DNA-bridges formation and DNA aggregation, which, in turn, may cause structural deformation in the DNA double helix responsible for increasing the enzymatic rate of the glycosylases themselves. This new biochemical property of Ape1 may be particularly interesting in the context of the highly repetitive telomeric sequences, in which the secondary and tertiary structures of DNA play a fundamental regulatory function that influences genome stability.

Further studies along these lines are warranted and will deserve particular attention. A crystal structure of full-length Ape1 protein with its cognate substrate would provide physical evidence to our biochemical observations. To date, all the available crystal structures of Ape1 employed an N-terminal truncated form of the protein (Mol et al. 2000; Freudenthal et al. 2015), thus limiting definitive conclusions on this unusual DNA repair enzyme.

An altered acetylation status of Ape1 K²⁷⁻³⁵ has been demonstrated in human cancers (Poletto et al. 2012; Bhakat et al. 2016). We may thus hypothesize that chromosomal instability in cancer development may result from defective coordination of Ape1 function at telomeres due to post-translational modifications on its N-terminal Lys residues. Specific experiments are needed to corroborate this hypothesis.

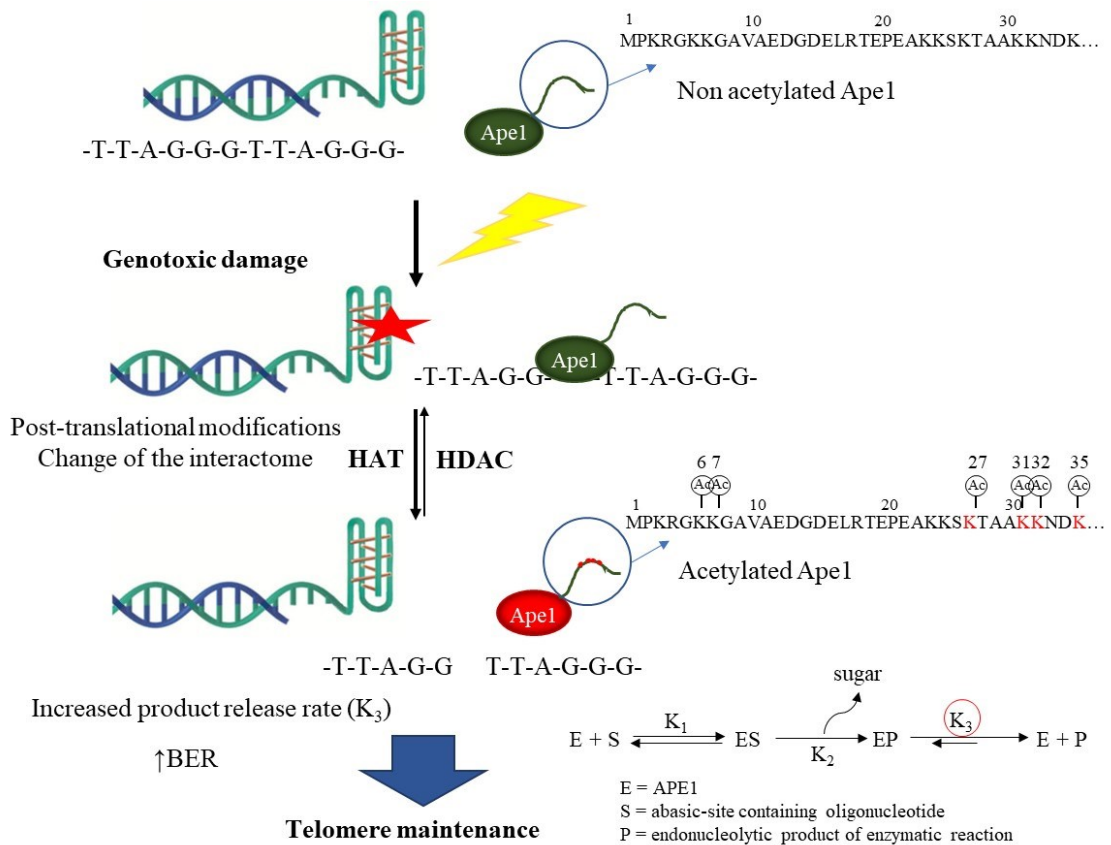


Figura 49 A model for the regulation of Ape1 activity during the repair of abasic sites in G4 DNA

Upon genotoxic damage, the generated damaged base is removed by a BER glycosylase, then the abasic site is handled by Ape1. After the intervention of acetyl-transferases, the lysine residues located in the N-terminal domain of Ape1 are acetylated. Consequently, this post-translational modification induces an increase of the release rate of the product upon the endonucleolytic cleavage. Consequently, acetylation may represent an efficient mechanism to regulate the activity of the protein also at the telomeric level.

8. Future perspectives

Ape1 N-terminus was defined as an essential domain for the interaction of the protein with nucleic acids, modulating the overall affinity of the protein. A recent work showed that Ape1, through its N-domain, can polymerize on DNA and that this induces a structural deformation of the double strand that could favor the activity of glycosylases thus increasing their cleavage rate (Kladova et al. 2018). This new highlighted property may be interesting to be further explored when considered in the context of telomeric repeats, which are characterized by the presence of secondary structures that influence their stability. Therefore, it would be interesting to obtain a crystal structure of the full length protein complexed with its substrate, as up to now the crystals were acquired using an N-terminal truncated form of the protein (Mol et al. 2000; Freudenthal et al. 2015), so partially excluding the contribution of an important functional domain for the enzyme.

As human cancer cells display an altered acetylation status for lysine residues K²⁷, K³¹, K³² and K³⁵, a correlation between chromosome instability and post translational modification dysregulation may exist (Poletto et al. 2012; Bhakat et al. 2016). So further investigation of this aspect could allow us to better define the precise association between acetylation and Ape1 function at the telomeres with specific *in vivo* experiments.

Experiments are underway to better describe the functional role of the N-terminus and for the Lysine residues here located in telomere physiology. We are interested in analyzing whether telomeres show significant variations in cells expressing these mutant forms of Ape1 in place of the wild type protein in term of length, integrity and chromosomal aberrations such as translocations or fusions.

It was demonstrated that Ape1 interacts with TRF2 and that this interaction at the telomeric level allows the correct positioning of the shelterin component on the interested site (Madlener et al. 2013). Next, it would be useful to assess the interaction between Ape1 acetylation mutants and the remaining sheltering proteins to define the interplay between the endonuclease and the other components responsible for telomere protection and stability.

Finally, based on the discovery that Ape1 may process abasic RNA, defining the interaction between Ape1 and TERRA RNA would be useful to enrich the characterization of the interaction of the telomeric transcript and the proteins implied in telomeric maintenance. TERRA interacts with TRF1 and TRF2 (Deng et al. 2009), folds

in a parallel G4 structure, participates in 3' telomeric overhang erosion (Cusanelli and Chartrand 2015) and can form hybrid quadruplexes pairing with complementary DNA (Xu and Komiyama 2012). So, this RNA molecule takes active part in several processes related with telomere maintenance, heterochromatinization, transcription activation and acts as a multiple protein partner and a scaffold that proteins employ to recruit other interactors. For these reasons it may have a key role in fundamental cellular processes in which also Ape1 takes part. Consequently, the interplay between the endonuclease and the telomeric transcript could represent a worthy crosstalk to be studied to better detail the scenario involving Ape1 in the context of transcription and RNA processing.

9. Materials and Methods

9.1. Protein expression and FPLC purification

BL21 cells were transformed with the proper pGEX-3X (GST tag) or pET-15b (His tag) plasmid following the manufacturer's instructions. In order to produce the protein, the culture was harvested at 37°C at 230 rpm until the reaching of OD₆₀₀ ~0.7. Finally, the culture was induced with 1 mM of IPTG (Sigma) for 4 hours and then was collected upon centrifugation. The pellet was lysed in the presence of Protease inhibitor 2.1 mg/ml (Sigma) and Lysozyme 0.3 mg/ml (Sigma) through sonication and the sample was centrifuged at 23,000 g for 20 minutes at 4° C, then the supernatants were purified through the appropriate column for affinity purification.

GST-tagged proteins (Ape1 WT and mutants) were purified through a GStrap column (GE Healthcare) and they were eluted through at increasing range of GSH (Sigma) concentration following the manufacturer's instructions. Then the proteins were incubated with Factor X (Amersham) to remove the tag; the enzyme was separated from the protein through a benzamidine column (GE Healthcare) and finally a cation exchange purification was performed.

His-tagged NPM1 protein were purified through a His-Trap column (GE Healthcare) and they were eluted through 3 steps at increasing imidazole (Sigma) concentrations. The protein was dialyzed and then purified through a cation exchange purification column.

All protein fractions were stored in a buffer containing 25 mM Tris pH 7.5, 100 mM NaCl, 1 mM DTT, 10% glycerol.

9.2. Oligonucleotides synthesis, purification and annealing

Oligonucleotides (ODN) reported in Table 1 were synthesized on a Millipore Cyclone Plus DNA synthesizer using standard solid phase β -cyanoethyl phosphoramidite chemistry at 1 μ mol scale. The synthesis were performed by using Fast Deprotection DNA 3'-phosphoramidites, a 5'-dimethoxytrityl-3'-phosphoramidite-1',2'-dideoxyribose (dSpacer, dS, Link Technologies) for the insertion of an abasic site mimic moiety and IRDye 800 phosphoramidite (LI-COR Biosciences) for the introduction of a Near IR fluorescent dye at the 5'-end of each ODN sequence. The oligomers were detached from the support and deprotected by treatment with concentrated aqueous ammonia in the dark for 1.5 hour at room temperature. The oligomers were purified by HPLC (Nucleosil C18

column Macherey–Nagel, 100-5; EC250/4.6) using standard methods. The fractions of the oligomers were collected and successively desalted by Sep-pak cartridges (C-18). The isolated oligomers proved to be >98% pure by HPLC. To perform *in vitro* experiments, some selected ODN sequences used previously (Virgilio et al., 2012) were employed and produced homemade as explained in the previous paragraph. A poly dT ODN of 23 bases, holding an abasic site (F) in 16th position (Poly dT-F) and an IRDye 800 at the 5' was synthesized by Metabion, purified through HPLC and checked in Mass Check. This probe was used as negative control as it is unable to acquire secondary structures. All the ODN were resuspended in DNase-free water at 100 μ M and annealing was performed at a final concentration of 5 μ M in a solution containing 70 mM KCl, 20 mM KH₂PO₄ and 0.2 mM EDTA, at pH 7.0, heated at 70°C and cooling down over night. A double-stranded ODN, named ds-F, which is composed of 26 bases and it holds a tetrahydrofuran mimicking the abasic site in position 15, was also synthesized by Metabion, purified through HPLC and checked in Mass Check. This latter ODN was annealed in 10 mM Tris, 10 mM MgCl₂, 1 mM EDTA pH 7.5, heated at 95°C and let to cool down. All ODN sequences are listed in Table 1.

ODN name	Sequences	Length of the product
Nat	5'-TAG GGT TAGG GTT AGG GTT AGG G-3'	-
S4	5'-TAG GGT TAFG GTT AGG GTT AGG G -3'	8 nt
S8	5'-TAG GGT TAGG GTT AGF GTT AGG G-3'	15 nt
Poly dT-F	5'-TTT TTT TTTT TTT TTF TTT TTT T-3'	15 nt
ds-F	5'-AAT TCA CCG GTA CCF TCT AGA ATT CG-3' 3'-TTA AGT GGA CAT GGG AGA TCT TAA GC-5'	14 nt
Poly dT	5'-TTT TTT TTTT TTT TTT TTT TTT T-3'	-

Table 2: Sequences of the ODN used in this study

F: tetrahydrofuran abasic site analog. Nat, S4 and S8 substrates are single strand DNA folded in a G-quadruplex. Poly dT-F is an unstructured DNA single strand. ds-F is the only duplex DNA sequence. All the ODN are labeled with IRDye 800 at the 5' end.

9.3. Circular dichroism (CD) spectroscopy

CD samples of the IRDye-labelled oligonucleotides reported in Table 1 were prepared at an ODN concentration of 25 μ M by using a potassium phosphate buffer (20 mM KH₂PO₄/K₂HPO₄, 70 mM KCl, pH 7.0) and submitted to the annealing procedure (heating at 70°C and slowly cooling at RT). CD samples at 50 mM KCl were prepared

by diluting the samples at 70 mM KCl and adding the suitable amounts of Tris and MgCl₂ to final concentrations of 50 mM and 10 mM, respectively. CD samples at 5 mM KCl were prepared by dialyzing CD samples at 70 mM against a solution KCl 5 mM, Tris 5 mM and MgCl₂ 1 mM. CD spectra of all G-quadruplexes and CD melting curves were registered on a Jasco 715 CD spectrophotometer. For the CD spectra, the wavelength was varied from 220 to 320 nm at 100 nm min⁻¹ scan rate, and the spectra recorded with a response of 4 s, at 1.0 nm bandwidth and normalized by subtraction of the background scan with buffer. The temperature was kept constant at 20°C with a thermoelectrically-controlled cell holder (Jasco PTC-348). CD melting curves were registered as a function of temperature from 20°C to 70°C for all G-quadruplexes at their maximum Cotton effect wavelengths. The CD data were recorded in a 0.1 cm pathlength cuvette with a scan rate of 0.5°C/min.

9.4. SDS-PAGE and Western blotting

All recombinant proteins were loaded onto a 10% (w/v) sodium dodecyl sulphate-polyacrylamide (SDS-PAGE; acr:bis= 37.5:1) electrophoresis gel, which was subsequently stained using Coomassie Brilliant Blue stain (ThermoFisher). Each band, corresponding to the protein of interest, was quantified and normalized with BSA (bovine serum albumin) standardization curve. The image was finally developed by using NIR Fluorescence technology with an Odyssey CLx scanner (LI-COR GmbH). Bands were quantified and analyzed using the ImageStudio software (LI-COR GmbH).

Cell extracts samples were loaded onto a 12 (w/v) % SDS-PAGE electrophoresis gel. Proteins were then transferred onto nitrocellulose membranes (Schleicher & Schuell). Monoclonal α -Ape1 was from Novus Biologicals (1:5,000 dilution). Membranes were incubated with secondary antibodies labeled with IRDye (1:10,000 dilution) in 5% milk, PBS and Tween 0.1% and finally developed by using NIR Fluorescence technology with an Odyssey CLx scanner (LI-COR GmbH). Bands were quantified and analyzed using the ImageStudio software (LI-COR).

9.5. Electrophoretic mobility shift assay (EMSA)

EMSA assays were performed incubating 20 pmol of Ape1 protein (2 μ M) with 250 fmol of the substrate (0.025 μ M) for 1 hour at RT in 25 mM Tris, 100 mM KCl, 2 mM DTT, 10% glycerol, pH 7.5. Alternatively, EMSA assays were done with 3.5 pmol of NPM1 or with 7 pmol of Ape1^{WT} or Ape1^{N Δ 33}, co-incubated for 1 h at RT with increasing concentrations of NPM1 (varying between 3.5 and 17.5 pmol); 350 fmol of Nat substrate were added and left to incubate for 1 h at RT during the binding reactions. The mixtures were loaded on a native gel 6% polyacrylamide (acr: bis= 37.5: 1) then run in the cold apparatus (at 4°C) at 130 V for 4 hours using 0.5x TBE as buffer. Gels were scanned and band intensities were quantified using the Image Studio software (Odyssey CLx, LI-COR GmbH).

9.6. UV-crosslinking experiments

UV-crosslinking analysis were performed co-incubating 20 pmol of recombinant purified protein (Ape1^{WT}, of Ape1^{N Δ 33} or Ape1^{K4pleA}) for 1.5 h at 4°C with 250 fmol of S4 or S8 ODN. Alternatively, UV-crosslinking analysis were performed with Immunoprecipitated (IP) samples obtained from transfected U2OS cells employing 2 pmol of Ape1, co-incubated for 40 min at RT with 250 fmol of the G4-structured ODN in AP buffer containing 5 mM KCl and 1 mM MgCl₂.

The mixtures were UV-crosslinked using a Vilber Lourmat UV-crosslinker BLX-254 at 0.2 J/cm² and run onto SDS-PAGE 10% acrylamide.

9.7. Cell cultures, transfection and Co-immunoprecipitation

U2OS cells were grown in DMEM (EuroClone) medium supplemented with 10% fetal bovine serum (FBS, EuroClone), L-glutamine (2mM), penicillin (100 U/ml) and streptomycin (100 mg/ml) and cultured in a humidified incubator at 5% CO₂ at 37°C. HeLa stable clones were grown as indicated in (Vascotto et al. 2009) and harvested 10 days after the addition of doxycycline in the medium (Vascotto et al. 2009). OCI/AML2 and OCI/AML3 cells were grown in MEM- α (EuroClone) supplemented with 20% heat-inactivated FBS, L-glutamine (2mM), penicillin (100 U/ml) and streptomycin (100

mg/ml) and cultured in a humidified incubator at 5% CO₂ at 37°C. CH12F3 cells were grown in RPMI 1640 (EuroClone) supplemented with non-essential amino acids, Na pyruvate, 10% FBS, Hepes (25 mM), β-mercaptoethanol (50 μM), L-glutamine (2mM), penicillin (100 U/ml) and streptomycin (100 mg/ml) and cultured in a humidified incubator at 5% CO₂ at 37°C (Masani, Han, and Yu 2013).

Co-immunoprecipitation studies were carried out with whole cell extracts from U2OS cells transfected with FLAG-tagged Ape1 mutants (Ape1^{WT}-Flag, Ape1^{NΔ33}-Flag, Ape1^{K4pleA}-Flag, Ape1^{K4pleQ}-Flag and Ape1^{K4pleR}-Flag). The cells were transiently transfected using 12 μg of DNA and 36 μL of Lipofectamine 3000 (Invitrogen). Cells were harvested 24 hours upon transfection, washed twice with PBS and re-suspended in lysis buffer (50 mM Tris HCl pH 7.4, 150 mM NaCl, 1 mM EDTA and 1 % Triton X-100) containing proteases inhibitor cocktail. After incubation for 20 minutes at 4°C under rotation, cell lysates were clarified by centrifugation at 12,000 × g for 10 minutes at 4°C and co-immunoprecipitation was performed with anti-FLAG M2 affinity gel (Sigma-Aldrich) at 4°C with gentle rocking for 3 hours. After washing three times with Tris-buffered saline (TBS), immunoprecipitates (IP) were then eluted by incubation with 0.15 mg/ml FLAG peptide in TBS and analyzed as indicated. Samples were then loaded onto a 12 w/vol % SDS-PAGE electrophoresis gel. Proteins were then transferred to nitrocellulose membranes (Schleicher & Schuell). Monoclonal α-Ape1 was from Novus Biologicals (1:5,000 dilution). Membranes were incubated with secondary antibodies labeled with IRDye (1:10,000 dilution) in 5% milk, PBS and Tween 0.1%. All gel images were captured with an Odyssey CLx scanner (LI-COR GmbH) and analyzed using the ImageStudio software (LI-COR GmbH).

9.8. Chromatin immunoprecipitation and quantitative PCR

Chromatin immunoprecipitation (ChIP) was performed using the Diagenode High cell number ChIP kit, according to the manual. After culturing HeLa cells stably carrying p3XFLAG-CMV vectors in doxycycline 1 μg/ml, as previously described (Vascotto et al. 2009), the cells were crosslinked with 1% formaldehyde for 10 minutes at RT, and sonicated with the Diagenode bioruptor. Samples were immunoprecipitated overnight with anti-FLAG (Sigma-Aldrich). Telomeric DNA sequences were amplified by PCR using SensiFAST SYBR No-ROX Kit (Bioline).

The primer sequences were telomere forward primer (Tel 1) 5'-GGTTTTTGAGGG-TGAGGGTGAGGGTGAGGGTGAGGGT-3'; telomere reverse primer (Tel 2), 5'-TCCCGACTATCCCTATCCCTATCCCTATCCCTATCCCTATCCCTA-3'; 36B4 forward primer, 5'-CAGCAAGTGGGAAGGTGTAATCC-3'; 36B4 reverse primer, 5'-CCCATTCTATCATCAACGGGTACAA-3' (Gil and Coetzer 2004; O'Callaghan et al. 2008). Samples were run on a C1000 Thermal Cycler CFX96 Real-Time System (BIORAD). Each sample was analyzed in triplicate. 36B4, a single-copy gene that encodes the acidic ribosomal phosphoprotein P0, was used as a reference (O'Callaghan et al. 2008). PCR reactions (15 μ L) were set up as follows: 1 μ L of recovered ChIP DNA, 2 \times SYBR Green master mix (Bioline), and the forward and reverse primers each at 100 nM final concentration. The thermal cycling conditions were as follows: 10 min at 95 $^{\circ}$ C, followed by 40 cycles of 95 $^{\circ}$ C for 15 s and 60 $^{\circ}$ C for 1 min for both telomere and 36B4 amplification.

9.9. AP site incision assays

Cleavage assays were performed either at high ionic strength (Tris 50 mM, KCl 50 mM, MgCl₂ 10 mM, BSA 1 μ g/ μ l, triton X-100 0.05%) or at low ionic strength (Tris 5 mM, KCl 5 mM, MgCl₂ 1 mM, BSA 0.1 μ g/ μ l, triton X-100 0.005%). A fixed amount of substrate (250 fmol) was incubated with an increasing amount of Ape1 proteins for 40 minutes at 37 $^{\circ}$ C. Alternatively, 10 pmol of Ape1^{WT} were incubated for 1h at RT with increasing amounts of NPM1, varying between 5 and 200 pmol. Then the substrate S8 was added for the reaction for 40 min at 37 $^{\circ}$ C in a solution containing 50 mM KCl (final volume 10 μ l). The reactions were in any case stopped by adding an equal volume of stop solution containing formamide (10 mM EDTA, 0.5 % bromophenol blue, 80 % formamide), followed by heating for 5 minutes at 95 $^{\circ}$ C. The mixtures were loaded on a 7 M urea 20% acrylamide gel and run in 0.5x TBE at 130 V for 50 minutes. The intensity of the obtained bands was determined using a fluorescence scanner (Odyssey CLx, LI-COR GmbH) and the quantification was obtained calculating the ratio between the product intensity over the sum between the intensities of the product and the substrate. The signals of the non-incised substrate (S) and the incision product (P) bands were quantified using Image Studio software.

9.10. Surface Plasmon Resonance (SPR) experiments

Real-time binding assays were performed at 25 °C on a Biacore 3000 Surface Plasmon Resonance (SPR) instrument (GE Healthcare). For immobilization, 5'-biotinylated Nat and Poly dT ODN were injected at a concentration of 20 µM on a SA Biacore sensor chip until the desired level of immobilization was achieved (averaged value of 700 RU) in an injection time of 7 min. Binding assays were carried out by injecting 90 µL of analyte, at 20 µL x min⁻¹. Experiments were carried out at pH 7.4 using HBS (10 mM Hepes, 150 mM NaCl, 3 mM EDTA, pH 7.4). The association phase (k_{on}) was followed for 270 s, whereas the dissociation phase (k_{off}) was followed for 300 s. The reference chip sensorgrams were properly subtracted to sample sensorgrams. After each cycle, the sensor chip surface was regenerated with a 1.0 M NaCl solution for 30 s followed by multiple buffer injections to yield a stable baseline for the following cycles. Analyte concentrations were in the range 50-1000 nM, for all proteins. Experiments were carried out in duplicates. Kinetic parameters were estimated assuming a 1:1 binding model and using version 4.1 Evaluation Software (GE Healthcare).

9.11. Telomeric length assay

Telomere length analysis was performed employing TeloTAGGG Telomere Length Assay Kit (Roche). Genomic DNA was isolated from OCI/AML2, OCI/AML3, CH12F3 cells using the Blood & Cell Culture DNA Midi kit (Qiagen). OCI/AML2 were treated with #3 500 nM (G. Rai et al. 2010), or with DMSO as control, for 7 days. After digestion with Hinf I and Rsa I, DNA was separated on 0.8% agarose gel. Following denaturation, the DNA was transferred to a HybondN+ membrane (Boehringer Mannheim) and hybridized with a digoxigenin-labeled telomeric probe included in the kit. Non-radioactive telomeric signal intensity was scanned with high resolution chemiluminescence settings using a Molecular Imager Chemidoc XRS scanner (Bio Rad) with Image Lab™ Software (Bio Rad). The length of the fragments was quantified using the TeloTool software version 1.3 (Matlab) (Göhrling et al. 2014).

9.12. GST pull-down assay

300 pmol of NPM1 were added, together with 100 pmol of GST or Ape1-GST, to 15 µl of glutathione-sepharose 4B beads (GE healthcare). Binding was performed in AP buffer

1x at 4°C for 2h, under rotation. The beads were washed three times with PBS 1x supplemented with 0.1% w/v Igepal (CA-630 Sigma). Elution was performed with GSH 10 mM and the obtained samples were analyzed through western blot. Anti-GST (Sigma H9658) and anti-NPM1 (Invitrogen 32-5200) antibodies were employed.

9.13. Statistical analysis

Statistical analyses were performed by using the Student's *t* test. $P < 0.05$ was considered as statistically significant.

10. References

- Abeldenov, Sailau, Ibtissam Talhaoui, Dmitry O. Zharkov, Alexander A. Ishchenko, Erlan Ramanculov, Murat Saparbaev, and Bekbolat Khassenov. 2015. "Characterization of DNA Substrate Specificities of Apurinic/Apyrimidinic Endonucleases from *Mycobacterium Tuberculosis*." *DNA Repair* 33 (September): 1–16. <https://doi.org/10.1016/j.dnarep.2015.05.007>.
- Akbari, Mansour, Marya Morevati, Deborah Croteau, and Vilhelm A. Bohr. 2015. "The Role of DNA Base Excision Repair in Brain Homeostasis and Disease." *DNA Repair* 32 (August): 172–79. <https://doi.org/10.1016/j.dnarep.2015.04.029>.
- Ancelin, Katia, Michele Brunori, Serge Bauwens, Catherine-Elaine Koering, Christine Brun, Michelle Ricoul, Jean-Patrick Pommier, Laure Sabatier, and Eric Gilson. 2002. "Targeting Assay to Study the Cis Functions of Human Telomeric Proteins: Evidence for Inhibition of Telomerase by TRF1 and for Activation of Telomere Degradation by TRF2." *Molecular and Cellular Biology* 22 (10): 3474–87.
- Antoniali, Giulia, Lisa Lirussi, Chiara D’Ambrosio, Fabrizio Dal Piaz, Carlo Vascotto, Elena Casarano, Daniela Marasco, Andrea Scaloni, Federico Fogolari, and Gianluca Tell. 2014. "SIRT1 Gene Expression upon Genotoxic Damage Is Regulated by APE1 through NCaRE-Promoter Elements." *Molecular Biology of the Cell* 25 (4): 532–47. <https://doi.org/10.1091/mbc.E13-05-0286>.
- Antoniali, Giulia, Lisa Lirussi, Mattia Poletto, and Gianluca Tell. 2014. "Emerging Roles of the Nucleolus in Regulating the DNA Damage Response: The Noncanonical DNA Repair Enzyme APE1/Ref-1 as a Paradigmatic Example." *Antioxidants & Redox Signaling* 20 (4): 621–39. <https://doi.org/10.1089/ars.2013.5491>.
- Antoniali, Giulia, Fabrizio Serra, Lisa Lirussi, Mikiei Tanaka, Chiara D’Ambrosio, Shiheng Zhang, Slobodanka Radovic, et al. 2017. "Mammalian APE1 Controls MiRNA Processing and Its Interactome Is Linked to Cancer RNA Metabolism." *Nature Communications* 8 (1). <https://doi.org/10.1038/s41467-017-00842-8>.
- Arora, Rajika, Yongwoo Lee, Harry Wischnewski, Catherine M. Brun, Tobias Schwarz, and Claus M. Azzalin. 2014. "RNaseH1 Regulates TERRA-Telomeric DNA Hybrids and Telomere Maintenance in ALT Tumour Cells." *Nature Communications* 5 (October): 5220. <https://doi.org/10.1038/ncomms6220>.
- Awate, Sanket, and Robert Brosh, Jr. 2017. "Interactive Roles of DNA Helicases and Translocases with the Single-Stranded DNA Binding Protein RPA in Nucleic Acid Metabolism." *International Journal of Molecular Sciences* 18 (6): 1233. <https://doi.org/10.3390/ijms18061233>.
- Azzalin, Claus M., Patrick Reichenbach, Lela Khoriantuli, Elena Giulotto, and Joachim Lingner. 2007. "Telomeric Repeat Containing RNA and RNA Surveillance Factors at Mammalian Chromosome Ends." *Science (New York, N.Y.)* 318 (5851): 798–801. <https://doi.org/10.1126/science.1147182>.
- Babinský, Martin, Radovan Fiala, Iva Kejnovská, Klára Bednářová, Radek Marek, Janos Sagi, Vladimír Sklenář, and Michaela Vorlíčková. 2014. "Loss of Loop Adenines

- Alters Human Telomere d[AG3(TTAG3)3] Quadruplex Folding.” *Nucleic Acids Research* 42 (22): 14031–41. <https://doi.org/10.1093/nar/gku1245>.
- Bailey, S. M. 2006. “Telomeres, Chromosome Instability and Cancer.” *Nucleic Acids Research* 34 (8): 2408–17. <https://doi.org/10.1093/nar/gkl303>.
- Balasubramanian, Shankar, Laurence H. Hurley, and Stephen Neidle. 2011. “Targeting G-Quadruplexes in Gene Promoters: A Novel Anticancer Strategy?” *Nature Reviews Drug Discovery* 10 (4): 261–75. <https://doi.org/10.1038/nrd3428>.
- Bañuelos, Sonia, Benoît Lectez, Stefka G. Taneva, Georgina Ormaza, Marián Alonso-Mariño, Xabier Calle, and María A. Urbaneja. 2013. “Recognition of Intermolecular G-Quadruplexes by Full Length Nucleophosmin. Effect of a Leukaemia-Associated Mutation.” *FEBS Letters* 587 (14): 2254–59. <https://doi.org/10.1016/j.febslet.2013.05.055>.
- Bauer, Nicholas C., Anita H. Corbett, and Paul W. Doetsch. 2015. “The Current State of Eukaryotic DNA Base Damage and Repair.” *Nucleic Acids Research* 43 (21): 10083–101. <https://doi.org/10.1093/nar/gkv1136>.
- Baumann, P., and T. R. Cech. 2001. “Pot1, the Putative Telomere End-Binding Protein in Fission Yeast and Humans.” *Science (New York, N.Y.)* 292 (5519): 1171–75. <https://doi.org/10.1126/science.1060036>.
- Berquist, Brian R., Daniel R. McNeill, and David M. Wilson III. 2008. “Characterization of Abasic Endonuclease Activity of Human Ape1 on Alternative Substrates, as Well as Effects of ATP and Sequence Context on AP Site Incision.” *Journal of Molecular Biology* 379 (1): 17–27. <https://doi.org/10.1016/j.jmb.2008.03.053>.
- Bhakat, Kishor K., Shiladitya Sengupta, Victor F. Adeniyi, Shrabasti Roychoudhury, Somsubhra Nath, Larry J. Bellot, Dan Feng, et al. 2016. “Regulation of Limited N-Terminal Proteolysis of APE1 in Tumor via Acetylation and Its Role in Cell Proliferation.” *Oncotarget* 7 (16): 22590–604.
- Blanpain, Cedric, Mary Mohrin, Panagiota A. Sotiropoulou, and Emmanuelle Passegué. 2011. “DNA-Damage Response in Tissue-Specific and Cancer Stem Cells.” *Cell Stem Cell* 8 (1): 16–29. <https://doi.org/10.1016/j.stem.2010.12.012>.
- Blasco, María A. 2003. “Mammalian Telomeres and Telomerase: Why They Matter for Cancer and Aging.” *European Journal of Cell Biology* 82 (9): 441–46. <https://doi.org/10.1078/0171-9335-00335>.
- Blasco, Maria A. 2007. “Telomere Length, Stem Cells and Aging.” *Nature Chemical Biology* 3 (10): 640–49. <https://doi.org/10.1038/nchembio.2007.38>.
- Bochman, Matthew L., Katrin Paeschke, and Virginia A. Zakian. 2012. “DNA Secondary Structures: Stability and Function of G-Quadruplex Structures.” *Nature Reviews. Genetics* 13 (11): 770–80. <https://doi.org/10.1038/nrg3296>.
- Broxson, Christopher, Jaelyn N. Hayner, Joshua Beckett, Linda B. Bloom, and Silvia Tornaletti. 2014. “Human AP Endonuclease Inefficiently Removes Abasic Sites within

- G4 Structures Compared to Duplex DNA.” *Nucleic Acids Research* 42 (12): 7708–19. <https://doi.org/10.1093/nar/gku417>.
- Bugaut, Anthony, and Patrizia Alberti. 2015. “Understanding the Stability of DNA G-Quadruplex Units in Long Human Telomeric Strands.” *Biochimie* 113 (June): 125–33. <https://doi.org/10.1016/j.biochi.2015.04.003>.
- Busso, Carlos S., Michael W. Lake, and Tadahide Izumi. 2010. “Posttranslational Modification of Mammalian AP Endonuclease (APE1).” *Cellular and Molecular Life Sciences: CMLS* 67 (21): 3609–20. <https://doi.org/10.1007/s00018-010-0487-3>.
- Celli, Giulia B., and Titia de Lange. 2005. “DNA Processing Is Not Required for ATM-Mediated Telomere Damage Response after TRF2 Deletion.” *Nature Cell Biology* 7 (7): 712–18. <https://doi.org/10.1038/ncb1275>.
- Cesare, Anthony J., and Roger R. Reddel. 2008. “Telomere Uncapping and Alternative Lengthening of Telomeres.” *Mechanisms of Ageing and Development* 129 (1–2): 99–108. <https://doi.org/10.1016/j.mad.2007.11.006>.
- Chen, Tianran, Chuan Liu, Heng Lu, Mingzhen Yin, Changjuan Shao, Xiaoding Hu, Jiaxue Wu, and Yajie Wang. 2017. “The Expression of APE1 in Triple-Negative Breast Cancer and Its Effect on Drug Sensitivity of Olaparib.” *Tumour Biology: The Journal of the International Society for Oncodevelopmental Biology and Medicine* 39 (10): 1010428317713390. <https://doi.org/10.1177/1010428317713390>.
- Chiarella, Sara, Antonella De Cola, Giovanni Luca Scaglione, Erminia Carletti, Vincenzo Graziano, Daniela Barcaroli, Carlo Lo Sterzo, et al. 2013. “Nucleophosmin Mutations Alter Its Nucleolar Localization by Impairing G-Quadruplex Binding at Ribosomal DNA.” *Nucleic Acids Research* 41 (5): 3228–39. <https://doi.org/10.1093/nar/gkt001>.
- Choi, Jee-Hye, Na Young Min, Jina Park, Jin Hong Kim, Soo Hyun Park, Young Jong Ko, Yoonsung Kang, et al. 2010. “TSA-Induced DNMT1 down-Regulation Represses HTERT Expression via Recruiting CTCF into Demethylated Core Promoter Region of HTERT in HCT116.” *Biochemical and Biophysical Research Communications* 391 (1): 449–54. <https://doi.org/10.1016/j.bbrc.2009.11.078>.
- Ciccia, Alberto, and Stephen J. Elledge. 2010. “The DNA Damage Response: Making It Safe to Play with Knives.” *Molecular Cell* 40 (2): 179–204. <https://doi.org/10.1016/j.molcel.2010.09.019>.
- Cohen, Scott B., Mark E. Graham, George O. Lovrecz, Nicolai Bache, Phillip J. Robinson, and Roger R. Reddel. 2007. “Protein Composition of Catalytically Active Human Telomerase from Immortal Cells.” *Science (New York, N.Y.)* 315 (5820): 1850–53. <https://doi.org/10.1126/science.1138596>.
- Colombo, E., P. Bonetti, E. Lazzerini Denchi, P. Martinelli, R. Zamponi, J.-C. Marine, K. Helin, B. Falini, and P. G. Pelicci. 2005. “Nucleophosmin Is Required for DNA Integrity and P19Arf Protein Stability.” *Molecular and Cellular Biology* 25 (20): 8874–86. <https://doi.org/10.1128/MCB.25.20.8874-8886.2005>.

- Correa, Elisa M. E., Luisina De Tullio, Pablo S. Vélez, Mariana A. Martina, Carlos E. Argaraña, and José L. Barra. 2013. "Analysis of DNA Structure and Sequence Requirements for *Pseudomonas Aeruginosa* MutL Endonuclease Activity." *Journal of Biochemistry* 154 (6): 505–11. <https://doi.org/10.1093/jb/mvt080>.
- Cusanelli, Emilio, and Pascal Chartrand. 2015. "Telomeric Repeat-Containing RNA TERRA: A Noncoding RNA Connecting Telomere Biology to Genome Integrity." *Frontiers in Genetics* 6: 143. <https://doi.org/10.3389/fgene.2015.00143>.
- Cusanelli, Emilio, Carmina Angelica Perez Romero, and Pascal Chartrand. 2013. "Telomeric Noncoding RNA TERRA Is Induced by Telomere Shortening to Nucleate Telomerase Molecules at Short Telomeres." *Molecular Cell* 51 (6): 780–91. <https://doi.org/10.1016/j.molcel.2013.08.029>.
- Dai, Jixun, Megan Carver, Chandanamali Punchihewa, Roger A. Jones, and Danzhou Yang. 2007. "Structure of the Hybrid-2 Type Intramolecular Human Telomeric G-Quadruplex in K⁺ Solution: Insights into Structure Polymorphism of the Human Telomeric Sequence." *Nucleic Acids Research* 35 (15): 4927–40. <https://doi.org/10.1093/nar/gkm522>.
- Dai, Jixun, Megan Carver, and Danzhou Yang. 2008. "Polymorphism of Human Telomeric Quadruplex Structures." *Biochimie* 90 (8): 1172–83. <https://doi.org/10.1016/j.biochi.2008.02.026>.
- De Vitis, Marco, Francesco Berardinelli, and Antonella Sgura. 2018. "Telomere Length Maintenance in Cancer: At the Crossroad between Telomerase and Alternative Lengthening of Telomeres (ALT)." *International Journal of Molecular Sciences* 19 (2). <https://doi.org/10.3390/ijms19020606>.
- Demple, Bruce, and Jung-Suk Sung. 2005. "Molecular and Biological Roles of Ape1 Protein in Mammalian Base Excision Repair." *DNA Repair, The Dale W. Mosbaugh Commemorative DNA Repair Issue*, 4 (12): 1442–49. <https://doi.org/10.1016/j.dnarep.2005.09.004>.
- Deng, Zhong, Julie Norseen, Andreas Wiedmer, Harold Riethman, and Paul M. Lieberman. 2009. "TERRA RNA Binding to TRF2 Facilitates Heterochromatin Formation and ORC Recruitment at Telomeres." *Molecular Cell* 35 (4): 403–13. <https://doi.org/10.1016/j.molcel.2009.06.025>.
- Di Maso, Vittorio, María Gabriela Mediavilla, Carlo Vascotto, Francesco Lupo, Umberto Baccarani, Claudio Avellini, Gianluca Tell, Claudio Tiribelli, and Lory Saveria Crocè. 2015. "Transcriptional Up-Regulation of APE1/Ref-1 in Hepatic Tumor: Role in Hepatocytes Resistance to Oxidative Stress and Apoptosis." *PloS One* 10 (12): e0143289. <https://doi.org/10.1371/journal.pone.0143289>.
- Doksani, Ylli, John Y. Wu, Titia de Lange, and Xiaowei Zhuang. 2013. "Super-Resolution Fluorescence Imaging of Telomeres Reveals TRF2-Dependent T-Loop Formation." *Cell* 155 (2): 345–56. <https://doi.org/10.1016/j.cell.2013.09.048>.
- Erzberger, J. P., and D. M. Wilson. 1999. "The Role of Mg²⁺ and Specific Amino Acid Residues in the Catalytic Reaction of the Major Human Abasic Endonuclease: New Insights from EDTA-Resistant Incision of Acyclic Abasic Site Analogs and Site-

- Directed Mutagenesis.” *Journal of Molecular Biology* 290 (2): 447–57.
<https://doi.org/10.1006/jmbi.1999.2888>.
- Esposito, Veronica, Luigi Martino, Giuseppe Citarella, Antonella Virgilio, Luciano Mayol, Concetta Giancola, and Aldo Galeone. 2010. “Effects of Abasic Sites on Structural, Thermodynamic and Kinetic Properties of Quadruplex Structures.” *Nucleic Acids Research* 38 (6): 2069–80. <https://doi.org/10.1093/nar/gkp1087>.
- Evans, A. R., M. Limp-Foster, and M. R. Kelley. 2000. “Going APE over Ref-1.” *Mutation Research* 461 (2): 83–108.
- Fagagna, Fabrizio d’Adda di, Philip M. Reaper, Lorena Clay-Farrace, Heike Fiegler, Philippa Carr, Thomas Von Zglinicki, Gabriele Saretzki, Nigel P. Carter, and Stephen P. Jackson. 2003. “A DNA Damage Checkpoint Response in Telomere-Initiated Senescence.” *Nature* 426 (6963): 194–98. <https://doi.org/10.1038/nature02118>.
- Fantini, Damiano, Carlo Vascotto, Marta Deganuto, Nicoletta Bivi, Stefano Gustincich, Gabriella Marcon, Franco Quadrioglio, et al. 2008. “APE1/Ref-1 Regulates PTEN Expression Mediated by Egr-1.” *Free Radical Research* 42 (1): 20–29.
<https://doi.org/10.1080/10715760701765616>.
- Fantini, Damiano, Carlo Vascotto, Daniela Marasco, Chiara D’Ambrosio, Milena Romanello, Luigi Vitagliano, Carlo Pedone, et al. 2010. “Critical Lysine Residues within the Overlooked N-Terminal Domain of Human APE1 Regulate Its Biological Functions.” *Nucleic Acids Research* 38 (22): 8239–56.
<https://doi.org/10.1093/nar/gkq691>.
- Federici, Luca, Alessandro Arcovito, Giovanni L. Scaglione, Flavio Scaloni, Carlo Lo Sterzo, Adele Di Matteo, Brunangelo Falini, Bruno Giardina, and Maurizio Brunori. 2010. “Nucleophosmin C-Terminal Leukemia-Associated Domain Interacts with G-Rich Quadruplex Forming DNA.” *The Journal of Biological Chemistry* 285 (48): 37138–49. <https://doi.org/10.1074/jbc.M110.166736>.
- Feng, J., W. D. Funk, S. S. Wang, S. L. Weinrich, A. A. Avilion, C. P. Chiu, R. R. Adams, E. Chang, R. C. Allsopp, and J. Yu. 1995. “The RNA Component of Human Telomerase.” *Science (New York, N.Y.)* 269 (5228): 1236–41.
- Fleming, Aaron M., and Cynthia J. Burrows. 2013. “G-Quadruplex Folds of the Human Telomere Sequence Alter the Site Reactivity and Reaction Pathway of Guanine Oxidation Compared to Duplex DNA.” *Chemical Research in Toxicology* 26 (4): 593–607. <https://doi.org/10.1021/tx400028y>.
- Fleming, Aaron M. and Cynthia J. Burrows. 2017. “8-Oxo-7,8-Dihydroguanine, Friend and Foe: Epigenetic-like Regulator versus Initiator of Mutagenesis.” *DNA Repair* 56: 75–83. <https://doi.org/10.1016/j.dnarep.2017.06.009>.
- Fleming, Aaron M., Yun Ding, and Cynthia J. Burrows. 2017. “Oxidative DNA Damage Is Epigenetic by Regulating Gene Transcription via Base Excision Repair.” *Proceedings of the National Academy of Sciences of the United States of America* 114 (10): 2604–9. <https://doi.org/10.1073/pnas.1619809114>.

- Fleming, Aaron M., Judy Zhu, Yun Ding, and Cynthia J. Burrows. 2017. "8-Oxo-7,8-Dihydroguanine in the Context of a Gene Promoter G-Quadruplex Is an On-Off Switch for Transcription." *ACS Chemical Biology* 12 (9): 2417–26. <https://doi.org/10.1021/acscchembio.7b00636>.
- Fleming, Aaron M., Judy Zhu, Yun Ding, Joshua A. Visser, Julia Zhu, and Cynthia J. Burrows. 2018. "Human DNA Repair Genes Possess Potential G-Quadruplex Sequences in Their Promoters and 5'-Untranslated Regions." *Biochemistry* 57 (6): 991–1002. <https://doi.org/10.1021/acs.biochem.7b01172>.
- Flores, Ignacio, and Maria A. Blasco. 2010. "The Role of Telomeres and Telomerase in Stem Cell Aging." *FEBS Letters* 584 (17): 3826–30. <https://doi.org/10.1016/j.febslet.2010.07.042>.
- Flynn, Rachel Litman, Richard C. Centore, Roderick J. O'Sullivan, Rekha Rai, Alice Tse, Zhou Songyang, Sandy Chang, Jan Karlseder, and Lee Zou. 2011. "TERRA and HnRNPA1 Orchestrate an RPA-to-POT1 Switch on Telomeric Single-Stranded DNA." *Nature* 471 (7339): 532–36. <https://doi.org/10.1038/nature09772>.
- Fontana, Gabriele A., Julia K. Reinert, Nicolas H. Thomä, and Ulrich Rass. 2018. "Shepherding DNA Ends: Rif1 Protects Telomeres and Chromosome Breaks." *Microbial Cell (Graz, Austria)* 5 (7): 327–43. <https://doi.org/10.15698/mic2018.07.639>.
- Fouché, Nicole, Anthony J. Cesare, Smaranda Willcox, Sezgin Ozgür, Sarah A. Compton, and Jack D. Griffith. 2006. "The Basic Domain of TRF2 Directs Binding to DNA Junctions Irrespective of the Presence of TTAGGG Repeats." *The Journal of Biological Chemistry* 281 (49): 37486–95. <https://doi.org/10.1074/jbc.M608778200>.
- Freudenthal, Bret D., William A. Beard, Matthew J. Cuneo, Nadezhda S. Dyrkheeva, and Samuel H. Wilson. 2015. "Capturing Snapshots of APE1 Processing DNA Damage." *Nature Structural & Molecular Biology* 22 (11): 924–31. <https://doi.org/10.1038/nsmb.3105>.
- Gallo, Angelo, Carlo Lo Sterzo, Mirko Mori, Adele Di Matteo, Ivano Bertini, Lucia Banci, Maurizio Brunori, and Luca Federici. 2012. "Structure of Nucleophosmin DNA-Binding Domain and Analysis of Its Complex with a G-Quadruplex Sequence from the c-MYC Promoter." *The Journal of Biological Chemistry* 287 (32): 26539–48. <https://doi.org/10.1074/jbc.M112.371013>.
- Georgiadis, M. M., M. Luo, R. K. Gaur, S. Delaplane, X. Li, and M. R. Kelley. 2008. "Evolution of the Redox Function in Mammalian Apurinic/Apyrimidinic Endonuclease." *Mutation Research* 643 (1–2): 54–63. <https://doi.org/10.1016/j.mrfmmm.2008.04.008>.
- Gil, Marcel E., and Thérèse L. Coetzer. 2004. "Real-Time Quantitative PCR of Telomere Length." *Molecular Biotechnology* 27 (2): 169–72. <https://doi.org/10.1385/MB:27:2:169>.
- Ginno, Paul A., Paul L. Lott, Holly C. Christensen, Ian Korf, and Frédéric Chédin. 2012. "R-Loop Formation Is a Distinctive Characteristic of Unmethylated Human CpG Island Promoters." *Molecular Cell* 45 (6): 814–25. <https://doi.org/10.1016/j.molcel.2012.01.017>.

- Göhring, Janett, Nick Fulcher, Jaroslaw Jacak, and Karel Riha. 2014. "TeloTool: A New Tool for Telomere Length Measurement from Terminal Restriction Fragment Analysis with Improved Probe Intensity Correction." *Nucleic Acids Research* 42 (3): e21–e21. <https://doi.org/10.1093/nar/gkt1315>.
- Gorman, M. A., S. Morera, D. G. Rothwell, E. de La Fortelle, C. D. Mol, J. A. Tainer, I. D. Hickson, and P. S. Freemont. 1997. "The Crystal Structure of the Human DNA Repair Endonuclease HAP1 Suggests the Recognition of Extra-Helical Deoxyribose at DNA Abasic Sites." *The EMBO Journal* 16 (21): 6548–58. <https://doi.org/10.1093/emboj/16.21.6548>.
- Grandér, D. 1998. "How Do Mutated Oncogenes and Tumor Suppressor Genes Cause Cancer?" *Medical Oncology (Northwood, London, England)* 15 (1): 20–26.
- Griffith, J., A. Bianchi, and T. de Lange. 1998. "TRF1 Promotes Parallel Pairing of Telomeric Tracts in Vitro." *Journal of Molecular Biology* 278 (1): 79–88. <https://doi.org/10.1006/jmbi.1998.1686>.
- Griffith, J. D., L. Comeau, S. Rosenfield, R. M. Stansel, A. Bianchi, H. Moss, and T. de Lange. 1999. "Mammalian Telomeres End in a Large Duplex Loop." *Cell* 97 (4): 503–14.
- Gros, Laurent, Alexander A. Ishchenko, Hiroshi Ide, Rhoderick H. Elder, and Murat K. Saparbaev. 2004. "The Major Human AP Endonuclease (Ape1) Is Involved in the Nucleotide Incision Repair Pathway." *Nucleic Acids Research* 32 (1): 73–81. <https://doi.org/10.1093/nar/gkh165>.
- Hadi, Masood Z., Krzysztof Ginalski, Lam H. Nguyen, and David M. Wilson. 2002. "Determinants in Nuclease Specificity of Ape1 and Ape2, Human Homologues of Escherichia Coli Exonuclease III." *Journal of Molecular Biology* 316 (3): 853–66. <https://doi.org/10.1006/jmbi.2001.5382>.
- Hanahan, Douglas, and Robert A. Weinberg. 2011. "Hallmarks of Cancer: The Next Generation." *Cell* 144 (5): 646–74. <https://doi.org/10.1016/j.cell.2011.02.013>.
- Hänsel-Hertsch, Robert, Dario Beraldi, Stefanie V Lensing, Giovanni Marsico, Katherine Zyner, Aled Parry, Marco Di Antonio, et al. 2016. "G-Quadruplex Structures Mark Human Regulatory Chromatin." *Nature Genetics* 48 (10): 1267–72. <https://doi.org/10.1038/ng.3662>.
- Harley, C. B., A. B. Futcher, and C. W. Greider. 1990. "Telomeres Shorten during Ageing of Human Fibroblasts." *Nature* 345 (6274): 458–60. <https://doi.org/10.1038/345458a0>.
- Harrington, L., W. Zhou, T. McPhail, R. Oulton, D. S. Yeung, V. Mar, M. B. Bass, and M. O. Robinson. 1997. "Human Telomerase Contains Evolutionarily Conserved Catalytic and Structural Subunits." *Genes & Development* 11 (23): 3109–15.
- Hass, Cathy S., Koonyee Lam, and Marc S. Wold. 2012. "Repair-Specific Functions of Replication Protein A." *The Journal of Biological Chemistry* 287 (6): 3908–18. <https://doi.org/10.1074/jbc.M111.287441>.

- Hayflick, L., and P. S. Moorhead. 1961. "The Serial Cultivation of Human Diploid Cell Strains." *Experimental Cell Research* 25 (December): 585–621.
- Heddi, Brahim, and Anh Tuân Phan. 2011. "Structure of Human Telomeric DNA in Crowded Solution." *Journal of the American Chemical Society* 133 (25): 9824–33. <https://doi.org/10.1021/ja200786q>.
- Hoeijmakers, J. H. 2001. "DNA Repair Mechanisms." *Maturitas* 38 (1): 17–22; discussion 22-23.
- Howard, Michael J., and Samuel H. Wilson. 2017. "Processive Searching Ability Varies among Members of the Gap-Filling DNA Polymerase X Family." *The Journal of Biological Chemistry* 292 (42): 17473–81. <https://doi.org/10.1074/jbc.M117.801860>.
- Huang, En, Dianbo Qu, Yi Zhang, Katerina Venderova, M. Emdadul Haque, Maxime W. C. Rousseaux, Ruth S. Slack, John M. Woulfe, and David S. Park. 2010. "The Role of Cdk5-Mediated Apurinic/Apyrimidinic Endonuclease 1 Phosphorylation in Neuronal Death." *Nature Cell Biology* 12 (6): 563–71. <https://doi.org/10.1038/ncb2058>.
- Hustedt, Nicole, and Daniel Durocher. 2016. "The Control of DNA Repair by the Cell Cycle." *Nature Cell Biology* 19 (1): 1–9. <https://doi.org/10.1038/ncb3452>.
- Ibáñez-Cabellos, José Santiago, Giselle Pérez-Machado, Marta Seco-Cervera, Ester Berenguer-Pascual, José Luis García-Giménez, and Federico V. Pallardó. 2018. "Acute Telomerase Components Depletion Triggers Oxidative Stress as an Early Event Previous to Telomeric Shortening." *Redox Biology* 14: 398–408. <https://doi.org/10.1016/j.redox.2017.10.004>.
- Ischenko, Alexander A., and Murat K. Sapparbaev. 2002. "Alternative Nucleotide Incision Repair Pathway for Oxidative DNA Damage." *Nature* 415 (6868): 183–87. <https://doi.org/10.1038/415183a>.
- Iyama, Teruaki, and David M. Wilson. 2013. "DNA Repair Mechanisms in Dividing and Non-Dividing Cells." *DNA Repair* 12 (8): 620–36. <https://doi.org/10.1016/j.dnarep.2013.04.015>.
- Izumi, T., W. D. Henner, and S. Mitra. 1996. "Negative Regulation of the Major Human AP-Endonuclease, a Multifunctional Protein." *Biochemistry* 35 (47): 14679–83. <https://doi.org/10.1021/bi961995u>.
- Izumi, Tadahide, David B. Brown, C. V. Naidu, Kishor K. Bhakat, Mark A. Macinnes, Hiroshi Saito, David J. Chen, and Sankar Mitra. 2005. "Two Essential but Distinct Functions of the Mammalian Abasic Endonuclease." *Proceedings of the National Academy of Sciences of the United States of America* 102 (16): 5739–43. <https://doi.org/10.1073/pnas.0500986102>.
- Jackson, Elias B., Corey A. Theriot, Ranajoy Chattopadhyay, Sankar Mitra, and Tadahide Izumi. 2005. "Analysis of Nuclear Transport Signals in the Human Apurinic/Apyrimidinic Endonuclease (APE1/Ref1)." *Nucleic Acids Research* 33 (10): 3303–12. <https://doi.org/10.1093/nar/gki641>.
- Kanoh, Yutaka, Seiji Matsumoto, Rino Fukatsu, Naoko Kakusho, Nobuaki Kono, Claire Renard-Guillet, Koji Masuda, et al. 2015. "Rif1 Binds to G Quadruplexes and

- Suppresses Replication over Long Distances.” *Nature Structural & Molecular Biology* 22 (11): 889–97. <https://doi.org/10.1038/nsmb.3102>.
- Kaur, Gagandeep, Ravi P. Cholia, Anil K. Mantha, and Raj Kumar. 2014. “DNA Repair and Redox Activities and Inhibitors of Apurinic/Apyrimidinic Endonuclease 1/Redox Effector Factor 1 (APE1/Ref-1): A Comparative Analysis and Their Scope and Limitations toward Anticancer Drug Development.” *Journal of Medicinal Chemistry* 57 (24): 10241–56. <https://doi.org/10.1021/jm500865u>.
- Kelley, Mark R., Millie M. Georgiadis, and Melissa L. Fishel. 2012. “APE1/Ref-1 Role in Redox Signaling: Translational Applications of Targeting the Redox Function of the DNA Repair/Redox Protein APE1/Ref-1.” *Current Molecular Pharmacology* 5 (1): 36–53.
- Kim, Wan-Cheol, Dustin King, and Chow H. Lee. 2010. “RNA-Cleaving Properties of Human Apurinic/Apyrimidinic Endonuclease 1 (APE1).” *International Journal of Biochemistry and Molecular Biology* 1 (1): 12–25.
- Kladova, Olga A., Milena Bazlekowa-Karaban, Sonia Bacconnais, Olivier Piétremont, Alexander A. Ishchenko, Bakhyt T. Matkarimov, Danila A. Iakovlev, et al. 2018. “The Role of the N-Terminal Domain of Human Apurinic/Apyrimidinic Endonuclease 1, APE1, in DNA Glycosylase Stimulation.” *DNA Repair* 64: 10–25. <https://doi.org/10.1016/j.dnarep.2018.02.001>.
- Lane, Andrew N., J. Brad Chaires, Robert D. Gray, and John O. Trent. 2008. “Stability and Kinetics of G-Quadruplex Structures.” *Nucleic Acids Research* 36 (17): 5482–5515. <https://doi.org/10.1093/nar/gkn517>.
- Lange, Titia de. 2004. “T-Loops and the Origin of Telomeres.” *Nature Reviews. Molecular Cell Biology* 5 (4): 323–29. <https://doi.org/10.1038/nrm1359>.
- . 2005. “Shelterin: The Protein Complex That Shapes and Safeguards Human Telomeres.” *Genes & Development* 19 (18): 2100–2110. <https://doi.org/10.1101/gad.1346005>.
- Lee, Ok-Hee, Hyeung Kim, Quanyuan He, Hwa Jin Baek, Dong Yang, Lih-Yow Chen, Jiancong Liang, et al. 2011. “Genome-Wide YFP Fluorescence Complementation Screen Identifies New Regulators for Telomere Signaling in Human Cells.” *Molecular & Cellular Proteomics: MCP* 10 (2): M110.001628. <https://doi.org/10.1074/mcp.M110.001628>.
- Li, Chun, Ming-Yao Wu, Ying-Rui Liang, and Xian-Ying Wu. 2003. “Correlation between Expression of Human Telomerase Subunits and Telomerase Activity in Esophageal Squamous Cell Carcinoma.” *World Journal of Gastroenterology* 9 (11): 2395–99.
- Li, Mengxia, Jens Völker, Kenneth J. Breslauer, and David M. Wilson III. 2014. “APE1 Incision Activity at Abasic Sites in Tandem Repeat Sequences.” *Journal of Molecular Biology* 426 (11): 2183–98. <https://doi.org/10.1016/j.jmb.2014.03.014>.

- Li, Mengxia, and David M. Wilson. 2014. "Human Apurinic/Apyrimidinic Endonuclease 1." *Antioxidants & Redox Signaling* 20 (4): 678–707. <https://doi.org/10.1089/ars.2013.5492>.
- Li, Mengxia, Xiao Yang, Xianfeng Lu, Nan Dai, Shiheng Zhang, Yi Cheng, Lei Zhang, et al. 2018. "APE1 Deficiency Promotes Cellular Senescence and Premature Aging Features." *Nucleic Acids Research*, May. <https://doi.org/10.1093/nar/gky326>.
- Limpose, Kristin L., Anita H. Corbett, and Paul W. Doetsch. 2017. "BERing the Burden of Damage: Pathway Crosstalk and Posttranslational Modification of Base Excision Repair Proteins Regulate DNA Damage Management." *DNA Repair* 56: 51–64. <https://doi.org/10.1016/j.dnarep.2017.06.007>.
- Lin, Ping, Maral E. Mobasher, Yasaman Hakakian, Veena Kakarla, Anum F. Naseem, Heliya Ziai, and Faizan Alawi. 2015. "Differential Requirements for H/ACA Ribonucleoprotein Components in Cell Proliferation and Response to DNA Damage." *Histochemistry and Cell Biology* 144 (6): 543–58. <https://doi.org/10.1007/s00418-015-1359-6>.
- Lirussi, Lisa, Giulia Antoniali, Chiara D'Ambrosio, Andrea Scaloni, Hilde Nilsen, Gianluca Tell, Lisa Lirussi, et al. 2016. "APE1 Polymorphic Variants Cause Persistent Genomic Stress and Affect Cancer Cell Proliferation." *Oncotarget* 7 (18): 26293–306.
- Lirussi, Lisa, Giulia Antoniali, Carlo Vascotto, Chiara D'Ambrosio, Mattia Poletto, Milena Romanello, Daniela Marasco, et al. 2012. "Nucleolar Accumulation of APE1 Depends on Charged Lysine Residues That Undergo Acetylation upon Genotoxic Stress and Modulate Its BER Activity in Cells." *Molecular Biology of the Cell* 23 (20): 4079–96. <https://doi.org/10.1091/mbc.E12-04-0299>.
- Liu, Dan, Matthew S. O'Connor, Jun Qin, and Zhou Songyang. 2004. "Telosome, a Mammalian Telomere-Associated Complex Formed by Multiple Telomeric Proteins." *The Journal of Biological Chemistry* 279 (49): 51338–42. <https://doi.org/10.1074/jbc.M409293200>.
- Liu, Pingfang, and Bruce Dimple. 2010. "DNA Repair in Mammalian Mitochondria: Much More than We Thought?" *Environmental and Molecular Mutagenesis* 51 (5): 417–26. <https://doi.org/10.1002/em.20576>.
- Loayza, Diego, and Titia De Lange. 2003. "POT1 as a Terminal Transducer of TRF1 Telomere Length Control." *Nature* 423 (6943): 1013–18. <https://doi.org/10.1038/nature01688>.
- López de Silanes, Isabel, Martina Stagno d'Alcontres, and Maria A. Blasco. 2010. "TERRA Transcripts Are Bound by a Complex Array of RNA-Binding Proteins." *Nature Communications* 1 (June): 33. <https://doi.org/10.1038/ncomms1032>.
- Luke, Brian, and Joachim Lingner. 2009. "TERRA: Telomeric Repeat-Containing RNA." *The EMBO Journal* 28 (17): 2503–10. <https://doi.org/10.1038/emboj.2009.166>.
- Luo, Meihua, Jun Zhang, Hongzhen He, Dian Su, Qiuqia Chen, Michael L. Gross, Mark R. Kelley, and Millie M. Georgiadis. 2012. "Characterization of the Redox Activity and

Disulfide Bond Formation in Apurinic/Apyrimidinic Endonuclease.” *Biochemistry* 51 (2): 695–705. <https://doi.org/10.1021/bi201034z>.

Madlener, Sibylle, Thomas Ströbel, Sarah Vose, Okay Saydam, Brendan D. Price, Bruce Dimple, and Nurten Saydam. 2013. “Essential Role for Mammalian Apurinic/Apyrimidinic (AP) Endonuclease Ape1/Ref-1 in Telomere Maintenance.” *Proceedings of the National Academy of Sciences of the United States of America* 110 (44): 17844–49. <https://doi.org/10.1073/pnas.1304784110>.

Malfatti, Matilde Clarissa, Sathya Balachander, Giulia Antoniali, Kyung Duk Koh, Christine Saint-Pierre, Didier Gasparutto, Hyongi Chon, Robert J. Crouch, Francesca Storici, and Gianluca Tell. 2017. “Abasic and Oxidized Ribonucleotides Embedded in DNA Are Processed by Human APE1 and Not by RNase H2.” *Nucleic Acids Research* 45 (19): 11193–212. <https://doi.org/10.1093/nar/gkx723>.

Manvilla, Brittney A., Edwin Pozharski, Eric A. Toth, and Alexander C. Drohat. 2013. “Structure of Human Apurinic/Apyrimidinic Endonuclease 1 with the Essential Mg²⁺ Cofactor.” *Acta Crystallographica. Section D, Biological Crystallography* 69 (Pt 12): 2555–62. <https://doi.org/10.1107/S0907444913027042>.

Marenstein, Dina R., David M. Wilson III, and George W. Teebor. 2004. “Human AP Endonuclease (APE1) Demonstrates Endonucleolytic Activity against AP Sites in Single-Stranded DNA.” *DNA Repair* 3 (5): 527–33. <https://doi.org/10.1016/j.dnarep.2004.01.010>.

Markkanen, Enni. 2017. “Not Breathing Is Not an Option: How to Deal with Oxidative DNA Damage.” *DNA Repair* 59: 82–105. <https://doi.org/10.1016/j.dnarep.2017.09.007>.

Masai, Hisao, Naoko Kakusho, Rino Fukatsu, Yue Ma, Keisuke Iida, Yutaka Kanoh, and Kazuo Nagasawa. 2018. “Molecular Architecture of G-Quadruplex Structures Generated on Duplex Rif1 Binding Sequences.” *The Journal of Biological Chemistry*, September. <https://doi.org/10.1074/jbc.RA118.005240>.

Masani, S., L. Han, and K. Yu. 2013. “Apurinic/Apyrimidinic Endonuclease 1 Is the Essential Nuclease during Immunoglobulin Class Switch Recombination.” *Molecular and Cellular Biology* 33 (7): 1468–73. <https://doi.org/10.1128/MCB.00026-13>.

Masuda, Y., R. A. Bennett, and B. Dimple. 1998. “Dynamics of the Interaction of Human Apurinic Endonuclease (Ape1) with Its Substrate and Product.” *The Journal of Biological Chemistry* 273 (46): 30352–59.

Meier, U. Thomas. 2005. “The Many Facets of H/ACA Ribonucleoproteins.” *Chromosoma* 114 (1): 1–14. <https://doi.org/10.1007/s00412-005-0333-9>.

Miller, Adam S., Lata Balakrishnan, Noah A. Buncher, Patricia L. Opresko, and Robert A. Bambara. 2012. “Telomere Proteins POT1, TRF1 and TRF2 Augment Long-Patch Base Excision Repair in Vitro.” *Cell Cycle* 11 (5): 998–1007. <https://doi.org/10.4161/cc.11.5.19483>.

Mitrea, D. M., C. R. Grace, M. Buljan, M.-K. Yun, N. J. Pytel, J. Satumba, A. Nourse, et al. 2014. “Structural Polymorphism in the N-Terminal Oligomerization Domain of

- NPM1.” *Proceedings of the National Academy of Sciences* 111 (12): 4466–71. <https://doi.org/10.1073/pnas.1321007111>.
- Mol, C. D., D. J. Hosfield, and J. A. Tainer. 2000. “Abasic Site Recognition by Two Apurinic/Apyrimidinic Endonuclease Families in DNA Base Excision Repair: The 3’ Ends Justify the Means.” *Mutation Research* 460 (3–4): 211–29.
- Mol, C. D., T. Izumi, S. Mitra, and J. A. Tainer. 2000. “DNA-Bound Structures and Mutants Reveal Abasic DNA Binding by APE1 and DNA Repair Coordination.” *Nature* 403 (6768): 451–56. <https://doi.org/10.1038/35000249>.
- Moor, Nina A., Inna A. Vasil’eva, Rashid O. Anarbaev, Alfred A. Antson, and Olga I. Lavrik. 2015. “Quantitative Characterization of Protein–Protein Complexes Involved in Base Excision DNA Repair.” *Nucleic Acids Research* 43 (12): 6009–22. <https://doi.org/10.1093/nar/gkv569>.
- Mundle, Sophia T., James C. Delaney, John M. Essigmann, and Phyllis R. Strauss. 2009. “Enzymatic Mechanism of Human Apurinic/Apyrimidinic Endonuclease against a THF AP Site Model Substrate.” *Biochemistry* 48 (1): 19–26. <https://doi.org/10.1021/bi8016137>.
- Muntoni, Alessandra, Axel A. Neumann, Mark Hills, and Roger R. Reddel. 2009. “Telomere Elongation Involves Intra-Molecular DNA Replication in Cells Utilizing Alternative Lengthening of Telomeres.” *Human Molecular Genetics* 18 (6): 1017–27. <https://doi.org/10.1093/hmg/ddn436>.
- Ng, Laura J., Jennifer E. Croypley, Hilda A. Pickett, Roger R. Reddel, and Catherine M. Suter. 2009. “Telomerase Activity Is Associated with an Increase in DNA Methylation at the Proximal Subtelomere and a Reduction in Telomeric Transcription.” *Nucleic Acids Research* 37 (4): 1152–59. <https://doi.org/10.1093/nar/gkn1030>.
- O’Callaghan, Nathan, Varinderpal Dhillon, Philip Thomas, and Michael Fenech. 2008. “A Quantitative Real-Time PCR Method for Absolute Telomere Length.” *BioTechniques* 44 (6): 807–9. <https://doi.org/10.2144/000112761>.
- Oganesian, Liana, and Jan Karlseder. 2009. “Telomeric Armor: The Layers of End Protection.” *Journal of Cell Science* 122 (Pt 22): 4013–25. <https://doi.org/10.1242/jcs.050567>.
- Olovnikov, Alexey M. 1996. “Telomeres, Telomerase, and Aging: Origin of the Theory.” *Experimental Gerontology* 31 (4): 443–48. [https://doi.org/10.1016/0531-5565\(96\)00005-8](https://doi.org/10.1016/0531-5565(96)00005-8).
- Opresko, Patricia L., Jinshui Fan, Shamika Danzy, David M. Wilson, and Vilhelm A. Bohr. 2005. “Oxidative Damage in Telomeric DNA Disrupts Recognition by TRF1 and TRF2.” *Nucleic Acids Research* 33 (4): 1230–39. <https://doi.org/10.1093/nar/gki273>.
- Paeschke, Katrin, Matthew L. Bochman, P. Daniela Garcia, Petr Cejka, Katherine L. Friedman, Stephen C. Kowalczykowski, and Virginia A. Zakian. 2013. “Pif1 Family Helicases Suppress Genome Instability at G-Quadruplex Motifs.” *Nature* 497 (7450): 458–62. <https://doi.org/10.1038/nature12149>.

- Park, E. M., M. K. Shigenaga, P. Degan, T. S. Korn, J. W. Kitzler, C. M. Wehr, P. Kolachana, and B. N. Ames. 1992. "Assay of Excised Oxidative DNA Lesions: Isolation of 8-Oxoguanine and Its Nucleoside Derivatives from Biological Fluids with a Monoclonal Antibody Column." *Proceedings of the National Academy of Sciences of the United States of America* 89 (8): 3375–79.
- Pastukh, Viktor, Justin T. Roberts, David W. Clark, Gina C. Bardwell, Mita Patel, Abu-Bakr Al-Mehdi, Glen M. Borchert, and Mark N. Gillespie. 2015. "An Oxidative DNA 'Damage' and Repair Mechanism Localized in the VEGF Promoter Is Important for Hypoxia-Induced VEGF mRNA Expression." *American Journal of Physiology. Lung Cellular and Molecular Physiology* 309 (11): L1367-1375. <https://doi.org/10.1152/ajplung.00236.2015>.
- Pedroso, Ilene M., William Hayward, and Terace M. Fletcher. 2009. "The Effect of the TRF2 N-Terminal and TRFH Regions on Telomeric G-Quadruplex Structures." *Nucleic Acids Research* 37 (5): 1541–54. <https://doi.org/10.1093/nar/gkn1081>.
- Perillo, Bruno, Maria Neve Ombra, Alessandra Bertoni, Concetta Cuzzo, Silvana Sacchetti, Annarita Sasso, Lorenzo Chiariotti, Antonio Malorni, Ciro Abbondanza, and Enrico V. Avvedimento. 2008. "DNA Oxidation as Triggered by H3K9me2 Demethylation Drives Estrogen-Induced Gene Expression." *Science (New York, N.Y.)* 319 (5860): 202–6. <https://doi.org/10.1126/science.1147674>.
- Poletto, Mattia, Carla Di Loreto, Daniela Marasco, Elena Poletto, Fabio Puglisi, Giuseppe Damante, and Gianluca Tell. 2012. "Acetylation on Critical Lysine Residues of Apurinic/Apyrimidinic Endonuclease 1 (APE1) in Triple Negative Breast Cancers." *Biochemical and Biophysical Research Communications* 424 (1): 34–39. <https://doi.org/10.1016/j.bbrc.2012.06.039>.
- Poletto, Mattia, Matilde C. Malfatti, Dorjbal Dorjsuren, Pasqualina L. Scognamiglio, Daniela Marasco, Carlo Vascotto, Ajit Jadhav, et al. 2016. "Inhibitors of the Apurinic/Apyrimidinic Endonuclease 1 (APE1)/Nucleophosmin (NPM1) Interaction That Display Anti-Tumor Properties." *Molecular Carcinogenesis* 55 (5): 688–704. <https://doi.org/10.1002/mc.22313>.
- Poletto, Mattia, Carlo Vascotto, Pasqualina L. Scognamiglio, Lisa Lirussi, Daniela Marasco, and Gianluca Tell. 2013. "Role of the Unstructured N-Terminal Domain of the HAPE1 (Human Apurinic/Apyrimidinic Endonuclease 1) in the Modulation of Its Interaction with Nucleic Acids and NPM1 (Nucleophosmin)." *Biochemical Journal* 452 (3): 545–57. <https://doi.org/10.1042/BJ20121277>.
- Porro, Antonio, Sascha Feuerhahn, Patrick Reichenbach, and Joachim Lingner. 2010. "Molecular Dissection of Telomeric Repeat-Containing RNA Biogenesis Unveils the Presence of Distinct and Multiple Regulatory Pathways." *Molecular and Cellular Biology* 30 (20): 4808–17. <https://doi.org/10.1128/MCB.00460-10>.
- Postberg, Jan, Maksym Tsytlonok, Daniela Sparvoli, Daniela Rhodes, and Hans J. Lipps. 2012. "A Telomerase-Associated RecQ Protein-like Helicase Resolves Telomeric G-Quadruplex Structures during Replication." *Gene* 497 (2): 147–54. <https://doi.org/10.1016/j.gene.2012.01.068>.

- Rai, Ganesh, Vaddadi N. Vyjayanti, Dorjbal Dorjsuren, Anton Simeonov, Ajit Jadhav, David M. Wilson, and David J. Maloney. 2010. "Small Molecule Inhibitors of the Human Apurinic/Apyrimidinic Endonuclease 1 (APE1)." In *Probe Reports from the NIH Molecular Libraries Program*. Bethesda (MD): National Center for Biotechnology Information (US). <http://www.ncbi.nlm.nih.gov/books/NBK133448/>.
- Rai, Ganesh, Vaddadi N. Vyjayanti, Dorjbal Dorjsuren, Anton Simeonov, Ajit Jadhav, David M. Wilson, and David J. Maloney. 2012. "Synthesis, Biological Evaluation, and Structure-Activity Relationships of a Novel Class of Apurinic/Apyrimidinic Endonuclease 1 Inhibitors." *Journal of Medicinal Chemistry* 55 (7): 3101–12. <https://doi.org/10.1021/jm201537d>.
- Rai, Rekha, Yong Chen, Ming Lei, and Sandy Chang. 2016. "TRF2-RAP1 Is Required to Protect Telomeres from Engaging in Homologous Recombination-Mediated Deletions and Fusions." *Nature Communications* 7 (March): 10881. <https://doi.org/10.1038/ncomms10881>.
- Renaud, S., D. Loukinov, Z. Abdullaev, I. Guilleret, F. T. Bosman, V. Lobanenko, and J. Benhattar. 2007. "Dual Role of DNA Methylation inside and Outside of CTCF-Binding Regions in the Transcriptional Regulation of the Telomerase HTERT Gene." *Nucleic Acids Research* 35 (4): 1245–56. <https://doi.org/10.1093/nar/gkl1125>.
- Ribes-Zamora, Albert, Sandra M. Indiviglio, Ivana Mihalek, Christopher L. Williams, and Alison A. Bertuch. 2013. "TRF2 Interaction with Ku Heterotetramerization Interface Gives Insight into C-NHEJ Prevention at Human Telomeres." *Cell Reports* 5 (1): 194–206. <https://doi.org/10.1016/j.celrep.2013.08.040>.
- Rivkees, S. A., and M. R. Kelley. 1994. "Expression of a Multifunctional DNA Repair Enzyme Gene, Apurinic/Apyrimidinic Endonuclease (APE; Ref-1) in the Suprachiasmatic, Supraoptic and Paraventricular Nuclei." *Brain Research* 666 (1): 137–42.
- Robson, C. N., D. Hochhauser, R. Craig, K. Rack, V. J. Buckle, and I. D. Hickson. 1992. "Structure of the Human DNA Repair Gene HAP1 and Its Localisation to Chromosome 14q 11.2-12." *Nucleic Acids Research* 20 (17): 4417–21.
- Roychoudhury, Shrabasti, Somsubhra Nath, Heyu Song, Muralidhar L. Hegde, Larry J. Bellot, Anil K. Mantha, Shiladitya Sengupta, Sutapa Ray, Amarnath Natarajan, and Kishor K. Bhakat. 2016. "Human AP-Endonuclease (APE1) Is Acetylated at DNA Damage Sites in Chromatin and Acetylation Modulates Its DNA Repair Activity." *Molecular and Cellular Biology*, December. <https://doi.org/10.1128/MCB.00401-16>.
- Sanderson, B. J., C. N. Chang, A. P. Grollman, and W. D. Henner. 1989. "Mechanism of DNA Cleavage and Substrate Recognition by a Bovine Apurinic Endonuclease." *Biochemistry* 28 (9): 3894–3901.
- Scognamiglio, Pasqualina Liana, Concetta Di Natale, Marilisa Leone, Mattia Poletto, Luigi Vitagliano, Gianluca Tell, and Daniela Marasco. 2014. "G-Quadruplex DNA Recognition by Nucleophosmin: New Insights from Protein Dissection." *Biochimica et Biophysica Acta (BBA) - General Subjects* 1840 (6): 2050–59. <https://doi.org/10.1016/j.bbagen.2014.02.017>.

- Sengupta, S., A. K. Mantha, S. Mitra, and K. K. Bhakat. 2011. "Human AP Endonuclease (APE1/Ref-1) and Its Acetylation Regulate YB-1-P300 Recruitment and RNA Polymerase II Loading in the Drug-Induced Activation of Multidrug Resistance Gene MDR1." *Oncogene* 30 (4): 482–93. <https://doi.org/10.1038/onc.2010.435>.
- Simms, Carrie L., and Hani S. Zaher. 2016. "Quality Control of Chemically Damaged RNA." *Cellular and Molecular Life Sciences: CMLS* 73 (19): 3639–53. <https://doi.org/10.1007/s00018-016-2261-7>.
- Smogorzewska, A., B. van Steensel, A. Bianchi, S. Oelmann, M. R. Schaefer, G. Schnapp, and T. de Lange. 2000. "Control of Human Telomere Length by TRF1 and TRF2." *Molecular and Cellular Biology* 20 (5): 1659–68.
- Smogorzewska, Agata, Jan Karlseder, Heidi Holtgreve-Grez, Anna Jauch, and Titia de Lange. 2002. "DNA Ligase IV-Dependent NHEJ of Deprotected Mammalian Telomeres in G1 and G2." *Current Biology: CB* 12 (19): 1635–44.
- Sobol, R. W., J. K. Horton, R. Kühn, H. Gu, R. K. Singhal, R. Prasad, K. Rajewsky, and S. H. Wilson. 1996. "Requirement of Mammalian DNA Polymerase-Beta in Base-Excision Repair." *Nature* 379 (6561): 183–86. <https://doi.org/10.1038/379183a0>.
- Steenken, Steen, and Slobodan V. Jovanovic. 1997. "How Easily Oxidizable Is DNA? One-Electron Reduction Potentials of Adenosine and Guanosine Radicals in Aqueous Solution." *Journal of the American Chemical Society* 119 (3): 617–18. <https://doi.org/10.1021/ja962255b>.
- Su, Dian, Sarah Delaplane, Meihua Luo, Don L. Rempel, Bich Vu, Mark R. Kelley, Michael L. Gross, and Millie M. Georgiadis. 2011. "Interactions of Apurinic/Apyrimidinic Endonuclease with a Redox Inhibitor: Evidence for an Alternate Conformation of the Enzyme." *Biochemistry* 50 (1): 82–92. <https://doi.org/10.1021/bi101248s>.
- Sung, Jung-Suk, Michael S. DeMott, and Bruce Demple. 2005. "Long-Patch Base Excision DNA Repair of 2-Deoxyribonolactone Prevents the Formation of DNA-Protein Cross-Links with DNA Polymerase Beta." *The Journal of Biological Chemistry* 280 (47): 39095–103. <https://doi.org/10.1074/jbc.M506480200>.
- Takeshita, M., C. N. Chang, F. Johnson, S. Will, and A. P. Grollman. 1987. "Oligodeoxynucleotides Containing Synthetic Abasic Sites. Model Substrates for DNA Polymerases and Apurinic/Apyrimidinic Endonucleases." *Journal of Biological Chemistry* 262 (21): 10171–79.
- Tell, Gianluca, Giuseppe Damante, David Caldwell, and Mark R. Kelley. 2005. "The Intracellular Localization of APE1/Ref-1: More than a Passive Phenomenon?" *Antioxidants & Redox Signaling* 7 (3–4): 367–84. <https://doi.org/10.1089/ars.2005.7.367>.
- Tell, Gianluca, Franco Quadrifoglio, Claudio Tiribelli, and Mark R. Kelley. 2009. "The Many Functions of APE1/Ref-1: Not Only a DNA Repair Enzyme." *Antioxidants & Redox Signaling* 11 (3): 601–20. <https://doi.org/10.1089/ars.2008.2194>.

- Tell, Gianluca, David M. Wilson, and Chow H. Lee. 2010. "Intrusion of a DNA Repair Protein in the RNome World: Is This the Beginning of a New Era?" *Molecular and Cellular Biology* 30 (2): 366–71. <https://doi.org/10.1128/MCB.01174-09>.
- Thakur, S., M. Dhiman, G. Tell, and A. K. Mantha. 2015. "A Review on Protein-Protein Interaction Network of APE1/Ref-1 and Its Associated Biological Functions." *Cell Biochemistry and Function* 33 (3): 101–12. <https://doi.org/10.1002/cbf.3100>.
- Thakur, Shweta, Bibekananda Sarkar, Ravi P. Cholia, Nandini Gautam, Monisha Dhiman, and Anil K. Mantha. 2014. "APE1/Ref-1 as an Emerging Therapeutic Target for Various Human Diseases: Phytochemical Modulation of Its Functions." *Experimental & Molecular Medicine* 46 (July): e106. <https://doi.org/10.1038/emm.2014.42>.
- Theruvathu, Jacob A., Agus Darwanto, Chia Wei Hsu, and Lawrence C. Sowers. 2014. "The Effect of Pot1 Binding on the Repair of Thymine Analogs in a Telomeric DNA Sequence." *Nucleic Acids Research* 42 (14): 9063–73. <https://doi.org/10.1093/nar/gku602>.
- Tiacci, E, A Spanhol-Rosseto, M P Martelli, L Pasqualucci, H Quentmeier, V Grossmann, H G Drexler, and B Falini. 2012. "The NPM1 Wild-Type OCI-AML2 and the NPM1-Mutated OCI-AML3 Cell Lines Carry DNMT3A Mutations." *Leukemia* 26 (3): 554–57. <https://doi.org/10.1038/leu.2011.238>.
- Timofeyeva, N. A., V. V. Koval, D. G. Knorre, D. O. Zharkov, M. K. Saparbaev, A. A. Ishchenko, and O. S. Fedorova. 2009. "Conformational Dynamics of Human AP Endonuclease in Base Excision and Nucleotide Incision Repair Pathways." *Journal of Biomolecular Structure & Dynamics* 26 (5): 637–52. <https://doi.org/10.1080/07391102.2009.10507278>.
- Timofeyeva, Nadezhda A., Vladimir V. Koval, Alexander A. Ishchenko, Murat K. Saparbaev, and Olga S. Fedorova. 2011. "Lys98 Substitution in Human AP Endonuclease 1 Affects the Kinetic Mechanism of Enzyme Action in Base Excision and Nucleotide Incision Repair Pathways." *PloS One* 6 (9): e24063. <https://doi.org/10.1371/journal.pone.0024063>.
- Vascotto, C., L. Lirussi, M. Poletto, M. Tiribelli, D. Damiani, D. Fabbro, G. Damante, B. Demple, E. Colombo, and G. Tell. 2014. "Functional Regulation of the Apurinic/Apyrimidinic Endonuclease 1 by Nucleophosmin: Impact on Tumor Biology." *Oncogene* 33 (22): 2876–87. <https://doi.org/10.1038/onc.2013.251>.
- Vascotto, Carlo, Damiano Fantini, Milena Romanello, Laura Cesaratto, Marta Deganuto, Antonio Leonardi, J. Pablo Radicella, et al. 2009. "APE1/Ref-1 Interacts with NPM1 within Nucleoli and Plays a Role in the RRNA Quality Control Process." *Molecular and Cellular Biology* 29 (7): 1834–54. <https://doi.org/10.1128/MCB.01337-08>.
- Venteicher, Andrew S., Eladio B. Abreu, Zhaojing Meng, Kelly E. McCann, Rebecca M. Terns, Timothy D. Veenstra, Michael P. Terns, and Steven E. Artandi. 2009. "A Human Telomerase Holoenzyme Protein Required for Cajal Body Localization and

- Telomere Synthesis.” *Science (New York, N.Y.)* 323 (5914): 644–48.
<https://doi.org/10.1126/science.1165357>.
- Verdun, Ramiro E., and Jan Karlseder. 2006. “The DNA Damage Machinery and Homologous Recombination Pathway Act Consecutively to Protect Human Telomeres.” *Cell* 127 (4): 709–20. <https://doi.org/10.1016/j.cell.2006.09.034>.
- Virgilio, Antonella, Luigi Petraccone, Veronica Esposito, Giuseppe Citarella, Concetta Giancola, and Aldo Galeone. 2012. “The Abasic Site Lesions in the Human Telomeric Sequence d[TA(G3T2A)3G3]: A Thermodynamic Point of View.” *Biochimica et Biophysica Acta (BBA) - General Subjects* 1820 (12): 2037–43.
<https://doi.org/10.1016/j.bbagen.2012.09.011>.
- Vohhodina, Jekaterina, D. Paul Harkin, and Kieran I. Savage. 2016. “Dual Roles of DNA Repair Enzymes in RNA Biology/Post-Transcriptional Control.” *Wiley Interdisciplinary Reviews. RNA* 7 (5): 604–19. <https://doi.org/10.1002/wrna.1353>.
- Walker, L. J., C. N. Robson, E. Black, D. Gillespie, and I. D. Hickson. 1993. “Identification of Residues in the Human DNA Repair Enzyme HAP1 (Ref-1) That Are Essential for Redox Regulation of Jun DNA Binding.” *Molecular and Cellular Biology* 13 (9): 5370–76.
- Wallace. 2013. “DNA Glycosylases Search for and Remove Oxidized DNA Bases.” *Environmental and Molecular Mutagenesis* 54 (9): 691–704.
<https://doi.org/10.1002/em.21820>.
- Wang, Richard C., Agata Smogorzewska, and Titia de Lange. 2004. “Homologous Recombination Generates T-Loop-Sized Deletions at Human Telomeres.” *Cell* 119 (3): 355–68. <https://doi.org/10.1016/j.cell.2004.10.011>.
- Wilson, David M., and Vilhelm A. Bohr. 2007. “The Mechanics of Base Excision Repair, and Its Relationship to Aging and Disease.” *DNA Repair* 6 (4): 544–59.
<https://doi.org/10.1016/j.dnarep.2006.10.017>.
- Wilson, David M., and Anton Simeonov. 2010. “Small Molecule Inhibitors of DNA Repair Nuclease Activities of APE1.” *Cellular and Molecular Life Sciences: CMLS* 67 (21): 3621–31. <https://doi.org/10.1007/s00018-010-0488-2>.
- Xin, Huawei, Dan Liu, Ma Wan, Amin Safari, Hyeung Kim, Wen Sun, Matthew S. O’Connor, and Zhou Songyang. 2007. “TPP1 Is a Homologue of Ciliate TEBP-Beta and Interacts with POT1 to Recruit Telomerase.” *Nature* 445 (7127): 559–62.
<https://doi.org/10.1038/nature05469>.
- Xu, Yan, and Makoto Komiyama. 2012. “Structure, Function and Targeting of Human Telomere RNA.” *Methods (San Diego, Calif.)* 57 (1): 100–105.
<https://doi.org/10.1016/j.ymeth.2012.02.015>.
- Yamazaki, Satoshi, Motoshi Hayano, and Hisao Masai. 2013. “Replication Timing Regulation of Eukaryotic Replicons: Rif1 as a Global Regulator of Replication Timing.” *Trends in Genetics: TIG* 29 (8): 449–60.
<https://doi.org/10.1016/j.tig.2013.05.001>.

Ye, Jeffrey Zheng-Sheng, Dirk Hockemeyer, Andrew N. Krutchinsky, Diego Loayza, Sarah M. Hooper, Brian T. Chait, and Titia de Lange. 2004. "POT1-Interacting Protein PIP1: A Telomere Length Regulator That Recruits POT1 to the TIN2/TRF1 Complex." *Genes & Development* 18 (14): 1649–54. <https://doi.org/10.1101/gad.1215404>.

Yoshida, Akira, Yoshimasa Urasaki, Mark Waltham, Ann-Charlotte Bergman, Philippe Pourquier, Dominic G. Rothwell, Manabu Inuzuka, et al. 2003. "Human Apurinic/Apyrimidinic Endonuclease (Ape1) and Its N-Terminal Truncated Form (AN34) Are Involved in DNA Fragmentation during Apoptosis." *The Journal of Biological Chemistry* 278 (39): 37768–76. <https://doi.org/10.1074/jbc.M304914200>.

Yu, Tai-Yuan, Yu-wen Kao, and Jing-Jer Lin. 2014. "Telomeric Transcripts Stimulate Telomere Recombination to Suppress Senescence in Cells Lacking Telomerase." *Proceedings of the National Academy of Sciences of the United States of America* 111 (9): 3377–82. <https://doi.org/10.1073/pnas.1307415111>.

Yun, Maximina H., and Kevin Hiom. 2009. "CtIP-BRCA1 Modulates the Choice of DNA Double-Strand-Break Repair Pathway throughout the Cell Cycle." *Nature* 459 (7245): 460–63. <https://doi.org/10.1038/nature07955>.

Zaky, Amira, Carlos Busso, Tadahide Izumi, Ranajoy Chattopadhyay, Ahmad Bassiouny, Sankar Mitra, and Kishor K. Bhakat. 2008. "Regulation of the Human AP-Endonuclease (APE1/Ref-1) Expression by the Tumor Suppressor P53 in Response to DNA Damage." *Nucleic Acids Research* 36 (5): 1555–66. <https://doi.org/10.1093/nar/gkm1173>.

Zarakowska, Ewelina, Daniel Gackowski, Marek Foksinski, and Ryszard Olinski. 2014. "Are 8-Oxoguanine (8-OxoGua) and 5-Hydroxymethyluracil (5-HmUra) Oxidatively Damaged DNA Bases or Transcription (Epigenetic) Marks?" *Mutation Research. Genetic Toxicology and Environmental Mutagenesis* 764–765 (April): 58–63. <https://doi.org/10.1016/j.mrgentox.2013.09.002>.

Zhou, Jia, Jany Chan, Marie Lambelé, Timur Yusufzai, Jason Stumpff, Patricia L. Opresko, Markus Thali, and Susan S. Wallace. 2017. "NEIL3 Repairs Telomere Damage during S Phase to Secure Chromosome Segregation at Mitosis." *Cell Reports* 20 (9): 2044–56. <https://doi.org/10.1016/j.celrep.2017.08.020>.

Zhou, Jia, Aaron M. Fleming, April M. Averill, Cynthia J. Burrows, and Susan S. Wallace. 2015. "The NEIL Glycosylases Remove Oxidized Guanine Lesions from Telomeric and Promoter Quadruplex DNA Structures." *Nucleic Acids Research* 43 (8): 4039–54. <https://doi.org/10.1093/nar/gkv252>.

Zhou, Jia, Minmin Liu, Aaron M. Fleming, Cynthia J. Burrows, and Susan S. Wallace. 2013. "Neil3 and NEIL1 DNA Glycosylases Remove Oxidative Damages from Quadruplex DNA and Exhibit Preferences for Lesions in the Telomeric Sequence Context." *The Journal of Biological Chemistry* 288 (38): 27263–72. <https://doi.org/10.1074/jbc.M113.479055>.

Zhu, Xu-Dong, Laura Niedernhofer, Bernhard Kuster, Matthias Mann, Jan H. J. Hoeijmakers, and Titia de Lange. 2003. "ERCC1/XPF Removes the 3' Overhang from

Uncapped Telomeres and Represses Formation of Telomeric DNA-Containing Double Minute Chromosomes.” *Molecular Cell* 12 (6): 1489–98.



Zimmermann, Michal, and Titia de Lange. 2014. “53BP1: Pro Choice in DNA Repair.” *Trends in Cell Biology* 24 (2): 108–17. <https://doi.org/10.1016/j.tcb.2013.09.003>.

11. Published articles

Silvia Burra, D. Marasco, M. C. Malfatti, G. Antoniali, A. Virgilio, V. Esposito, B. Demple, A. Galeone and Gianluca Tell "*Human AP-endonuclease (Ape1) activity on telomeric G4 structures is modulated by acetyltable lysine residues in the N-terminal sequence*" DNA Repair 73 (2019) 129–143 <https://doi.org/10.1016/j.dnarep.2018.11.010>

12. Acknowledgements

Innanzitutto, mi pare doveroso ringraziare Gianluca, per essere stato un capo autorevole ma anche paterno. Grazie per avermi offerto la possibilità di completare questo percorso di studi nel tuo laboratorio, per tutti i consigli e le direttive e per aver sempre saputo intrecciare con perfetto equilibrio i rapporti lavorativi con quelli umani! Un ringraziamento sincero per essere capace di riconoscere il valore di ognuno oltre all'aspetto lavorativo e per avere così tanto a cuore le persone con cui collabori, non avrei potuto sperare in un PI migliore! Se al mondo ci fossero più persone come te, tutto funzionerebbe meglio.

Grazie alle mie insostituibili colleghe Giulia, Matilde, Giovanna e Marta, con cui ho condiviso dentro e fuori dal lab questo lungo e tortuoso percorso fatto di mainagioia e risate, momenti di sconforto e degustazioni di torte varie estorte ai tirocinanti, perché bisogna pur consolarsi quando "l'ipotesi è crollata"! Vi porterò sempre nel cuore, mentre la ricerca di base, di cui conserverò un ricordo agrodolce, la lascio sul bancone...  

Un ringraziamento non basta ai miei genitori, i miei due pilastri, i miei modelli di vita, senza i quali niente sarebbe stato possibile. Senza di voi non sarei arrivata fino a qui, grazie per amarmi e sostenermi sempre. ♥

Grazie alla mia sisterina unica che crede sempre in me. Ti voglio bene! ♥

Grazie infinite ad Anna, mia inseparabile amica per la pelle, mia complice e mia spalla. Grazie per il sorriso inossidabile che sempre mi rivolgi, il supporto che sei costantemente pronta a darmi, per tutti i momenti di confronto, i consigli spassionati e le opinioni sincere (*y muchas gracias* al Cantera che ci ha fatto incontrare)!

Grazie a Maurizio per il bene sincero che mi vuole e per essere sempre carinissimo con me. Grazie per la stima che hai in me, per le belle parole che mi hai sempre rivolto e per tutti gli incoraggiamenti che mi regali!

Grazie a tutti gli amici del ballo con cui passo il mio tempo libero, grazie a Marti, Cate, Nil, Simo, Ale, Stefano e tutti gli altri bailadores, siete davvero tanti ed è bellissimo avere una compagnia variegata con cui condividere questa passione irrefrenabile!

Grazie alla mia piccola grande Chiaretta per avermi consolata e rincuorata quando ne avevo bisogno. È bellissimo che alla fine siamo giunte al traguardo comunque insieme,

anche se su due strade diverse! 🌸 Grazie di cuore a tutta la famiglia Viotto che mi fa sempre sentire a casa!

Grazie a Vale per tutti gli incoraggiamenti e per le indimenticabili gite nella City. Grazie per trasmettami la tua energia dirompente e per farmi sognare con la tua vita straordinaria.

Un grazie affettuoso ad Alessandra che riesce sempre a farmi ridere di gusto!

Ringrazio Bruce per l'ospitalità che mi ha offerto durante la trasferta a Long Island e per avermi fatto apprezzare tanto NY quanto il FVG.

Grazie a Viviana per condividere le mie stesse paranoie e grazie anche a Max, Veronica e Anna con i quali ho in parte condiviso questo lungo percorso biotecnologico.

La scienza è amore per la scoperta, curiosità, tenacia. È costanza, determinazione, capacità di vedere oltre. È gioire di un risultato dopo decine di tentativi falliti. Tanta stima per tutti coloro che hanno la forza di continuare a fare ricerca con lo stesso slancio con cui si conduce i primi esperimenti!